&EPA
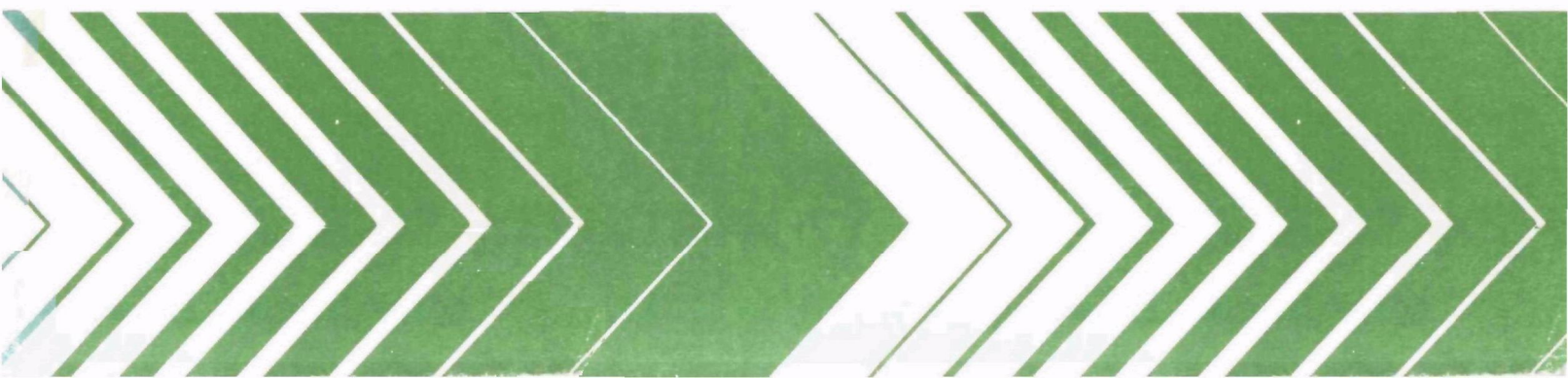
Airborne Measurements of Power Plant Plumes in West Virginia

Kammer and Mitchell Power Plants, 25 August — 11 September 1975

RESEARCH REPORTING SERIES

Research reports of the Office of Research and Development, U.S. Environmental Protection Agency, have been grouped into nine series. These nine broad categories were established to facilitate further development and application of environmental technology. Elimination of traditional grouping was consciously planned to foster technology transfer and a maximum interface in related fields. The nine series are:

1. Environmental Health Effects Research
2. Environmental Protection Technology
3. Ecological Research
4. Environmental Monitoring
5. Socioeconomic Environmental Studies
6. Scientific and Technical Assessment Reports (STAR)
7. Interagency Energy-Environment Research and Development
8. "Special" Reports
9. Miscellaneous Reports

This report has been assigned to the ENVIRONMENTAL MONITORING series.This series describes research conducted to develop new or improved methods and instrumentation for the identification and quantification of environmental pollutants at the lowest conceivably significant concentrations. It also includes studies to determine the ambient concentrations of pollutants in the environment and/or the variance of pollutants as a function of time or meteorological factors.

AIRBORNE MEASUREMENTS OF POWER PLANT PLUMES IN WEST VIRGINIA
Kammer and Mitchell Power Plants
25 August - 11 September 1975

by

Frank G. Johnson*, John L. Connolly, Roy B. Evans and Thomas M. Zeller
Monitoring Operations Division
Environmental Monitoring and Support Laboratory
Las Vegas, Nevada 89114

*On assignment from National Oceanic and Atmospheric Administration,
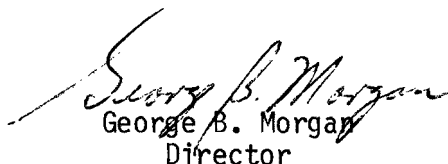U.S. Department of Commerce

DISCLAIMER

This report has been reviewed by the Environmental Monitoring and Support
Laboratory-Las Vegas, U.S. Environmental Protection Agency, and approved for
publication. Mention of trade names or commercial products does not
constitute endorsement or recommendation for use.

FOREWORD

Protection of the environment requires effective regulatory actions that are based on sound technical and scientific information. This information must include the quantitative description and linking of pollutant sources, transport mechanisms, interactions, and resulting effects on man and his environment. Because of the complexities involved, assessment of specific pollutants in the environment requires a total systems approach that transcends the media of air, water, and land. The Environmental Monitoring and Support Laboratory-Las Vegas contributes to the formation and enhancement of a sound monitoring data base for exposure assessment through programs designed to:

- develop and optimize systems and strategies for monitoring pollutants and their impact on the environment

- demonstrate new monitoring systems and technologies by applying them to fulfill special monitoring needs of the Agency's operating programs

This report presents the results of an air quality study made in the upper Ohio River Valley. Specifically, a helicopter-borne system was used to measure the plumes of the Kammer and Mitchell power plants near Wheeling, W. Va. In addition, a downward-looking LIDAR system was deployed for the same purpose. Additional information, not contained in this report, may be obtained from the Monitoring Operations Division of the Environmental Monitoring and Support Laboratory.

George B. Morgan
Director
Environmental Monitoring and Support Laboratory
Las Vegas, Nevada

iii

CONTENTS

FIGURES

TABLES

LIST OF ABBREVIATIONS AND SYMBOLS

ABBREVIATIONS

$\overset{\circ}{A}$	--	Angstrom
AGL	--	above ground level
b_{scat}	--	total light scattering
BCD	--	binary coded decimal
BTU	--	British thermal unit
°C	--	degree Celsius
cfm	--	cubic feet per minute
cm	--	centimeter
DCS	--	Bendix dynamic calibration system
DME	--	distance measuring equipment
EMSL-LV	--	Environmental Monitoring and Support Laboratory-Las Vegas
EPA	--	U.S. Environmental Protection Agency
EST	--	Eastern Standard Time
F	--	buoyancy flux
ft	--	feet
g	--	gravitational constant
h	--	centerline plume height
J	--	Joule
°K	--	degree Kelvin
kg	--	kilogram
km	--	kilometer
kn	--	knot (nautical mile per hour)
L	--	downwind distance where concentration at top of mixing layer is 1/10 of centerline
LIDAR	--	light detection and ranging
m	--	meter
mag	--	magnetic compass heading or bearing
max	--	maximum
MOD	--	Monitoring Operations Division
mm	--	millimeter
MSL	--	mean sea level
MTE	--	maximum terrain elevation
MW	--	molecular weight
MWe	--	megawatt electric
NBKI	--	neutral buffered potassium iodide
NBS	--	National Bureau of Standards
nmi	--	nautical mile
$NO\text{-}NO_x$	--	nitrous oxide-total oxides of nitrogen
sec	--	second
SO_2	--	sulfur dioxide

List of Abbreviations and Symbols (Continued)

SRM	--	standard reference method
STP	--	standard temperature and pressure
T	--	temperature
T_d	--	dewpoint temperature
u	--	horizontal wind speed
UV	--	ultra violet
VFR	--	visual flight rules
VORTAC	--	air navigation beacon
w	--	exit velocity
x	--	downwind distance

SYMBOLS

Δh	--	plume rise
μg	--	microgram
ρ	--	density
θ	--	potential temperature
σy	--	standard deviation in the crosswind direction
σz	--	standard deviation in the vertical direction
χ	--	centerline concentration

INTRODUCTION

In response to a request from the U.S. Environmental Protection Agency (EPA) Regional Administrator for Region III, the Monitoring Operations Division (MOD) of the Environmental Monitoring and Support Laboratory-Las Vegas (EMSL-LV) conducted a field study between 25 August and 11 September 1975 to measure parameters of effluent plumes from two large coal-fired electric generating stations near Wheeling, West Virginia. Concentrations of sulfur dioxide (SO_2) in the plumes had previously been estimated by the H.E. Cramer Company (1975) using standard Gaussian-type point source dispersion models. The MOD study was intended to measure plume parameters to compare with model calculations. Parameters of interest included plume height-of-rise, horizontal and vertical plume spread, and concentrations of SO_2 at the plume centerline and near the ground.

The two generating stations are located about 15 nautical miles (nmi)* south of Wheeling, on the Ohio River. The larger of the two, the Mitchell plant, has a capacity of approximately 1600 megawatts electric (MWe), a 365-meter stack and a maximum SO_2 emission rate of approximately 850,000 kilograms per day (kg/day). The Kammer plant has two 183-meter stacks, a capacity of approximately 800 MWe, and a SO_2 emission rate of about 389,000 kg/day (Walden 1973). Table 1 provides a more complete list of pertinent plant characteristics.

Plume parameters were observed during the field study with two airborne measurement systems.

1. A helicopter-borne air quality monitoring system measured gas concentrations of sulfur dioxide, nitric oxide, oxides of nitrogen, and ozone along with aerosol light scattering (with a nephelometer), air temperature and dew point, and location. This system was installed in a Sikorsky S-58 helicopter.

2. An airborne down-looking LIDAR system instantaneously measured aerosol light scattering versus altitude above ground level (AGL). The LIDAR was installed in a Beechcraft C-45 twin-engine airplane.

---

*Gases are reported in parts per million (ppm) by the helicopter data processing system in order to make the data compatible with extensive ground monitoring stations involved in the Regional Air Pollution Study, St. Louis, Missouri (Allen 1973). The amount of data involved in this report makes it impractical to convert concentrations to micrograms per cubic meter. In addition, all altimetry and navigational data are reported in nautical miles and feet, as those systems report directly in those units.

1 ft = 0.3048 m; 1 nmi = 1.84 km; $\mu g/m^3$ SO_2 = 2,667 X ppm SO_2

SUMMARY

Seventeen helicopter flights were made during the period 25 August to
11 September 1975, to make measurements in the effluent plumes from the Kammer
and Mitchell generating stations. LIDAR measurements were obtained on 4 days
during the period. From the helicopter data, 16 sulfur dioxide plume cross
sections and three horizontal plume concentration maps were prepared.
Additional plume dimensions were obtained on occasions when plume cross
sections were not constructed. The LIDAR flights yielded four plume cross
sections and several long range measurements perpendicular to the regional
gradient winds. The LIDAR was hampered by adverse weather and equipment
problems. Three of the LIDAR cross sections were performed simultaneously
with helicopter cross sections, providing a check on the validity of such
cross sectional patterns prepared from successive helicopter passes.

Figures 1 and 2 summarize plume widths determined by helicopter
observations. In the majority of cases, the two Kammer plumes combined to act
as a single plume, and only such cases are included in the summaries.
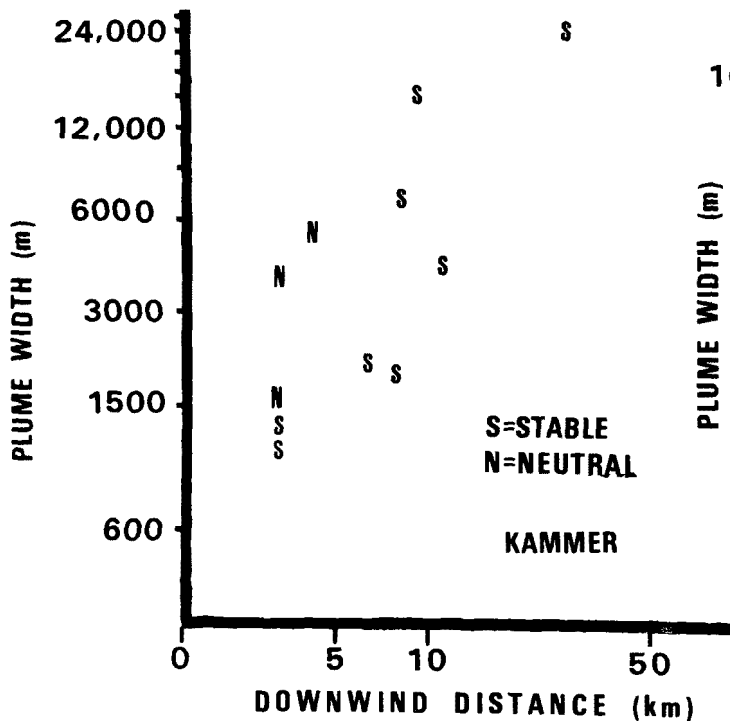
Figure 1. Combined Kammer plume width vs. downwind distance.
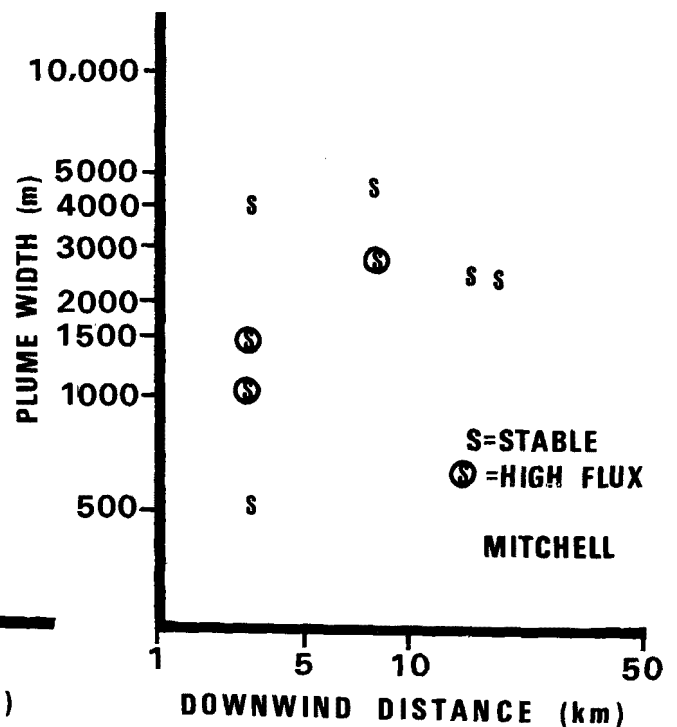
Figure 2. Mitchell plume width vs. downwind distance.

2

Figures 3 and 4 offer a comparison of normalized plume height,

$$h \text{ (meters)} \times u \text{ (meters/sec)} = hu \text{ (meters}^2\text{/sec)}$$

to downwind distance. The stability associated with each observation is noted. As shown in Figure 3, the Kammer plumes have for the stable cases, a mean normalized plume stabilization height of 4,632 m^2/sec with a standard deviation of 1,308 m^2/sec. In Figure 4, the mean normalized plume stabilization height of the Mitchell plume is 5,069 m^2/sec with a standard deviation of 608 m^2/sec. It is believed that this difference in variation about the mean may be attributed to the fact that the Kammer plume, originating from shorter stacks, exhibits a terrain-induced looping motion not found to as great an extent in the higher Mitchell plume.
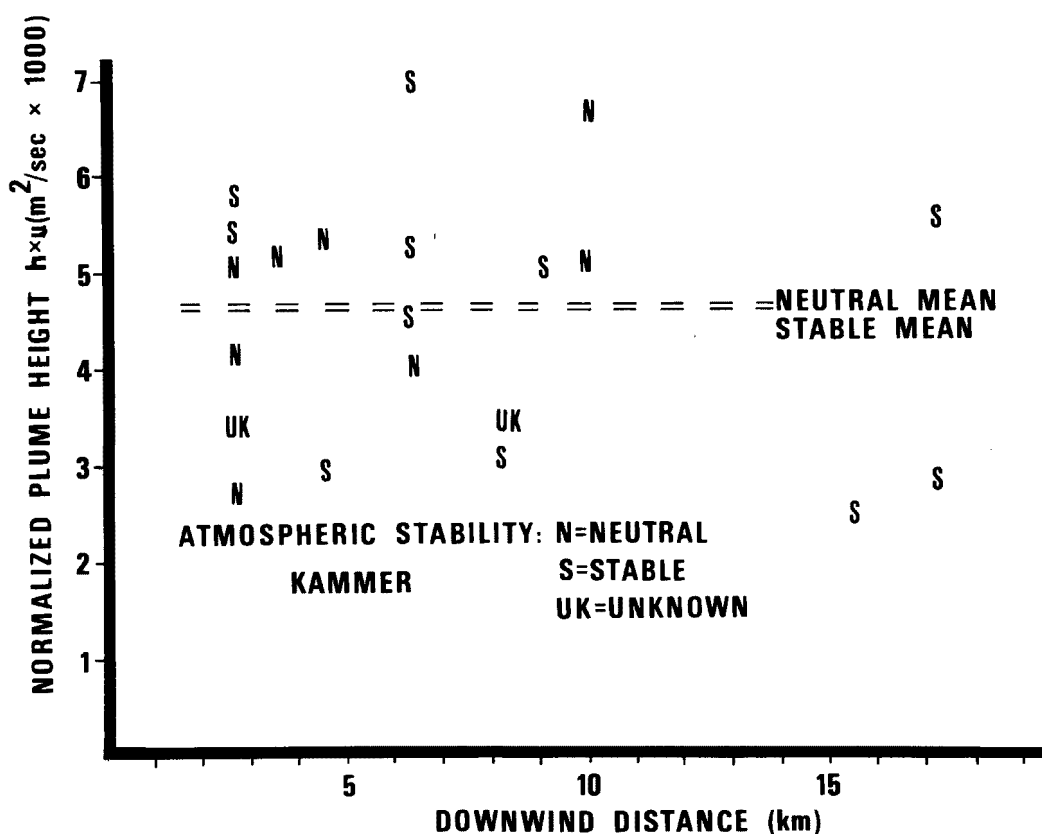
Figure 3. Normalized Kammer plume height vs. downwind distance.

3

25 AUGUST - SEPTEMBER 1975

NEUTRAL MEAN

ATMOSPHERIC STABILITY: N=NEUTRAL
MITCHELL   S=STABLE

STABLE MEAN

h×u(m²/sec×1000)

DOWNWIND DISTANCE (km)
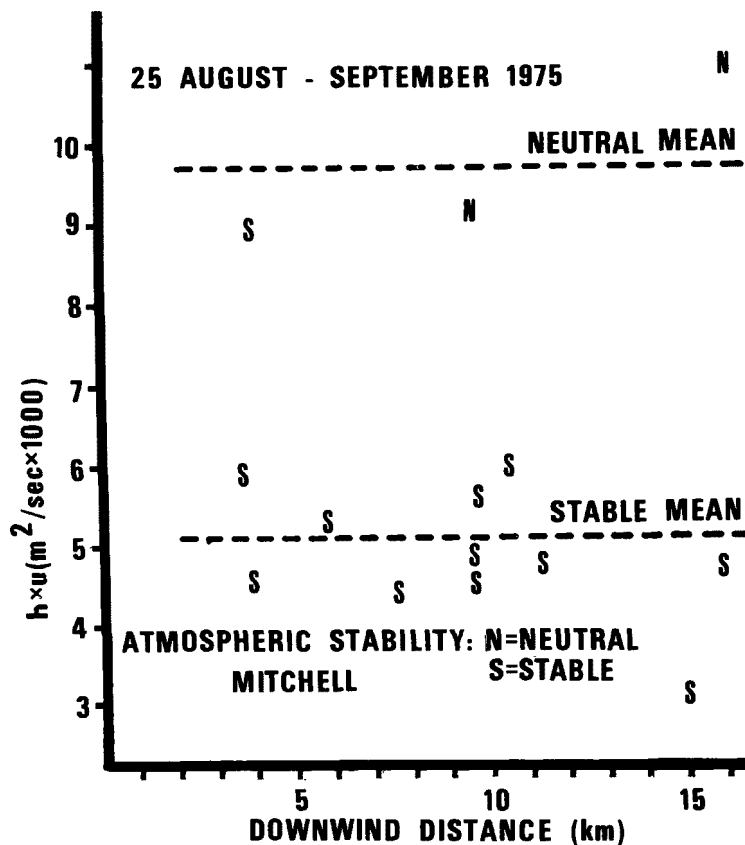
Figure 4. Normalized Mitchell plume height vs. downwind distance.

Figures 5 and 6 compare plume rise to the results obtained from use of the following formulae to compute plume rise.

For the Mitchell plant:

Δh = 2.0 $F^{1/2}u^{-1}x^{2/3}$, for periods of nominal loading, and
Δh = 980$e^{-0.21u}$ for periods of normal loading where
F = buoyancy flux (m^4sec^{-3})
u = wind speed (m/sec)
x = distance where plume stabilization takes place

For the Kammer plant:

Δh = 0.66 (2.0 $F^{1/3}u^{-1}x^{2/3}$).
 x was chosen arbitrarily as 1 km.

Appendix G presents details of the selection of these equations.

$$\odot = f(2.0F^{1/3} u^{-1} x^{2/3})$$

$$\oplus = f(980.0e^{-0.209u})$$

MITCHELL

DATE 1975

Figure 5. A comparison of observed and calculated plume rises for the Mitchell plant, 27 August - 11 September 75.

$$\Delta h = 0.66(2.0F^{1/3} u^{-1} x^{2/3})$$

KAMMER

Figure 6. A comparison of observed and calculated plume rises for the Kammer plant, 27 August - 11 September 75.

Figures 7 and 8 represent an attempt to normalize plume centerline sulfur dioxide concentrations. Centerline sulfur dioxide concentr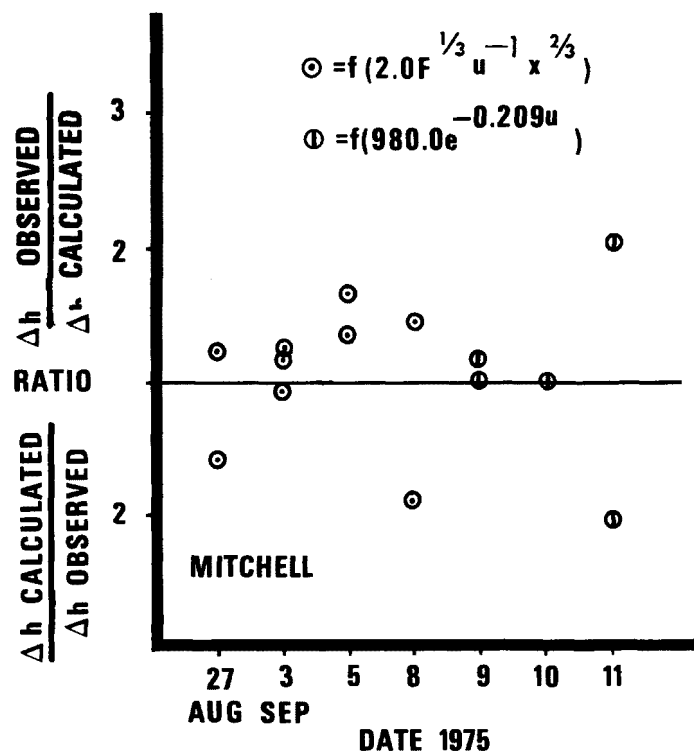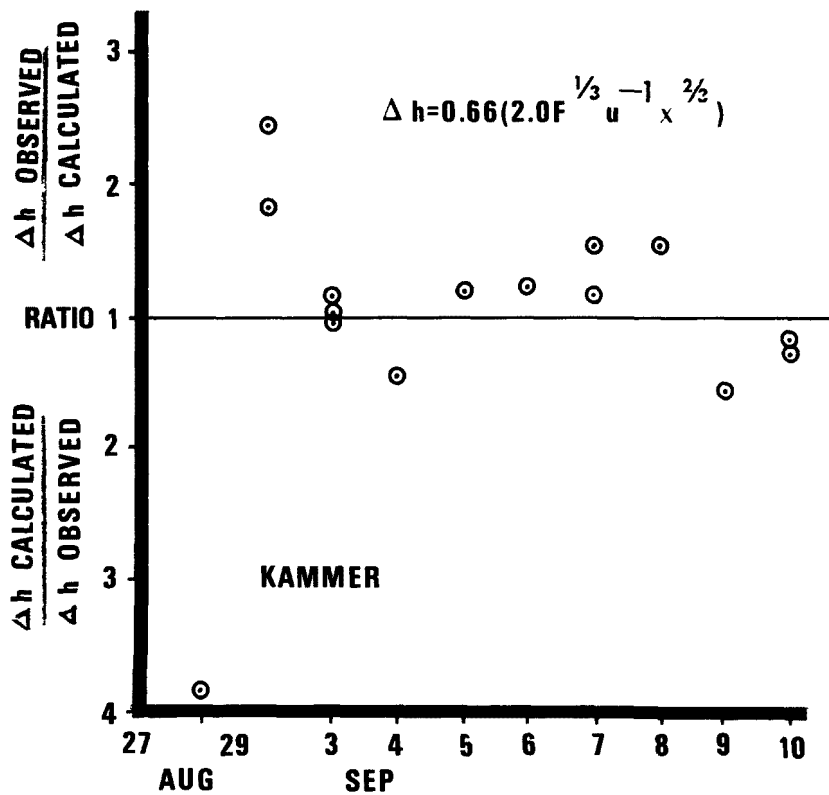ations in $\mu g/m^3$ were multiplied by the observed stack height winds (m/sec) and the standard deviations, $\sigma_y\sigma_z$ (m^2), of the plume concentration distributions in the horizontal and vertical dimensions to normalize the diluting effects of these two phenomena. The values of σ_y were obtained from actual plume measurements. The values of σ_y measured for the Mitchell plant were nearly those for flat terrain, while the σ_y for the Kammer plant were higher by a factor of two. The σ_z values were calculated based on σ_y values (see Appendix C). These normalized concentrations were plotted against distance from the plants. The product of centerline concentrations, wind speed and the standard deviations, $\chi u \sigma_y \sigma_z$ ($\mu g/sec$), represents the flux along the centerline. This may be used to estimate the plume centerline concentrations under a variety of wind and stability conditions. In order to eliminate the effects of a few very high or low values skewing the mean value, the midmean has been included. The midmean is defined as, "The arithmetic mean of all observations between and including the lower and upper quartiles" (Cleveland et al., 1976). The midmean value for the Mitchell plume is 1.0×10^9 $\mu g/sec$, and for the Kammer plumes, 1.8×10^9 $\mu g/sec$.
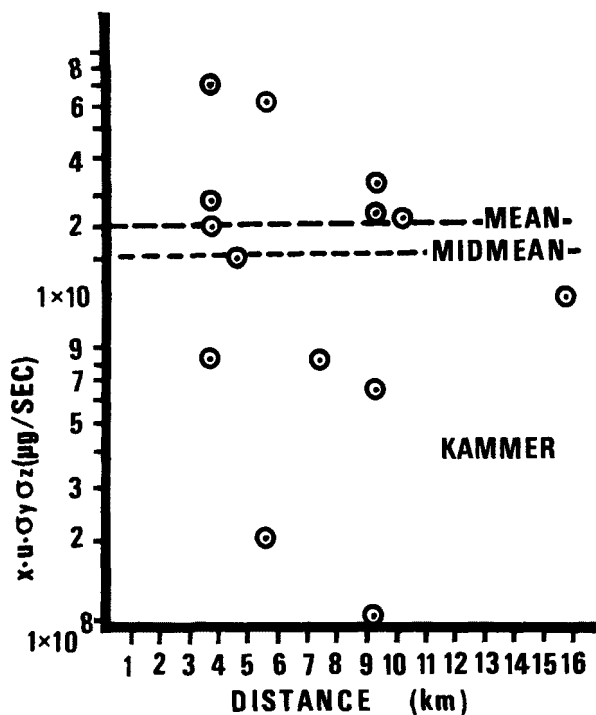

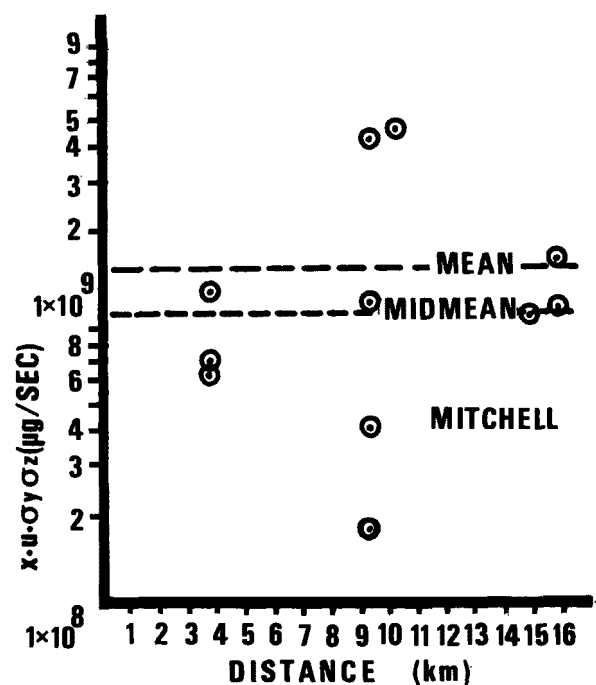Figure 7. Centerline flux vs. downwind distance for the Kammer plumes.

Figure 8. Centerline flux vs. downwind distance for the Mitchell plume.

6

Figures 9 and 10 present a more classical representation of centerline concentrations, i.e., the product of relative centerline concentration and wind speed vs. downwind distance. With the exception of the low flux days for the Mitchell plant, these data show a logical decrease with distance. The only difference that was noted for the anomalous data was the fact that the Mitchell plant was producing low volumetric emissions during the times of observation.
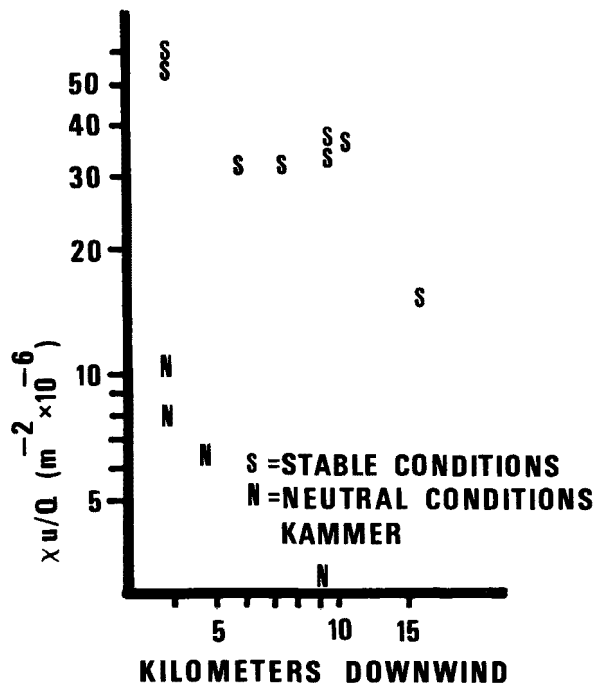
Figure 9. Kammer power plant centerline concentration times wind speed ($\frac{\chi}{Q}$ u) vs. downwind distance.
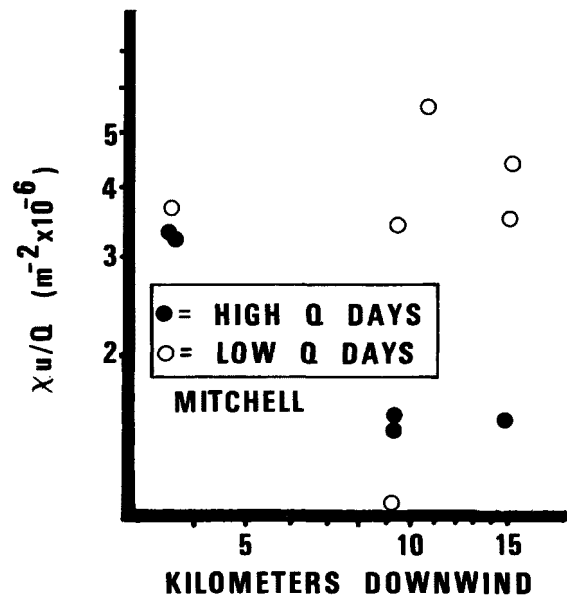
Figure 10. Mitchell power plant centerline concentration times wind speed ($\frac{\chi}{Q}$ u) vs. downwind distance.

LIDAR and helicopter cross sections were simultaneously constructed on 5 and 8 September 1975. Good general agreement was observed between the SO_2 and particulate distribution. However, the length of time required for the helicopter to construct its cross section (about an hour) and the LIDAR shot spacing (about one-half nautical mile) resulted in less than perfect agreement in some cases. A wide skew is shown for the SO_2 cross section (Figure A-42) due to lateral plume shift during the relatively long helicopter measurement, while a quick cross section by LIDAR measurement (Figure A-43) during the helicopter measurement shows a more "true picture" but with less structure detail and measurement precision.

7

LIDAR passes for a number of miles once again demonstrate the ability of this instrumentation to give relative particulate distribution over a large area (Eckert et al., 1975) (See Figures A-31, A-32, A-33, and A-55).

The Kammer plumes were observed to contact the ground surface on a number of occasions (27 and 29 August and 2, 3, 7 and 11 September). The Mitchell plume was visually observed at the surface on the afternoon of 9 September.

Estimates of sulfur dioxide fluxes in the Kammer plume were prepared from three separate cross sections and the associated transport wind data; all three cross sections were measured on 29 August under stable atmospheric conditions with moderately strong winds (17 knots at 2,000 ft, or 610 m, MSL). The three flux estimates from helicopter data agree within 10 percent with flux estimates derived from coal consumption and sulfur content data for the Kammer plant (See Appendix D).

DESCRIPTION OF PLANTS

The Kammer and Mitchell power plants are located on the east bank of the Ohio River in Marshall County, West Virginia. Within several kilometers, terrain elevations extend up to 180 meters above plant grade (See Figures 11 and 12). These two plants are described in Table 1.

TABLE 1. KAMMER AND MITCHELL POWER STATIONS - CHARACTERISTICS (WALDEN 1973)

	MITCHELL	KAMMER Stack 1	KAMMER Stack 2
Power production	$\simeq 1600$ MWe	$\simeq 800$ MWe (Total)	
Plant grade (m MSL)	201	195	195
Stack height (m)	365.8	183	183
Inside diameter (m)	10.06	4.75	3.35
Exit velocity (m sec^{-1})	30.3	34.6	34.7
Exit temperature (°K)	441.3	441.3	441.3
Rated capacity (BTU hr^{-1})	1.3446×10^{10}	3.871×10^{9}	1.936×10^{9}
Rated capacity (J hr^{-1})	1.4×10^{13}	4.1×10^{12}	2.0×10^{12}
Fuel (coal) (kg yr^{-1})	3.0×10^{9}	9.5×10^{10}	4.2×10^{8}
% Sulfur	3.7	4.0	4.0
SO_2 Emission rate (kg sec^{-1})			
Max. load	9.8	3.0	1.5
Nom. load	5.4	2.3	1.3

Both of these plants have high stack exit velocities. The Mitchell Power Plant has one of the tallest smoke stacks in the world.

Figure 11.   The Mitchell Power
Station.

Figure 12.   The Kammer Power Station
(Mitchell in background).

DESCRIPTION OF AIRCRAFT AND INSTRUMENTATION

A Sikorsky S-58 helicopter was used for in-plume measurements (See Figure 13). Its normal sampling speed is 60 knots (kn); its cruising speed is approximately 80 kn; its flight duration, at 80 kn, is approximately 4.0 hours, and its ceiling is approximately 9,000 feet (2,745 m) MSL. The helicopter was instrumented to measure the following parameters: ozone (Rem 216B), nitric oxide and oxides of nitrogen (Monitor Labs ML 844), and sulfur dioxide (Meloy SA160). Aerosol light scattering was measured with an integrating nephelometer (MRI 1550). Measurements were also made of temperature and dew point (CS-137), position (Collins DME-40), and altitude. Position was determined by continuous triangulation against two air navigation beacons (VORTAC's) and is accurate to $\pm$ 0.1 nmi. In addition, magnetic heading and indicated airspeed are recorded. Figure 14 is a block diagram of the instrument package. Analog and digital voltages are processed by an on board data acquisition system (Monitor Labs ML7200) at selected rate of scan of 2 to 5 seconds. The data system converts the output voltages to Binary Coded Decimal (BCD) characters recorded on magnetic tape (Copher 70). The magnetic tape is then processed by a digital computer and a printout of calibrated engineering units is obtained. In addition, any four analog outputs may be recorded on a strip chart recorder. Calibration procedures are described in Appendix F.

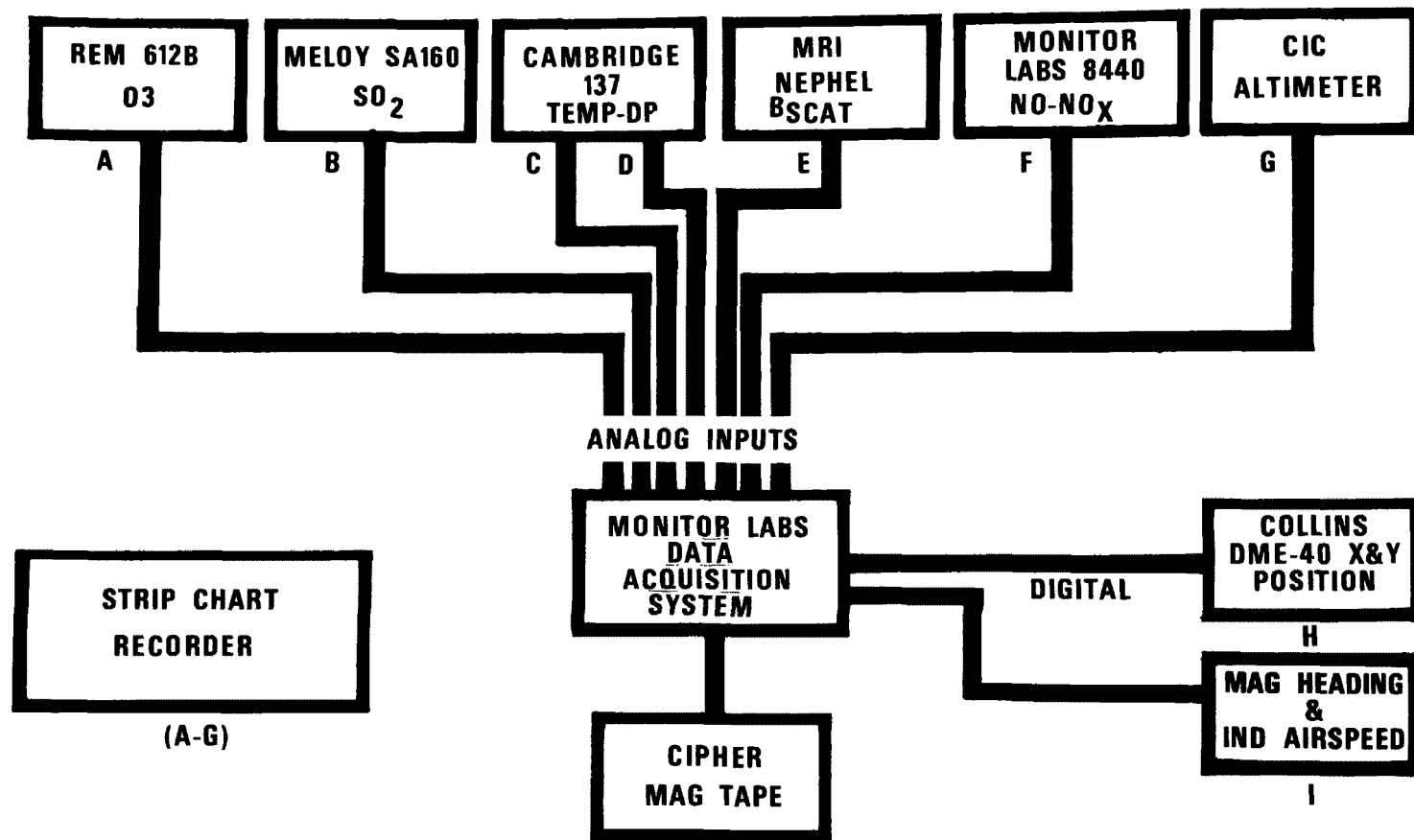Figure 13. Sikorsky S-58 helicopter.

11

Figure 14. Helicopter data system.

A twin-engine Beechcraft (C-45) was used to carry the LIDAR. Its normal cruising speed is 155 kn with a flight duration of 6 hours. The normal sampling speed is 100 kn. The LIDAR system is composed of a laser which generates a pulse of monochromatic light downward and a detection system to measure the returned scattered light. When the particles, whose largest dimension is small compared to the wavelength of the incident light, are measured, the volume of the particle is the most important consideration. Under these conditions, the amount of scattered flux varies directly to the square of the volume and the number of scatterers per unit volume (Johnson 1954). The laser must be fired through a cloud-free atmosphere from at least 7,500 feet above ground level (AGL) to protect ground based observers from possible eye damage.

The LIDAR includes a Q-switched ruby laser operating at a wavelength of 6934Å and a 38-centimeter (cm) fresnel lens receiving telescope. The returned signals are detected by a photomultiplier tube and digitized with an analog-to-digital converter with a storage capacity. This system has a vertical resolution of 15 m (Eckert et al., 1975) and a horizontal resolution dependent on the aircraft speed, LIDAR cycle time, and navigation data precision. Shot spacings averaged approximately one-half mile.

The data were recorded on board on a strip chart. These data were subsequently digitized and corrected for a $1/R^2$ (R is the range of the particle from the telescope) light divergence factor and placed on magnetic tape. The value given to the strength of a return from one altitude was given a relative value comparing it to returns from other altitudes. In this manner a series of vertical profiles was constructed and cross sections were drawn. The bar graphs for the constant heading flights represent a subjective evaluation of the total return signal associated with a shot to the strength of other returns received during the flight. This was done by plotting each profile on graph paper and measuring the area between each return and its baseline. Figure 15 is a block diagram of the LIDAR system.
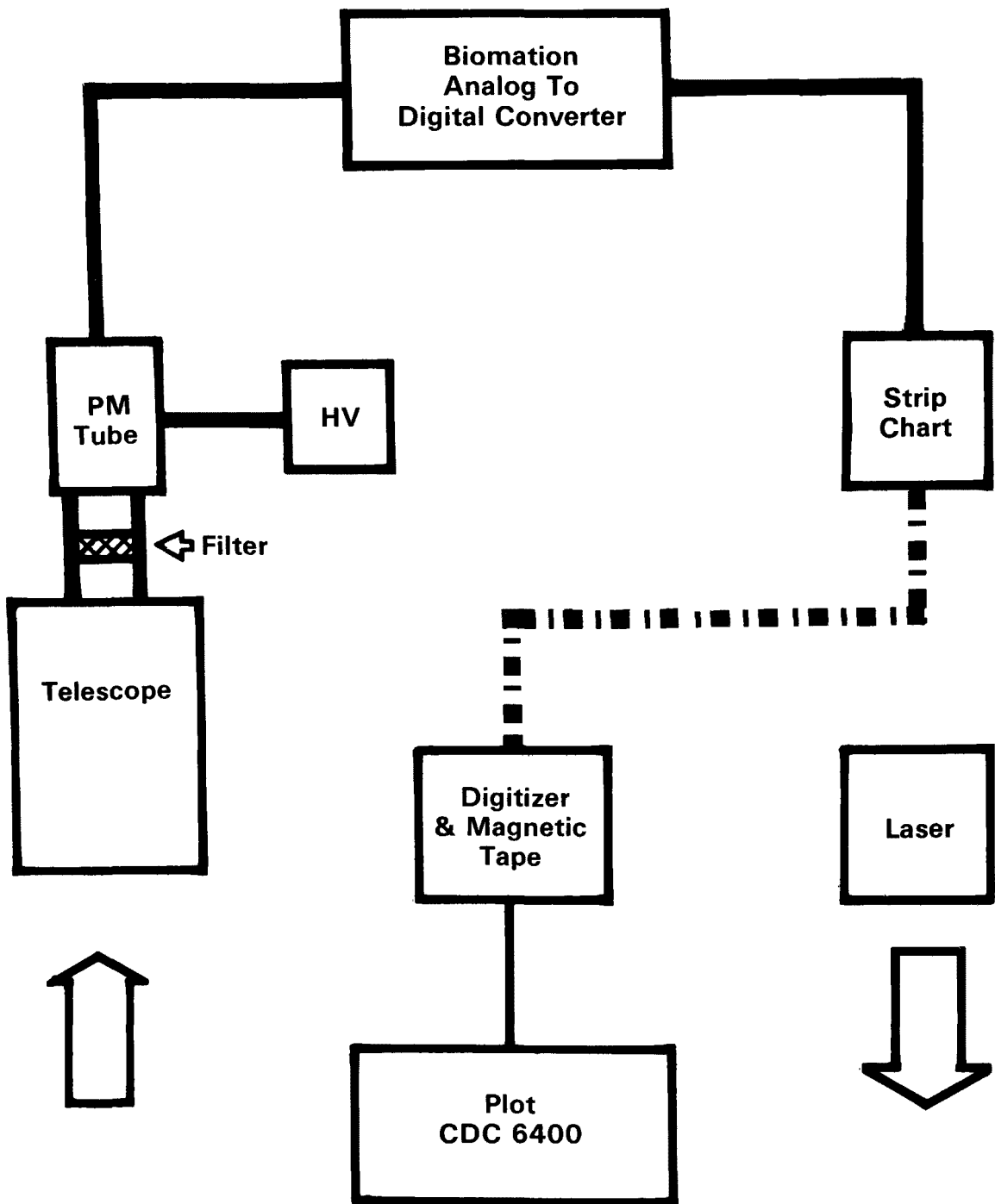
Figure 15. Airborne LIDAR system.

DESCRIPTION OF FLIGHT PATHS AND TECHNIQUES

The following types of missions were flown:

1. Plume dimensionalization flights were made under various atmospheric conditions. These consisted of slow spirals down through the plume at a known distance from the plant to determine the height of plume centerline. These were followed by traverses at the centerline height to determine the plume's lateral extent and to determine the centerline concentration.

2. Plume cross section flights were made. These flights consisted of a series of traverses through the plume, normal to the wind flow and over a given path, at various altitudes in order to determine the horizontal and vertical distribution of the various pollutants. Some of these cross sections were integrated and combined with wind speed to determine flux from the plant. (Appendix D)

3. "Zigzag" helicopter flights were made along the plume at constant altitudes to determine the axial and radial gradient of SO_2 within the plume. These flights extended for a number of miles and were accomplished by flying obliquely through the plume until the helicopter reached the plume edge. The helicopter would then change course 90° to re-enter the plume as quickly as possible.

4. Low altitude helicopter measurements were made to determine near ground-level concentrations of SO_2 during periods when the plumes were observed impating upon the surface.

5. Helicopter and LIDAR aircraft flights were made simultaneously along an identical radial from a VORTAC station. The radial was chosen so that it would be as normal as possible to the orientation of the plume. The helicopter SO_2 cross section was developed so that it could be compared with the particulate cross section obtained from an integration of the LIDAR soundings.

6. Long range LIDAR flights were made to determine particulate variations across the larger air mass. Flights were made along selected radials from various VORTAC stations for a number of miles. The radials were chosen to be as normal to the flow as possible. The fact that the aircraft was flying along a known radial allowed for precision navigation when distance measuring equipment (DME) information was recorded.

7. Flights were made to test equipment, aircraft, or weather effects problems.

The following table is a summation of the various types of missions flown:

TABLE 2. SUMMATION OF AIRCRAFT MISSIONS

Aircraft	Type of Mission	Number of Missions	Hours Flown
S-58	1	3	6.0
	2	8	19.1
	3	2	6.1
	4	2	2.1
	5	2	7.4
Total for S-58		17	40.7
C-45	5	2	8.6
	6	1	5.0
	7	2	3.1
Total for C-45		5	16.7

REFERENCES

Allen, D.W. "Regional air pollution study - an overview." Paper No. 73-21. Proceedings of the 66th Annual Meeting, Air Pollution Control Association (1973).

Briggs, G.A. Plume Rise. U.S. Atomic Energy Commission, Nuclear Safety Information Center, Oak Ridge National Laboratory, Oakridge, Tennessee, TID-25075. (1969).

Briggs, G.A., L. Van der Hoven, R. J. Englemann, and J. Holitsky. "Chapter 5. Processes other than natural turbulence affecting effluent concentrations." Meteorology and Atomic Energy. U.S. Atomic Energy Commission, Office of Information Services, Oak Ridge, Tennessee (1968).

Cleveland, W.S., B. Kleiner, and J.L. Warner. "Robust statistical methods and photochemical air pollution data." Journal of the Air Pollution Control Association (1976).

Cramer, H.E. Characteristics of the Stack Plumes from the Mitchell and Kammer Plants. Preliminary report for Region III, U.S. Environmental Protection Agency (1975).

Eckert, J.A., J.L. McElroy, D.H. Bundy, J.L. Guagliardo, and S.H. Melfi. "Downlooking LIDAR studies." Proceedings of the International Conference on Environmental Sensing and Assessment, Las Vegas, Nevada. IEEE (1975).

Johnson, J.C. Physical Meteorology. J. Wiley and Sons, Inc., New York, New York (1954).

McElroy, J.L., and F. Pooler, Jr. St. Louis Dispersion Study, Volume II - Analysis. National Air Pollution Control Administration Publication No. AP-53, Arlington, Virginia (1968).

Nickola, P.W., and G.H. Clark. "Estimation of mean crosswind concentration profiles from 'instantaneous' crosswind traverses." Pacific Northwest Laboratory Annual Report for 1973 to the U.S. Atomic Energy Commission Division of Biomedical and Environmental Research. Battelle Pacific Northwest Laboratories, Richland, Washington (1974).

Ramsdell, Jr., J.V., and W.T. Hinds. "A systematic error in the measurement of plume crosswind concentration distribution with moving samplers." Pacific Northwest Laboratory Annual Report for 1974 to the U.S. Atomic Energy Commission Division of Biomedical and Environmental Research. Battelle Pacific Northwest Laboratories, Richland, Washington (1975).

17

Schiermeier, F.A. "Study of effluents from large power plants." Presented at the American Industrial Hygiene Association Conference, Toronto, Canada (1971).

Sutton, O.G. "A theory of eddy diffusion in the atmosphere." Proceedings of the Royal Society, Series A, vol. 135. pp. 143-165 (1932).

Turner, D.B. Workbook of Atmospheric Dispersion Estimates. U.S. Department of Health, Education, and Welfare, National Air Pollution Control Administration, Cincinnati, Ohio (1969).

Walden Research Corporation. "Modeling analysis of power plants for compliance extensions." Report for the Source Receptor Analysis Branch, Monitoring and Data Analysis Division of the Office of Air Quality Planning and Standards, Office of Air and Water Programs, U.S. Environmental Protection Agency. (1973).

APPENDIX A - DESCRIPTION AND RESULTS OF FLIGHTS

The following are descriptions and the results of each flight. Included are maps, temperature soundings, cross sections and other geographical presentations as applicable. The primary pollutant of interest was sulfur dioxide (SO_2). The cross sections of SO_2 concentrations have been visually adjusted to compensate for the lag time of the sampling system and the rise and fall times of the instrument. Figure A-1 is an example of an unadjusted cross section, while Figure A-2 illustrates the magnitude of the adjustments that have been made. In addition, the response time will result in conservative measurements of maximum concentrations and increase the apparent width of the plume profiles. However, any mean or integrated measurements should show a higher degree of representativeness. It has been demonstrated by Nickola and Clark (1974) that the standard error in measurements made by aircraft can be reduced by repetitive sampling and that peak values are much more stochastic than integrated values. In addition, Ramsdell and Hinds (1975) have shown that concentration fluctuations become greater at greater distances from the plume axis, although the absolute intensity of fluctuations decreases as the distance from the axis is increased.
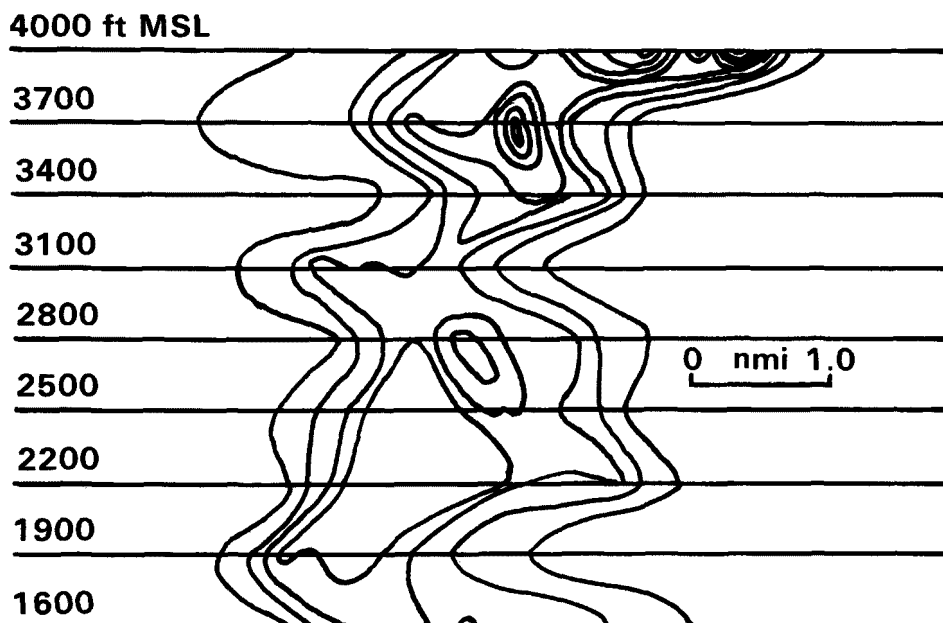

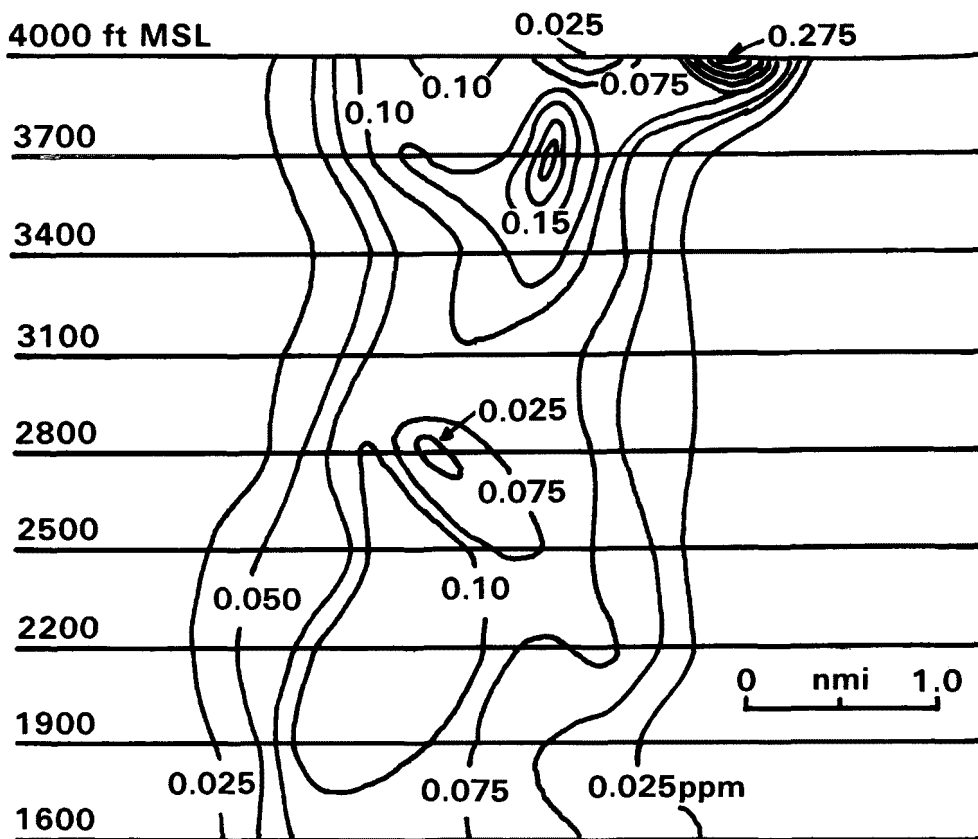Figure A-1. Example of an unadjusted SO_2 cross section.

19

Figure A-2. Example of an adjusted SO₂ cross section.

The plant emissions and plume data tables show both the known plant emission rates and the measured plume dimensions for reader convenience. A separation is made in these tables to show that correlation is not expected. The tables of pibal wind information show the number of balloon soundings, under the heading "Number of Observations", over which the presented data were averaged.

25 AUGUST 1975, 0739-0921 EST

The purpose of this flight was to obtain information on the height and concentration of the Mitchell plume at 2, 5, and 12 nautical miles (nmi). In addition, values for plume width were measured, with plume width being defined as the distance through the centerline and between two points on opposite edges of the plume where one tenth of the centerline concentration is measured. No SO_2 information was obtained due to a malfunction of the instrument; dimensional information was obtained from the $NO-No_x$ instrument. A weak inversion was noted at the beginning of the flight; by 0833 EST near-isothermal conditions existed, indicating stable conditions. No wind measurements were available.

nmi
0   5   N 10
N
5
Wheeling Vortac
Airport
Wheeling
Bellaire Vortac
Moundsville 12nmi
5nmi
2nmi
MTE=1400
Kammer
Mitchell
MTE=1360
MTE=1280
Traverses at 2,5,&12nmi
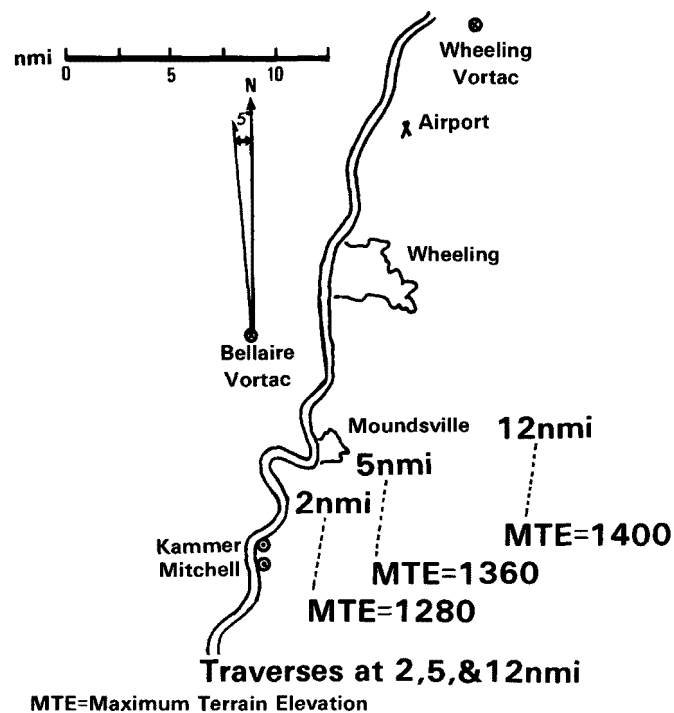MTE=Maximum Terrain Elevation

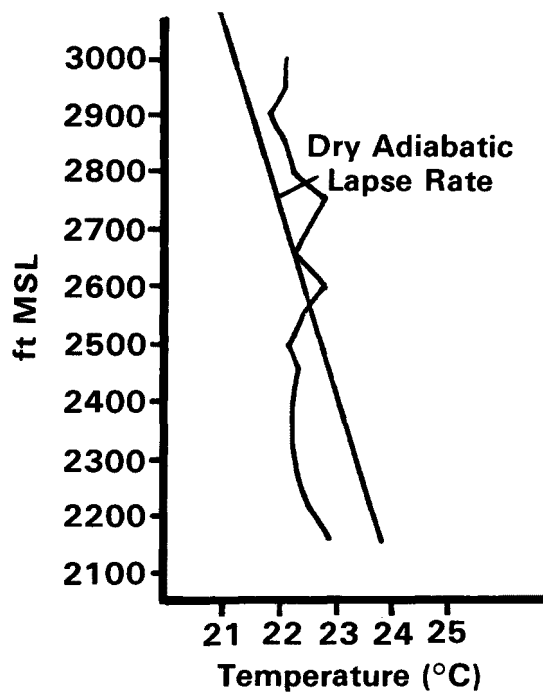Figure A-3. Helicopter flight, 25 August 75.

Figure A-4. Temperature sounding, 25 August 75,
0705-0710 EST

21

TABLE A-1. MITCHELL PLANT EMISSIONS (CRAMER 1976)* AND PLUME DATA,
25 AUGUST 75, 0739-0921 EST

Volumetric Emission Rate (m^3/sec)	SO_2 Emission Rate (g/sec)	Distance (nmi)	Plume Width (ft)	Visual Plume Height (ft MSL)
635	3,770	2	--	2,400
		2	1,520	2,500
		5	4,050	2,250
		12	8,100	2,800

Volumetric emission rates are under stack conditions of temperature and pressure.

*H.E. Cramer, 1976, personal communication.

26 AUGUST 1975, 0859-0959

The purpose of this mission was to obtain information on the Kammer plume. The data system failed after measurements were made at approximately 2 nmi. The temperature probe was not operational.
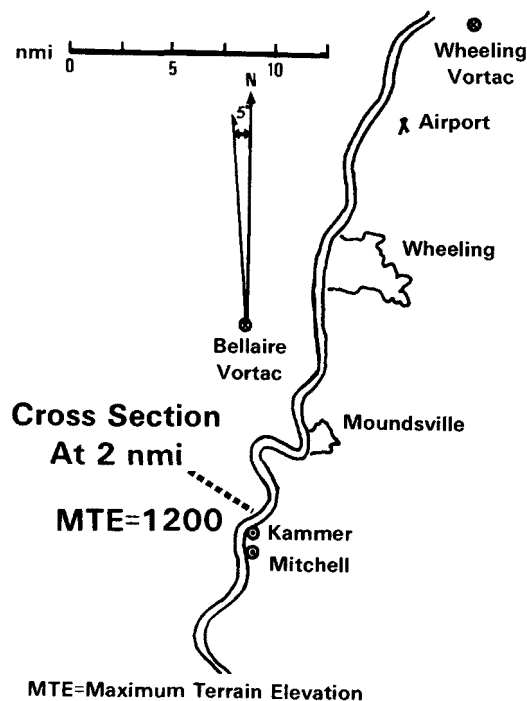

Figure A-5. Helicopter flight path, 26 August 75.

TABLE A-2. PIBAL WIND INFORMATION, 26 AUGUST 75, 0900-1000 EST

Number of Observations	Height (ft MSL)	Direction (degrees mag)	Measured Speed (m/sec)	Speed (knots)
3	993	182	4.5	9
	1,307	194	4.8	9
	1,621	198	5.4	11
	1,935	223	5.8	11

Wind speed and direction are averages of the total observations.

TABLE A-3. KAMMER PLANT EMISSIONS AND PLUME DATA, 26 AUGUST 75, 0859-0959 EST. The emissions are for both Kammer stacks.

Volumetric Emission Rate (m^3/sec)	SO_2 Emission Rate (g/sec)	Distance (nmi)	Plume Width (ft)	Plume Height (ft MSL)	Centerline Concentration SO_2 (ppm)
950	4,970	2	3,550	2,800	0.93

27 AUGUST 1975, 1005-1318 EST

The purpose of this flight was to construct cross sections of the Kammer and Mitchell plumes at 2 and 6 nmi. The temperature profile indicated near neutral conditions to 2,300 ft MSL. Light northeasterly flow was observed to 4,000 ft MSL.
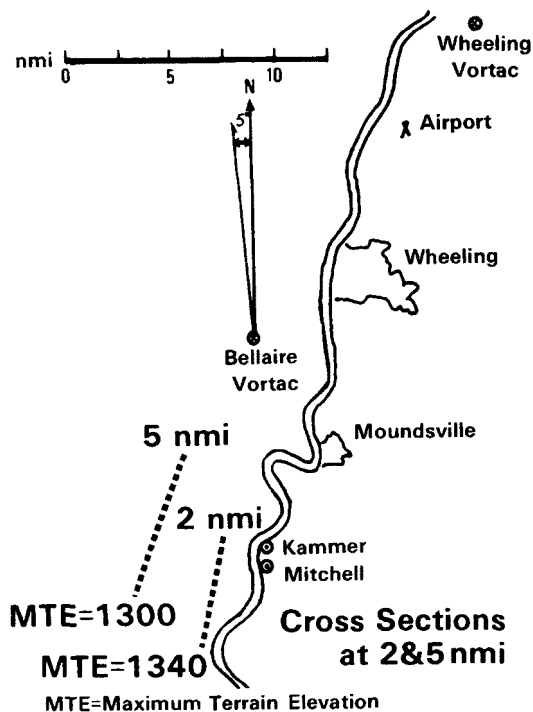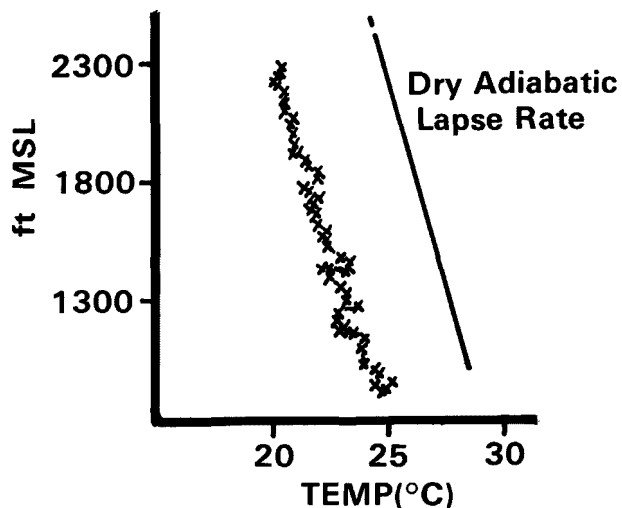
Figure A-6. Helicopter flight, 27 August 75.

Figure A-7. Temperature sounding, 27 August 75, 1028-1033 EST.
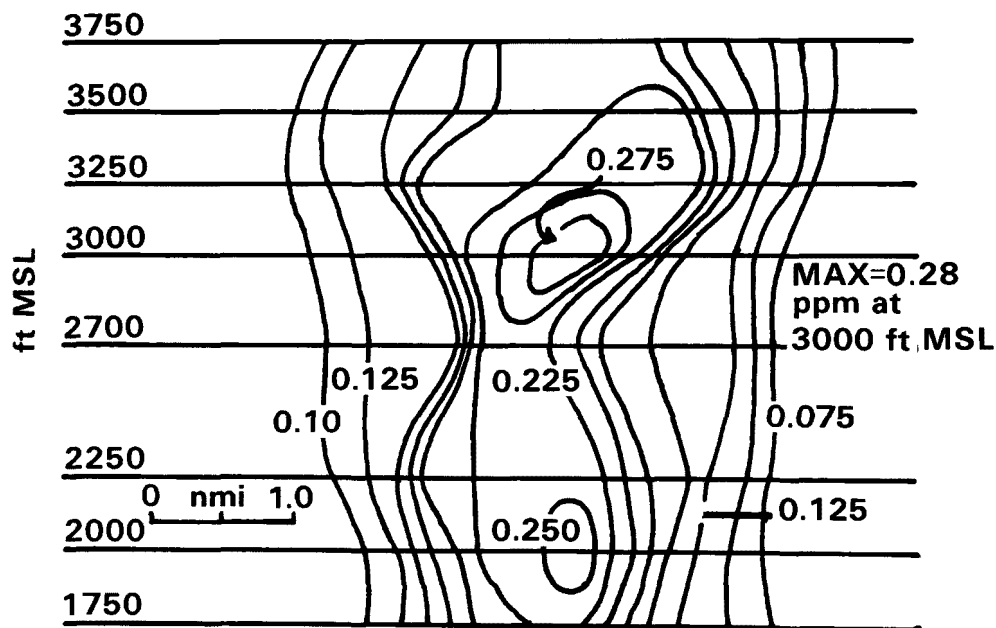

Figure A-8. Sulfur dioxide cross section of the Kammer and Mitchell plumes at 5 nmi, 27 August 75, 1156-1244 EST.
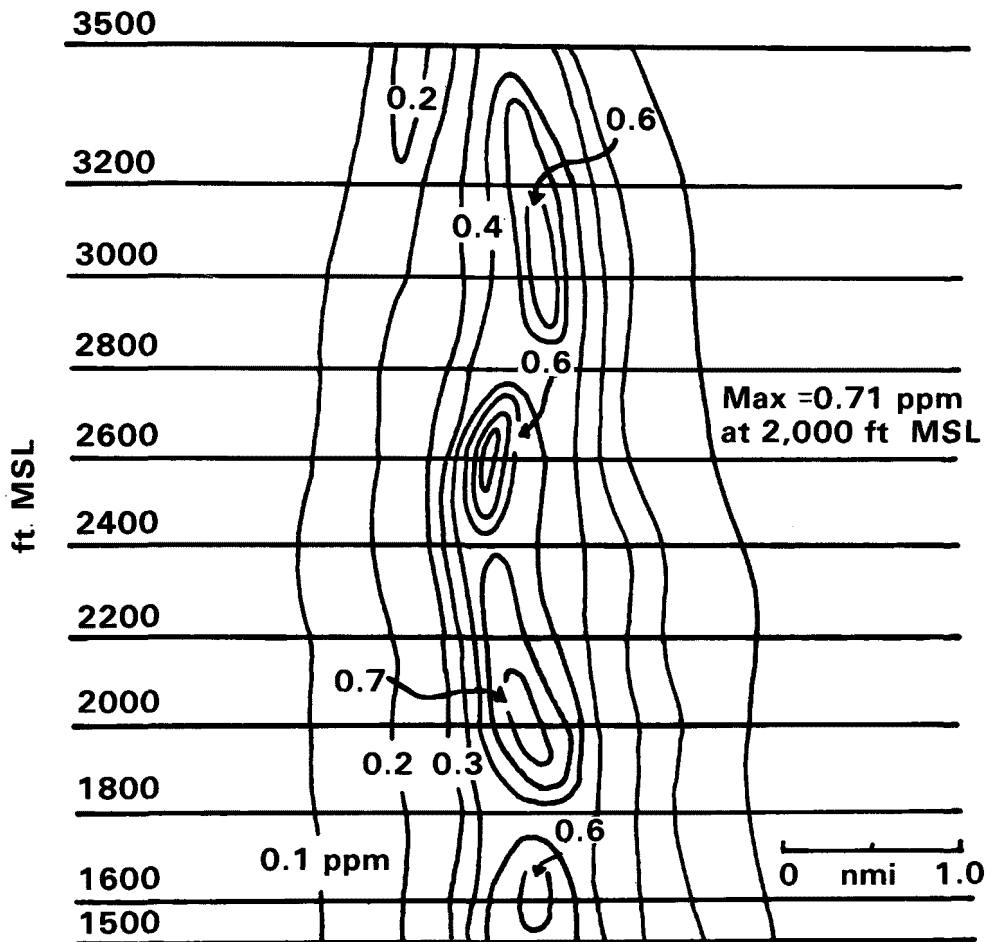
24

Figure A-9. Sulfur dioxide cross section of the Kammer and Mitchell plumes, 2 nmi west of the plants, 27 August 75, 1051-1131 EST.

TABLE A-4. PIBAL WIND INFORMATION, 27 AUGUST 75, 1010-1210 EST

Number of Observations	Height (ft MSL)	Direction (degrees mag)	Measured Speed (m/sec)	Speed (knots)
5	993	335	3.2	6
	1,307	18	1.4	3
	1,621	40	2.2	4
	1,935	42	2.7	5
	2,249	48	2.4	5
	2,563	62	3.0	6
	2,876	64	3.7	7
	3,190	62	4.1	8
	3,504	49	3.8	7
	3,818	48	3.6	7
	4,132	50	4.2	8
	4,446	47	5.2	10
	4,759	55	5.2	10
	5,073	57	4.6	9
	5,387	62	4.3	8
	5,701	52	5.5	11

TABLE A-5. KAMMER PLANT EMISSIONS AND PLUME DATA, 27 AUGUST 75, 1005-1318 EST

Volumetric Emission Rate (m^3/sec)	SO_2 Emission Rate (g/sec)	Distance (nmi)	Plume Width (ft)	Plume Height (ft MSL)	Centerline Concentration (ppm)
988	5,040	2	15,200	2,600	0.80
				2,000	
				1,600	
		6	Unknown	2,000	0.26

At 2 nmi, the Kammer plume was looping over the hills to the west of the plant. This is the reason for the three plume heights recorded by the helicopter. During the traverse at 1,500 ft MSL (as low as 50 ft AGL) a maximum concentration of 0.52 ppm SO_2 was recorded.

TABLE A-6.   MITCHELL PLANT EMISSIONS AND PLUME DATA, 27 AUGUST 75,
             1005-1318 EST

Volumetric Emission Rate (m³/sec)	SO_2 Emission Rate (g/sec)	Distance (nmi)	Plume Width (ft)	Plume Height (ft MSL)	Centerline Concentration SO_2 (ppm)
205	1,960	3	14,000	3,000	0.68
		6	Unknown	3,000	0.28

The plume widths were undeterminable at 6 nmi due to the low centerline
concentrations and the high ambient SO_2 levels.

28 AUGUST 1975, 0914-1217 EST

    The purpose of this flight was to investigate the horizontal gradients of
the Kammer plume. The plume was tracked for approximately 70 km by flying
through the plume at oblique angles. As quickly as possible after leaving the
plume, the helicopter changed course by 90° in order to reenter the plume. A
downstream track was completed at 2,200 ft MSL; this was followed by an upwind
track at 1,500 ft MSL, within 180 ft AGL. Both of these tracks have been
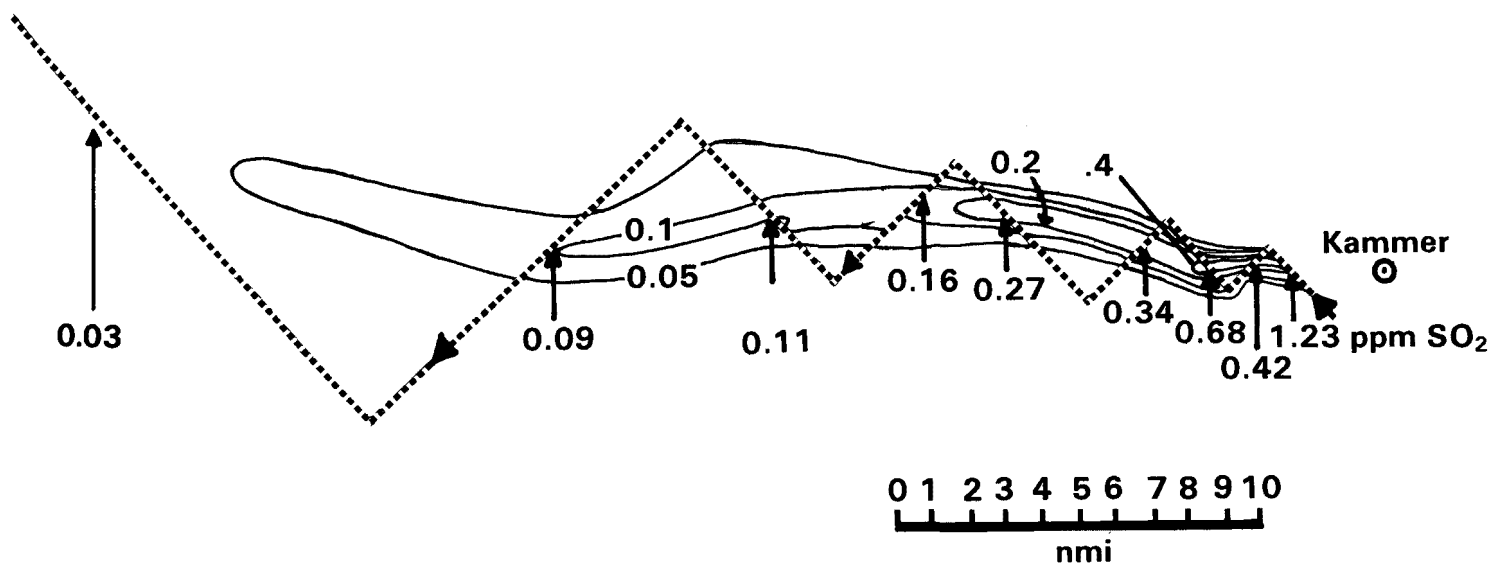plotted for SO_2 concentrations (Figures A-10 and A-11).

Figure A-10. Flight at 2,200 ft MSL along the plume of the Kammer power
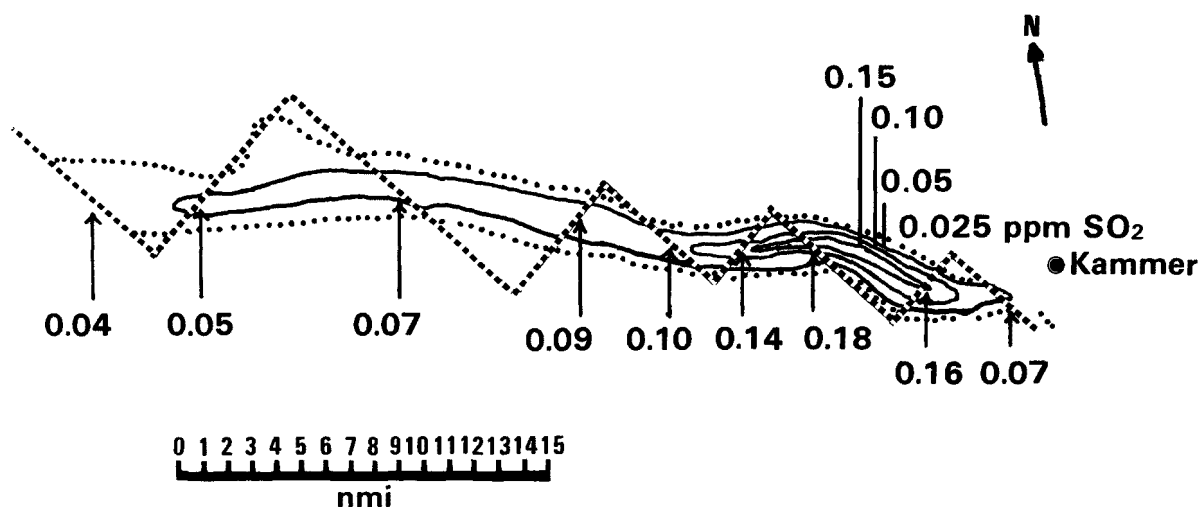station, 28 August 75, 1001-1046 EST.

Figure A-11. Flight at 1,500 ft MSL along the plume of the Kammer power station, 28 August 1975, 1050-1055 EST.
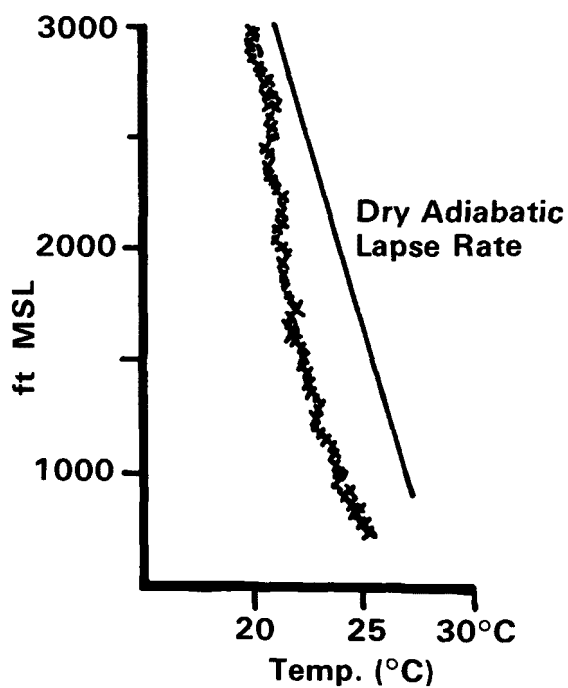

Figure A-12. Temperature sounding, 28 August 75, 0931-0946 EST.

Stable conditions were observed to 3,000 ft MSL at 0931 EST (See Figure A-12). At 1,500 ft, the area equal to or greater than 0.15 ppm SO_2 extended some 20 km from the plant. The highest concentration noted at 1,500 ft was 0.19 ppm SO_2. An attempt has been made to generalize these data. Observed centerline concentrations, $\chi(\mu g/m^3)$, were divided by source emission, Q(g/sec), and multiplied by wind speed, u(m/sec). The results were plotted against distance. (See Figure A-13). The graph for 1,500 ft appears to be a logical extension for taller stacks and greater distances of Turner's graphs for estimating ground level concentrations. The Mitchell plant was not in operation. The volumetric emission rate of the Kammer plant was 1,000 m³/sec and the SO_2 emission rate was 5,157 g/sec.

The average winds were as follows:

TABLE A-7. PIBAL WIND INFORMATION, 28 AUGUST 75, 1000-1100 EST

Number of Observations	Height (ft MSL)	Direction (degrees mag)	Speed (knots)	Measured Speed (m/sec)
3	993	38	7	3.3
	1,307	81	4	2.0
	1,621	88	9	4.5
	1,935	87	11	5.6
	2,249	95	15	7.9
	2,563	96	21	10.8
	2,876	96	19	9.9
	3,190	101	20	10.1
	3,504	106	17	8.8
	3,818	112	17	8.6
	4,132	116	11	6.1
	4,446	118	8	4.1
	4,759	107	8	4.1
	5,073	95	12	4.1

TABLE A-8. KAMMER PLANT EMISSIONS, 0914-1217 EST, 28 AUGUST 75

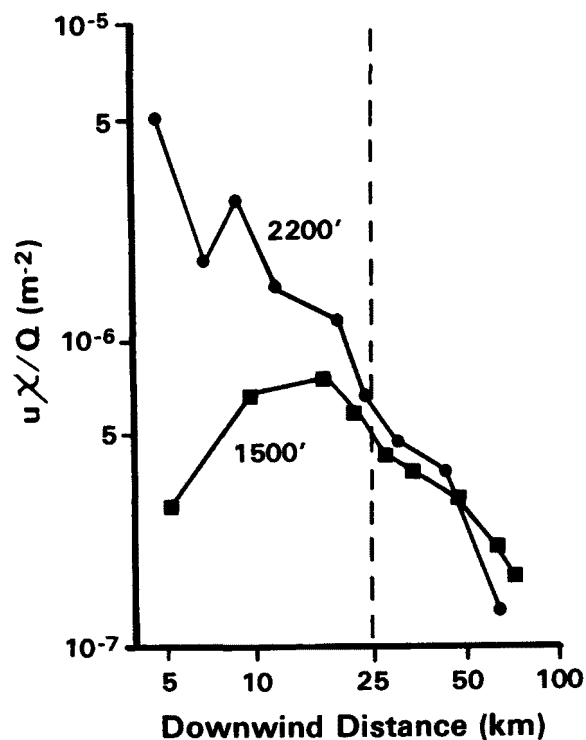| Volumetric Emission Rate (m³/sec)	Emission Rate for SO_2 (g/sec)
1,000	5,157

Figure A-13. Normalized centerline SO$_2$ concentration vs. downwind distance at 1,500 ft MSL and at 2,200 ft MSL of the Kammer plume, 28 August 75.
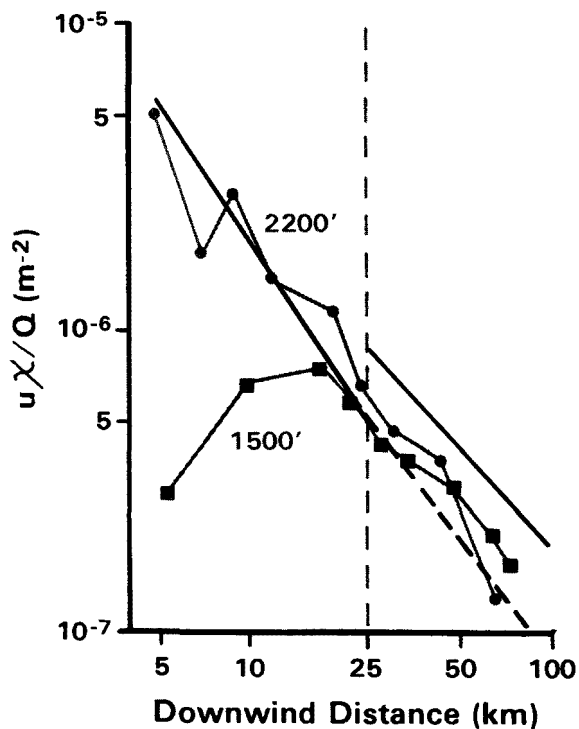

Figure A-14. Calculated normalized downwind SO$_2$ concentration using the methods of Turner (1969) compared to measured parameter, 28 August 75.

Referring to Figure 3 and recognizing an 8 m/sec wind speed and a stable atmosphere, the plume centerline is estimated to be very close to the 2,200 ft MSL altitude where the measurements were taken. The sounding (Figure A-12) suggests that the top of the mixing layer is at approximately 2,500 ft MSL. The method of Turner (1969) computes the distance downwind ($2x_L$) at which vertical mixing should be complete to be 29 km (15.7 nmi), applying Pasquill-Gifford stability category D. Therefore, at distances up to 29 km, the diffusion condition equation applies, and downwind of 29 km, the equation concerning vertical homogeneity should apply.

The data show excellent agreement for the determination of 29 km as the point where complete vertical mixing occurs. Figure A-13 indicates that mixing is complete at about 25 km, the point where the two curves assume the same slope. The concentration discrepancy between 2,200 ft data and 1,500 ft data at this point is not fully understood, but the measurements were not corrected for altitude (pressure) and this consideration can propagate such differences. With the exception of the 65 km data point for the 2,200 ft data set, the 1,500 ft and the 2,200 ft curves appear to parallel each other, downwind of 25 km, which indicates vertical homogeneity with probable measurement discrepancy.

Calculation of expected downwind concentration using the Turner (1960) diffusion condition equation shows excellent correlation to the measured data from 2,200 ft MSL out to 25 km (Figure A-14).

$$X = \frac{Q}{2\pi \, \sigma_y \, \sigma_z \, u}$$

where X = downwind concentration at distance x,
 Q = stack emission concentration,
 u = wind speed, and
 σ_y and σ_z = parameters from Turner (1969).

These data and the data from both flight levels downwind of 25 km agree very well to calculated estimates, although a slope change is evident and the data are beginning to depart the calculated curve.

At this point, Turner (1960) suggests an equation to apply during conditions of vertical homogeneity.

$$X = \frac{Q}{\sqrt{2\pi} \, \sigma_y \, Lu}$$

where X, Q, σ_y, and u are as above, and
 L = thickness of the mixing layer.

This calculation yields an approximation of downwind concentration with a slope which agrees nicely with the measured data, but there is a noticeable offset toward overestimation of downwind concentration (Figure A-14). In this

31

case, it appears that the best estimate of downwind concentration is derived using the diffusion equation exclusively even though vertical dispersion has apparently ceased.

28 AUGUST 1975, 1430-1655 EST

The purpose of this flight was to construct a cross section of the Kammer power plant plume at 2.5 nmi. The Mitchell plant was not in operation. Near neutral conditions were observed. It is unknown whether the plume was oscillating between 2,540 and 5,500 ft MSL, whether the plumes associated with the two stacks had maintained their identities, or whether pollution from another source was measured. There was, however, a definite core at 4,000 ft MSL.
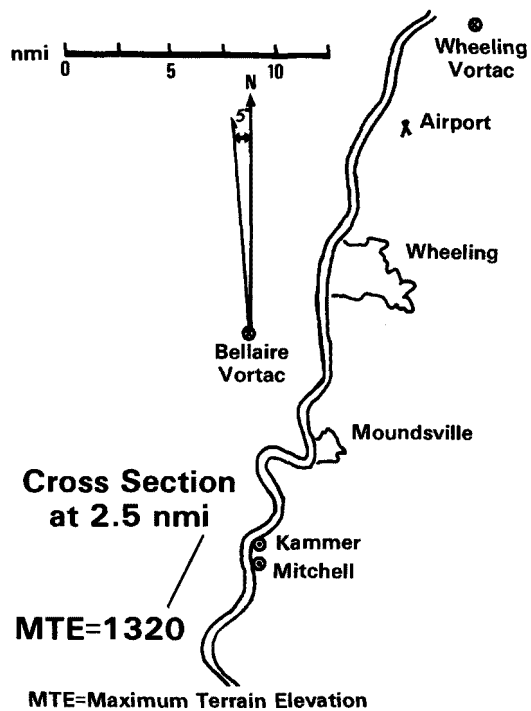
Figure A-15. Helicopter flight, 28 August 75, second flight.
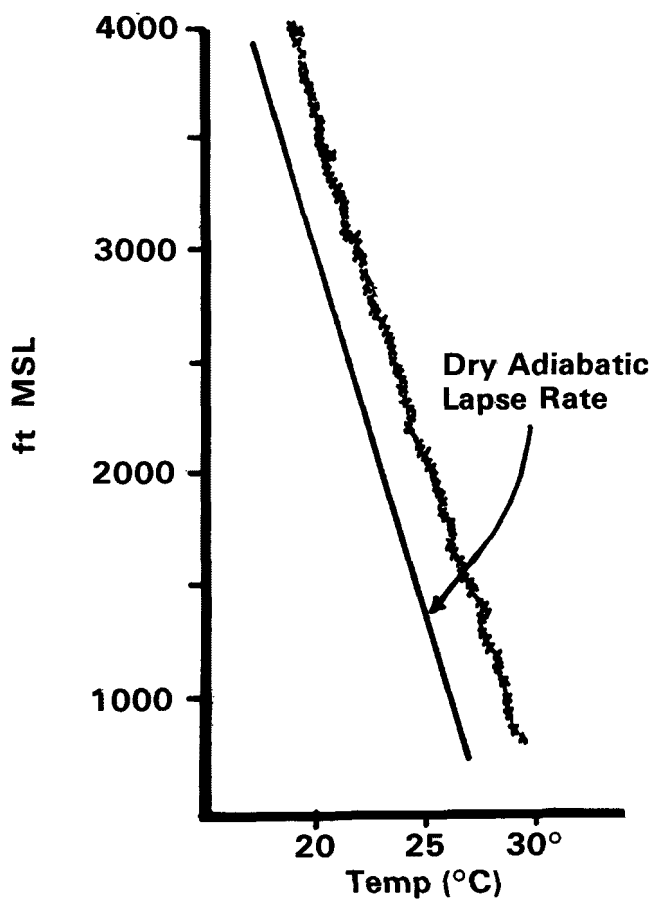
Figure A-16. Temperature sounding, 28 August 75, 1438-1449 EST.

33
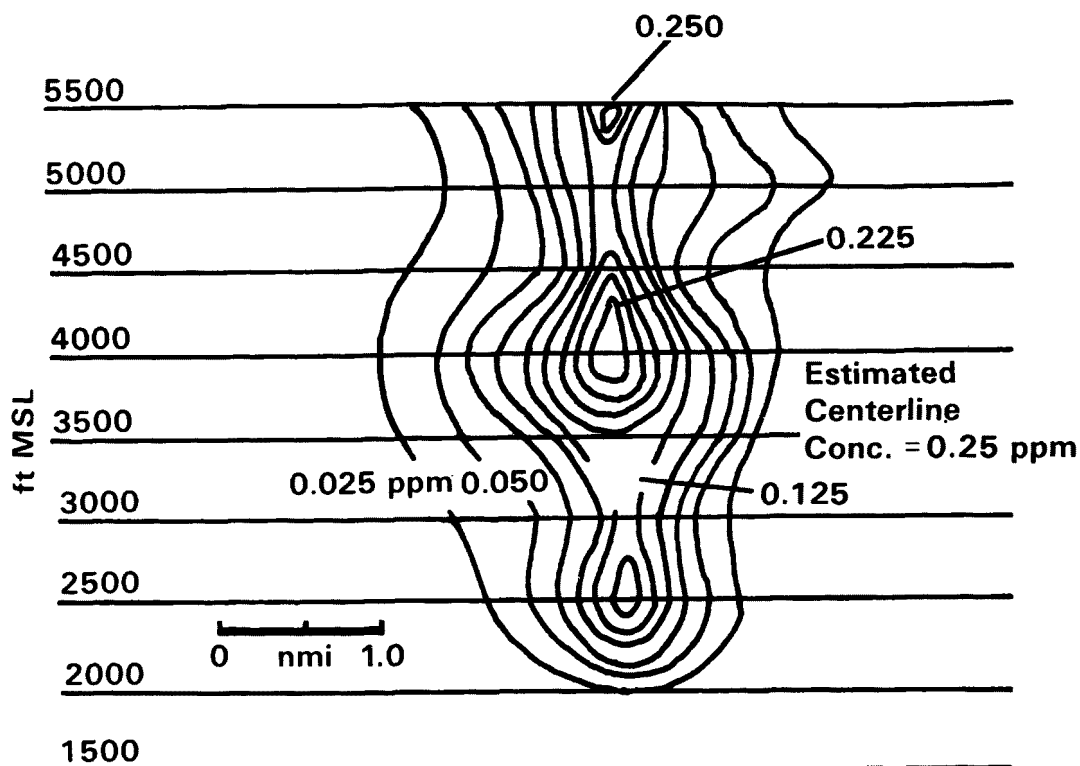
Figure A-17. SO$_2$ cross section of the Kammer plume at 2.5 nmi west of the plant, 28 August 75, 1457-1550 EST.

TABLE A-9. PIBAL WIND INFORMATION, 28 AUGUST 75, 1430-1600 EST

Number of Observations	Height (ft MSL)	Direction (degrees mag)	Measured Speed (m/sec)	Speed (knots)
4	993	96	4.2	8
	1,307	107	3.5	7
	1,621	104	4.9	10
	1,935	106	5.3	10
	2,249	105	5.2	10
	2,563	101	4.2	8
	2,876	107	3.7	7
	3,190	103	4.3	8
	3,504	114	3.7	7
	3,818	122	4.3	8
	4,132	119	4.5	9
	4,446	120	3.1	6
	4,759	121	4.3	8
	5,073	120	4.9	10
	5,387	129	4.7	9

34

TABLE A-10. KAMMER PLANT EMISSIONS AND PLUME DATA, 28 AUGUST 75, 1430-1655 EST

Volumetric Emission Rate (m^3/sec)	SO$_2$ Emission Rate (g/sec)	Distance (nmi)	Plume Width (ft)	Plume Height (ft MSL)	Centerline Concentration (ppm)
1,020	5,160	2.5	18,240	4,000	0.25

29 AUGUST 1975, 0750-1107 EST

This flight provided information which was used to construct three cross sections of the Kammer plume, two at 2 nmi and one at 4 nmi. Two cross sections were developed at 2 nmi because these cross sections were to be used as a basis for calculations of the flux of SO$_2$ from the Kammer plant (See Appendix E). Stable conditions were observed to 3,200 ft MSL. The Mitchell plant was not in operation. Only one stack of the Kammer plume was operating.
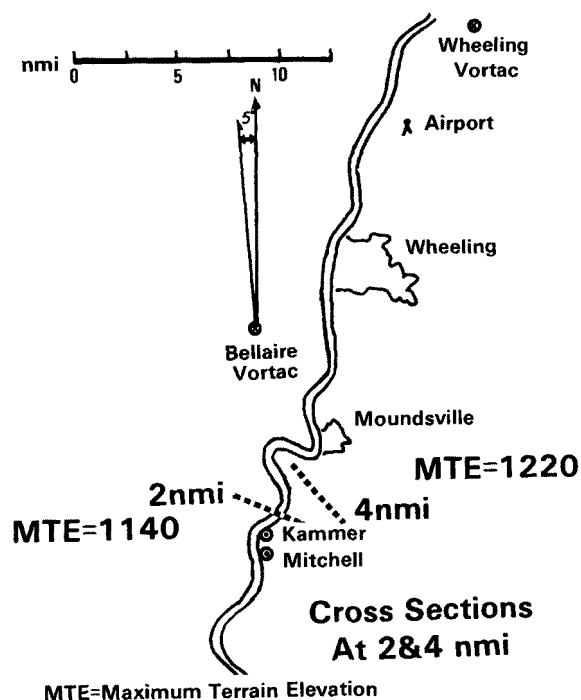
Figure A-18. Helicopter flight, 29 August 75.
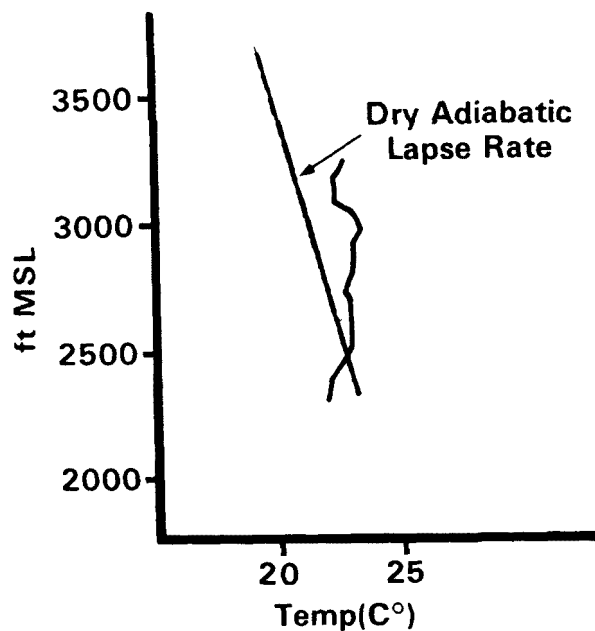
Figure A-19. Temperature sounding, 29 August 75, 0825-0828 EST.

2750 ft MSL

Estimated Centerline Conc. = 1.00 ppm at 2,200 MSL
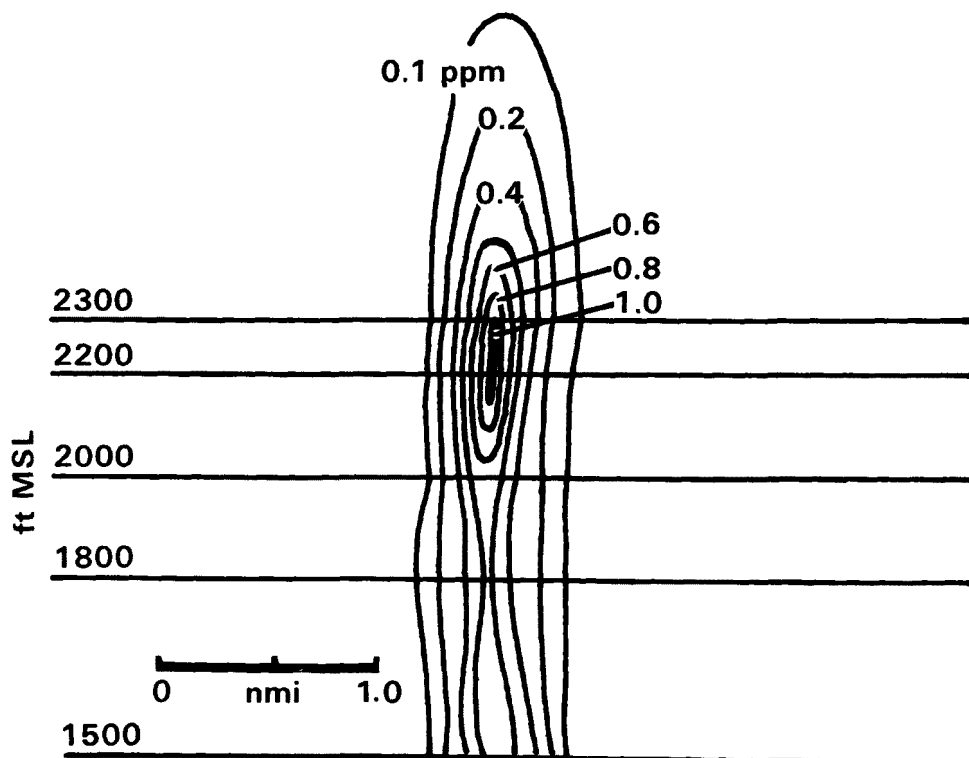
Figure A-20. Sulfur dioxide cross section of the Kammer plume at 2 nmi northeast of plant, 29 August 75, 0855-0913 EST.

36
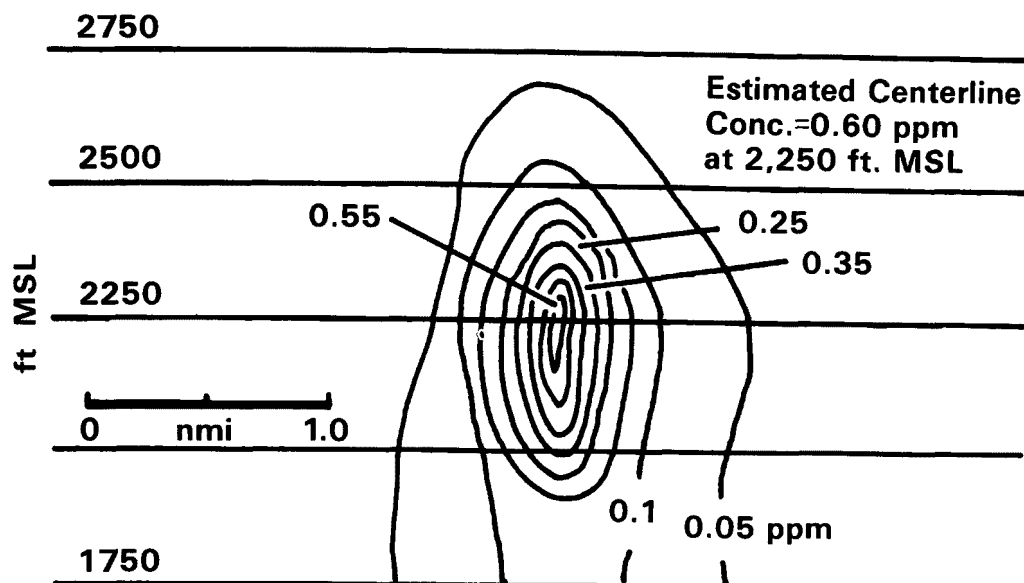
Figure A-21. Sulfur dioxide cross section of Kammer at 4 nmi northeast of plant, 29 August 75, 0923-0943 EST.
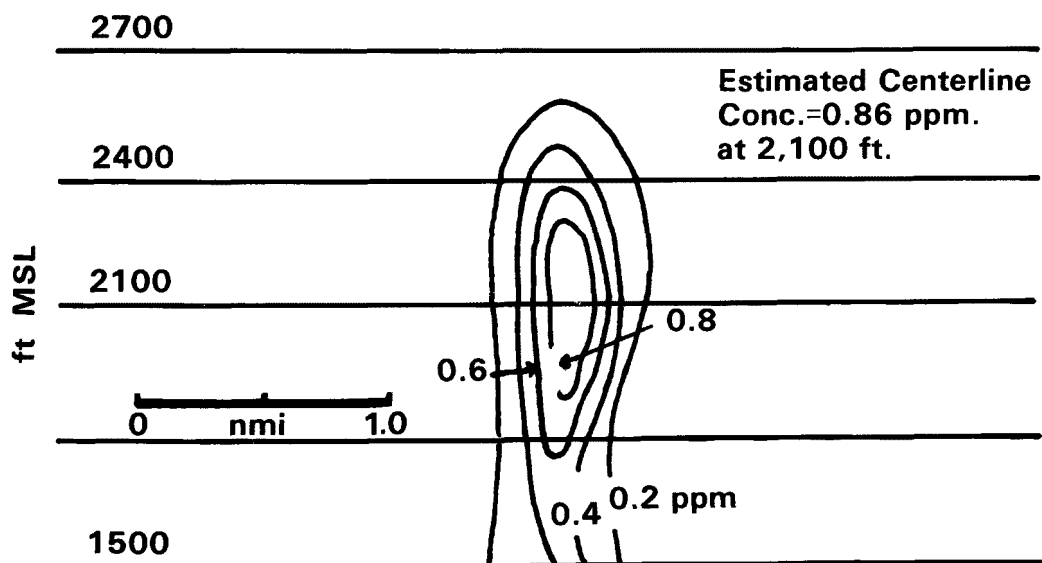
Figure A-22. Sulfur dioxide cross section of Kammer at 2 nmi northeast of plant, 29 August 75, 1022-1040 EST.

TABLE A-11. PIBAL WIND DATA, 29 AUGUST 75, 0800-1130 EST

Number of Observations	Height (ft MSL)	Direction (degrees mag)	Measured Speed (m/sec)	Speed (knots)
8	993	197	3.3	6
	1,307	198	3.6	7
	1,621	201	4.6	9
	1,935	210	7.2	14
	2,249	223	8.8	17
	2,563	223	10.5	21
	2,876	243	11.3	22
	3,190	251	11.7	23
	3,504	224	11.5	22
	3,818	257	12.4	24
	4,132	261	11.8	23

TABLE A-12. KAMMER PLANT EMISSIONS AND PLUME DATA, 29 AUGUST 75, 0750-1107 EST

| Volumetric Emission Rate (m^3/sec)	SO_2 Emission Rate (g/sec)	Distance (nmi)	Plume Width (ft)	Plume Height (ft MSL)	Centerline Concentration (ppm)
675	3,830	2	4,560	2,200	0.99
		4	7,095	2,250	0.70
		2	5,570	2,100	0.86

After the cross sections were completed, it was noted that the plume was beginning to impact on a hill approximately 3.7 nmi north of the plant. The helicopter was flown as close to the hill as possible. A maximum reading of 0.15 ppm SO_2 was recorded. An additional traverse was made at approximately 2 nmi from the plant and as close to the ground as possible (approximately 200 ft AGL). A maximum concentration of 0.67 ppm was noted. From the previous measurements of the centerline concentration at this distance, it is concluded that the centerline was near the surface at this time.

A cross section of the Kammer plume was constructed at approximately 3.5 nmi east of the plant. Near neutral conditions coupled with flow normal to the hills east of the plant were causing the plume to impact at the surface at various distances from the plant. While constructing the cross section at 3.5 nmi, a traverse of the plume at 1,750 ft MSL (140-740 ft AGL), a maximum SO_2 concentration of 0.46 ppm was noted. A series of six traverses made at 1,700 ft MSL and approximately 2.5 nmi east of the plant recorded SO_2 concentrations up to 0.16 ppm. The average maximum concentration was 0.08 ppm with a standard deviation of 0.04 ppm. These six traverses were over the same line. The standard deviation is a good indication that the plume was indeed looping at 1,700 ft MSL. During additional passes, one at approximately 400 ft above the point of plume impact and 1.5 nmi from the plant and another at about 300 ft AGL and 1 nmi from the plant, maximum SO_2 concentrations of 0.45 and 1.2 ppm were measured. An additional series of five passes was made approximately 3.5 nmi from the plant at an altitude of 1,700 ft MSL. Values as high as 1.6 ppm were recorded. The average peak value was 0.46 ppm and the standard deviation was 0.65 ppm. One traverse was made at 3.5 nmi from the plant at approximately 1,650 ft MSL, as low as safety factors would allow, and a reading of 1.02 ppm SO_2 was obtained.
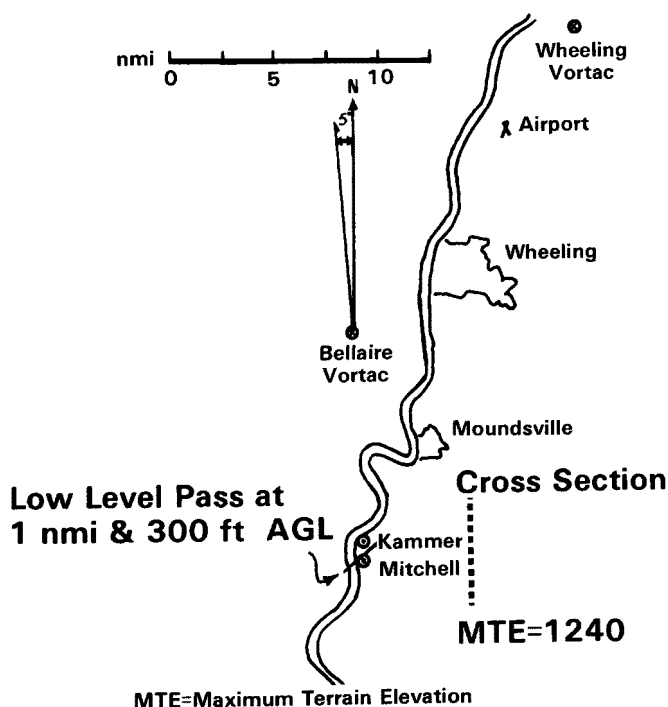
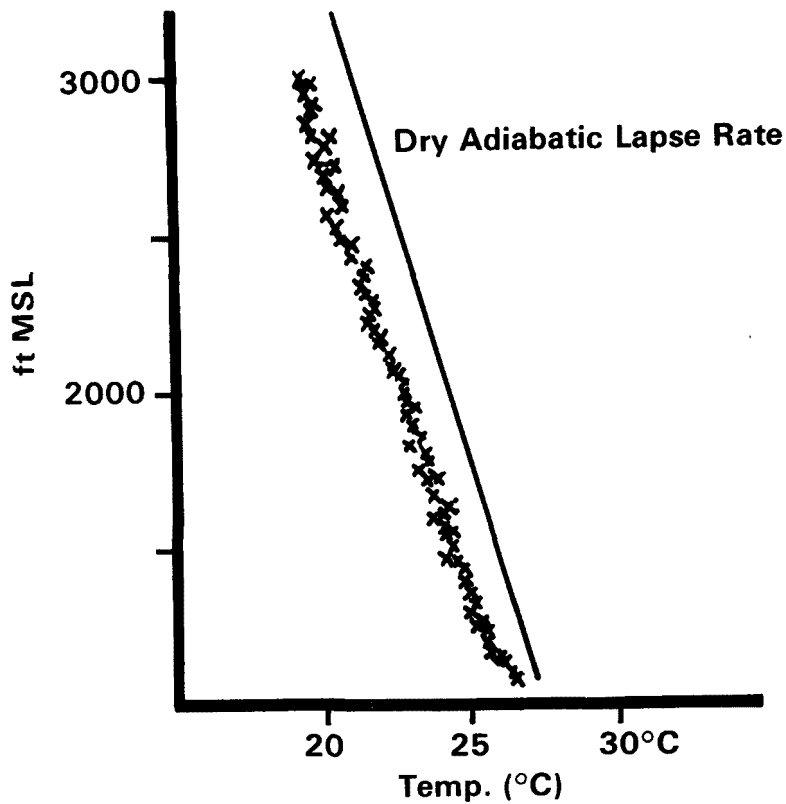Figure A-23. Helicopter flight, 2 September 75.

Figure A-24. Temperature sounding, 2 September 75, 1050-1058 EST.
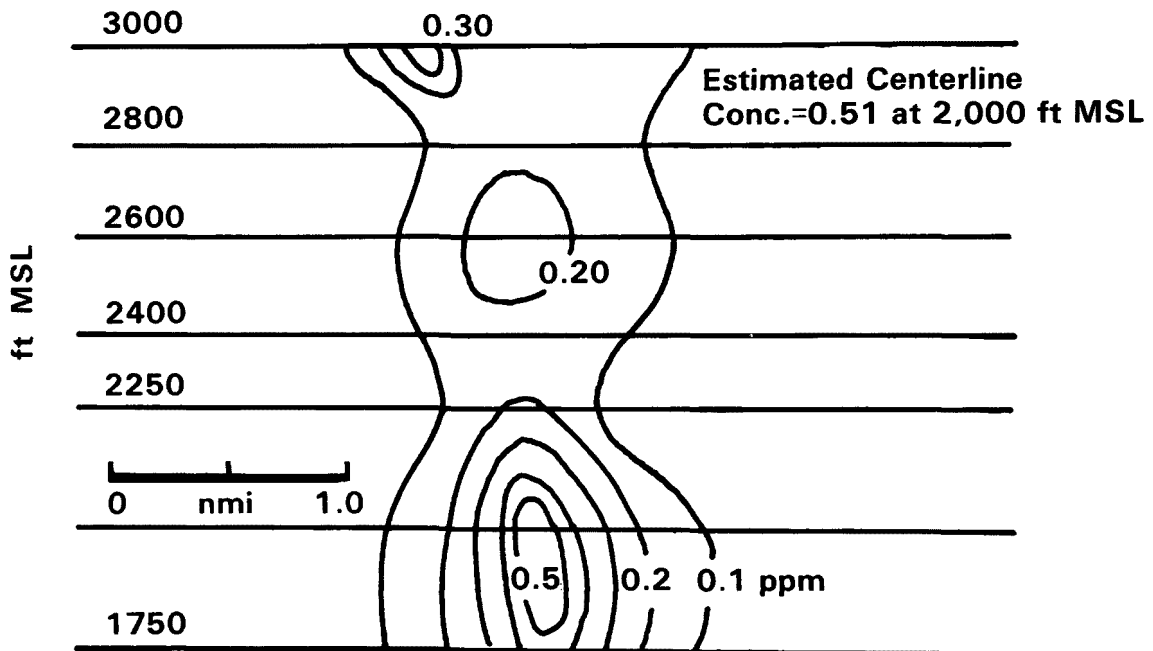
Figure A-25. Sulfur dioxide cross sections of Kammer, 2 nmi east of plant, 2 September 75, 1115-1151 EST.

40

TABLE A-13. PIBAL WIND INFORMATION, 2 SEPTEMBER 75, 1030-1300 EST

Number of Observations	Height (ft MSL)	Direction (degrees mag)	Measured Speed (m/sec)	Speed (knots)
6	993	301	3.3	6
	1,307	301	3.5	7
	1,621	292	3.5	7
	1,935	291	4.6	9
	2,249	284	3.4	7
	2,562	299	3.3	6
	2,876	289	3.8	7
	3,190	296	4.2	8
	3,504	328	5.0	10
	3,818	305	4.6	9
	4,132	331	4.3	8
	4,446	300	4.6	9
	4,759	348	4.3	8

TABLE A-14. KAMMER PLANT EMISSIONS AND PLUME DATA, 2 SEPTEMBER 75
            1024-1320 EST

Volumetric Emission Rate (m^3/sec)	SO_2 Emission Rate (g/sec)	Distance (nmi)	Plume Width (ft)	Plume Height (ft MSL)	SO_2 Centerline Concentration (ppm)
935	4,550	3.5	5.070	2,000	0.51

3 SEPTEMBER 1975, 0919-1234 EST

The purpose of this flight was to measure the Kammer and Mitchell plumes at 3, 5 and 10 nmi. Stable conditions were observed at the begining of the mission. The two Kammer plumes maintained their identity to 10 nmi. Three maxima were found at this distance. No pibal wind information was available. The following are winds derived from helicopter wind drift measurements (See Appendix C).

41
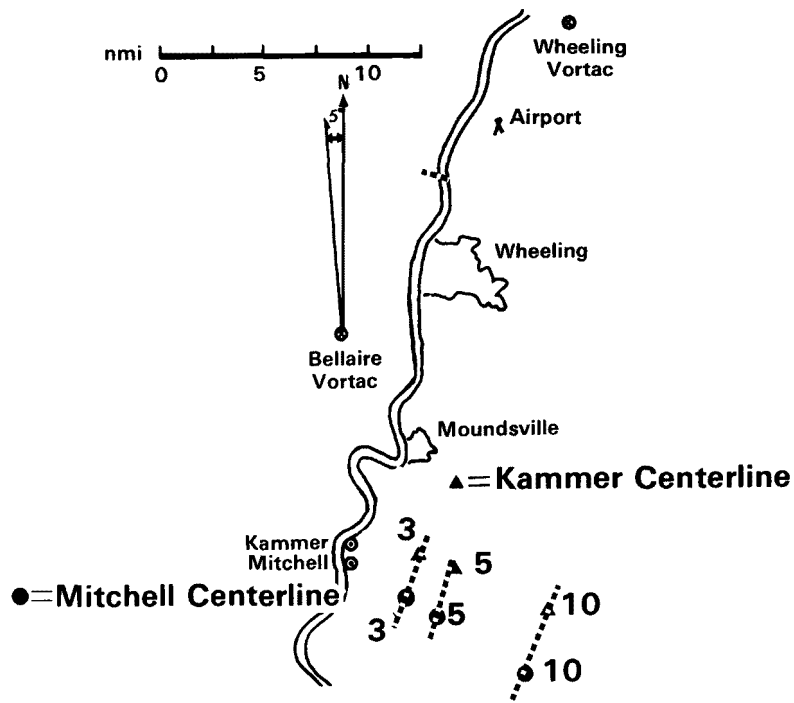
Figure A-26. Helicopter flight, 3 September 75, first flight.
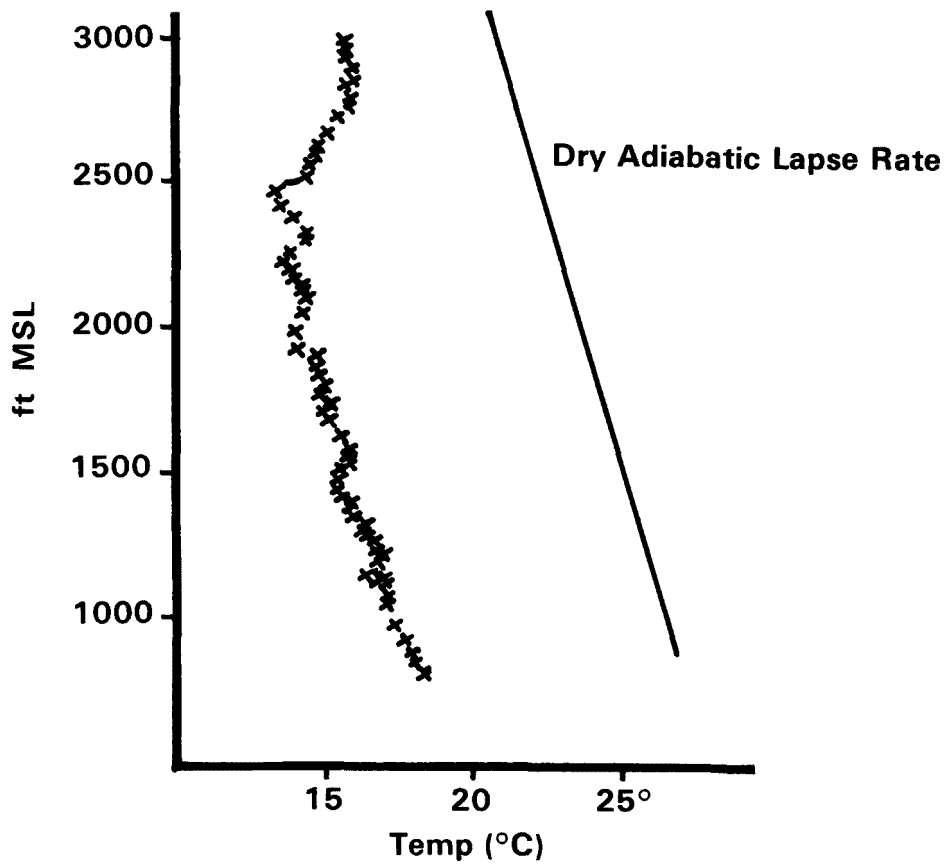
Figure A-27. Temperature sounding, 3 September 75, 0938-0944 EST.

TABLE A-15. HELICOPTER WIND MEASUREMENTS

Direction (Degrees mag)	Speed (knots)	Altitude (ft MSL)
257	6	2,260
279	8	1,900

TABLE A-16. KAMMER PLANT EMISSIONS AND PLUME DATA, 3 SEPTEMBER 75, 0919-1234 EST

Volumetric Emission Rate (m^3/sec)	SO_2 Emission Rate (g/sec)	Distance (nmi)	Plume Width (ft)	Plume Height (ft MSL)	SO_2 Centerline Concentration (ppm)
1,000	4,490	3	30,130	2,750	5.05
		3	9,630	3,000	3.21
		5	10,640	3,000	3.52
		5	10,640	2,850	3.12
		10	13,680	3,100	1.09
		10	12,670	2,850	0.86

TABLE A-17. MITCHELL PLANT EMISSIONS AND PLUME DATA, 3 SEPTEMBER 75, 0919-1234 EST

Volumetric Emission Rate (m^3/sec)	SO_2 Emission Rate (g/sec)	Distance (nmi)	Plume Width (ft)	Plume Height (ft MSL)	SO_2 Centerline Concentration (ppm)
255	5,210	3	4,560	3,500	
		5	14,690	3,200	2.48
		10	15,700	3,100	1.62

The plume was held by an inversion at 0943 EST; by 1213 EST the inversion had dissipated. This may explain why the plume height at 10 nmi, which was measured first, was lower than the other plume heights.

3 SEPTEMBER 1975, 1350-1531 EST

On the afternoon flight, near-neutral conditions were observed. A visual estimate of both the Kammer and Mitchell initial plume heights was made as 3,900 ft MSL. In spite of this high initial plume rise, looping conditions caused the Kammer plume to hit the ground further downwind. A series of low level plume traverses was made east of the plant. The most significant of these was a series of eight passes between 1449 and 1507 EST at 1,500 ft MSL, within 380 ft AGL. Values as high as 0.80 ppm SO_2 were recorded, while the mean maximum recorded for the eight passes was 0.50 ppm SO_2.

In the afternoon, the LIDAR aircraft made flights along selected radials of the Clarksburg, Ellwood City, and Wheeling VORTACs. Each LIDAR return signal was given a relative value compared with other returns dependent upon the integrated value of the total return within the mixing layer and the vertical baseline. These relative values have been plotted along the flight paths and are presented as examples of the log range measurements of relative particulate distribution along these tracks. No pibal wind information is available.
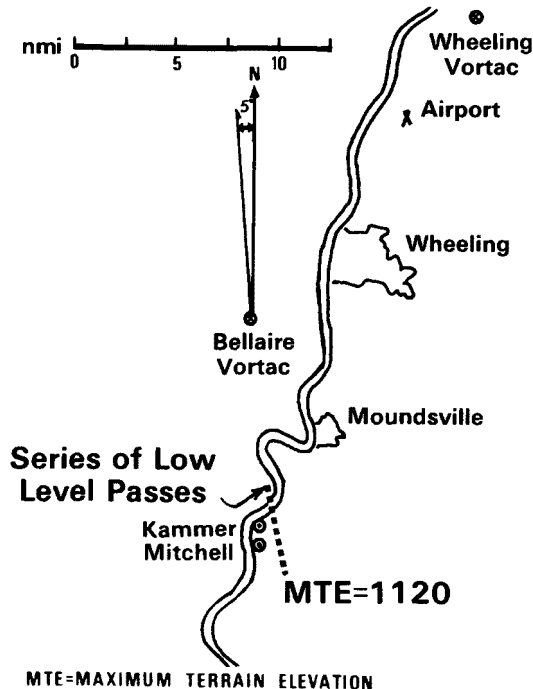
Figure A-28. Helicopter flight, 3 September 75, second flight.
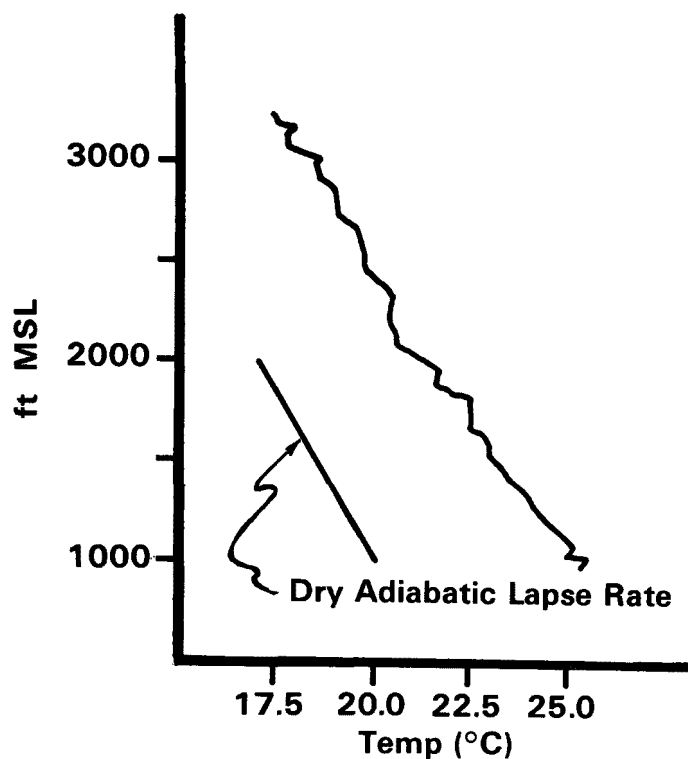
Figure A-29. Temperature sounding, 1418-1422, 3 September 75.
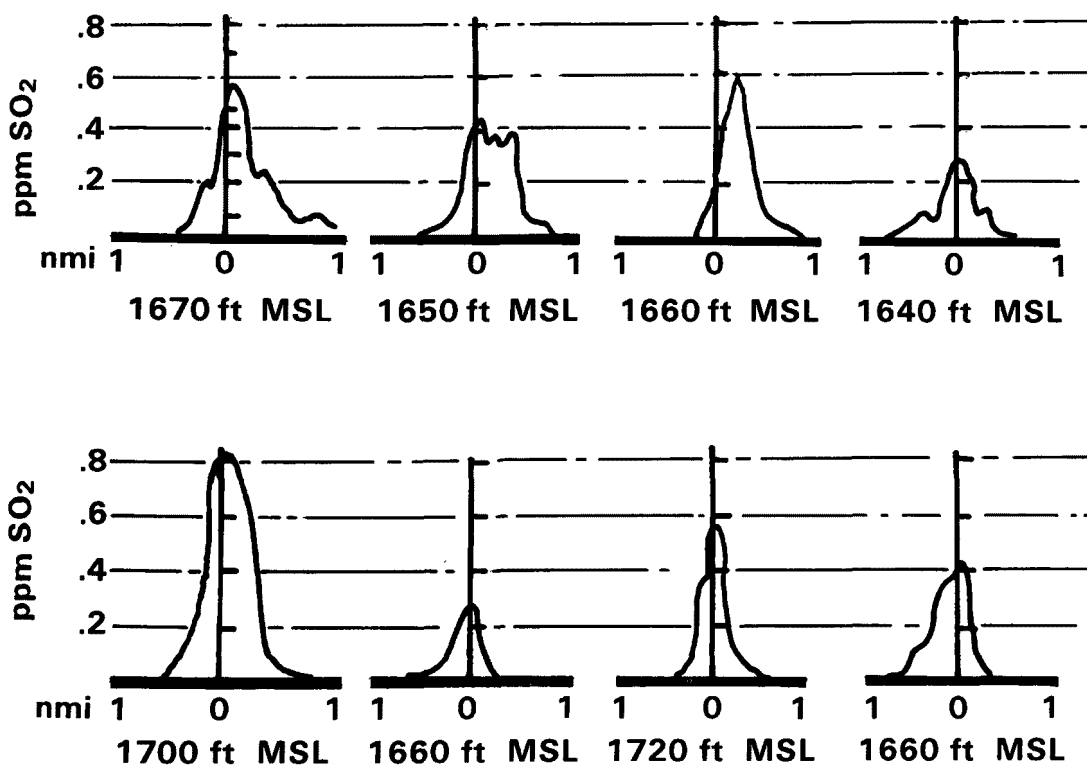
Figure A-30. Series of low-level measurements of the Kammer plume, 3 September 75.

Steubenville

Wheeling
Vortac

No Data

No Data

Wheeling

Bellaire
Vortac

No Data
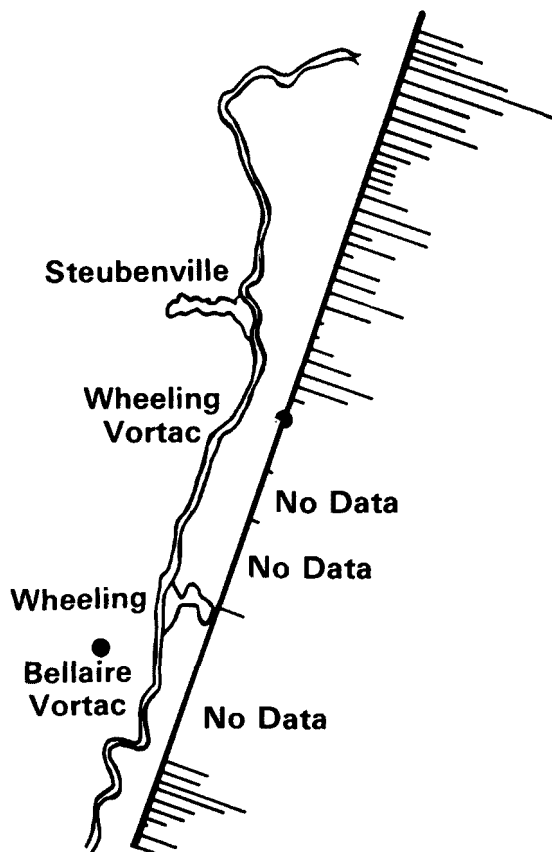
Figure A-31. LIDAR flight along
019°/199° radial of Wheeling VORTAC,
1352-1419 EST, 5 September 75.

Ellwood City

Ellwood City
Vortac

Steubenville

Pittsburgh

No Data
Washington

Wheeling

No Data

Bellaire
Vortac
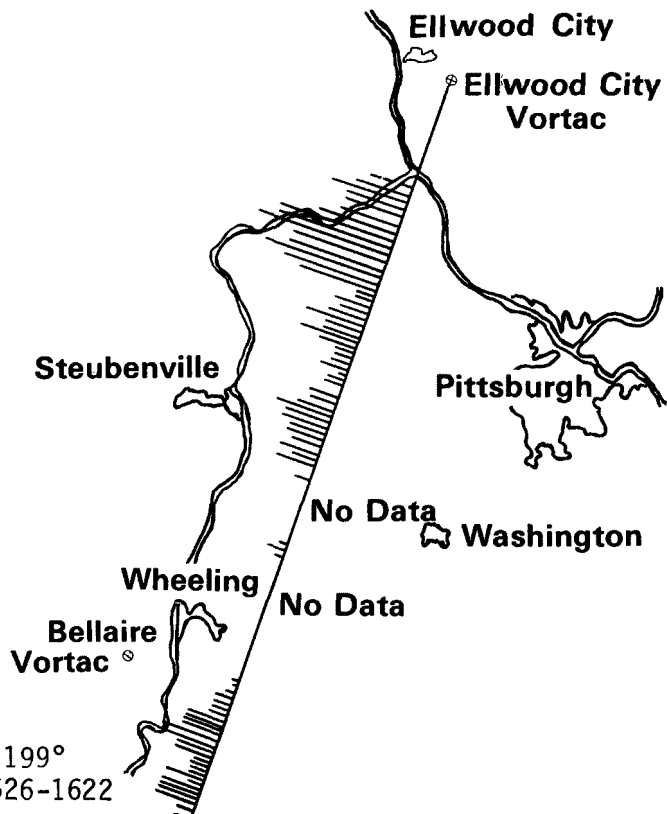
Figure A-32. LIDAR flight along 199°
radial of Ellwood City VORTAC, 1526-1622
EST, 3 September 75.

46
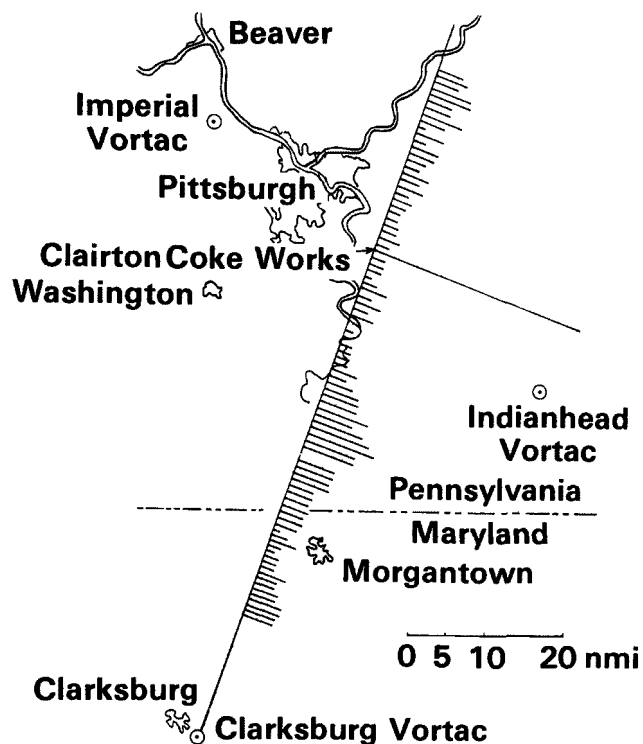
Figure A-33. LIDAR flight along 019° radial of Clarksburg
VORTAC, 1626-1642 EST, 3 September 75.

TABLE A-18. PLANT EMISSIONS DATA, 3 SEPTEMBER 75, 1350-1531

Plant	Volumetric Emission Rate (m^3/sec)	SO_2 Emission Rate (g/sec)
Mitchell	260	5,208
Kammer	1,030	4,448

A cross section of the Mitchell and Kammer plumes was constructed under near neutral conditions at approximately 6 nmi south southeast of the plants. Traverses of the plume were made 1,600 to 4,000 ft MSL where low visibility prevented completion of the upper portion of the cross section. The traverse at 1,600 ft MSL (300-920 ft AGL) measured a maximum value of 0.11 ppm SO_2. After the cross section was completed, it was noted that apparent high levels of pollutants were pooled in the sheltered valley associated with Fish Creek which empties into the Ohio River south of the plants. The source of the pollutants was not determined. The helicopter entered the valley approximately 7 nmi upstream and flew well below the ridge line to the Ohio River. Values as high as 0.66 ppm SO_2 were observed. Pibal wind data were not obtained. However, the helicopter did determine the winds based on drift information.
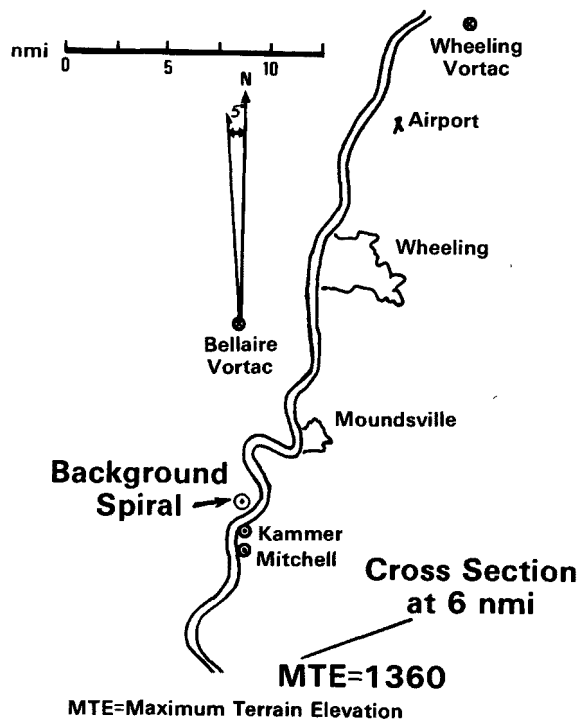
Figure A-34. Helicopter flight, 4 September 75.
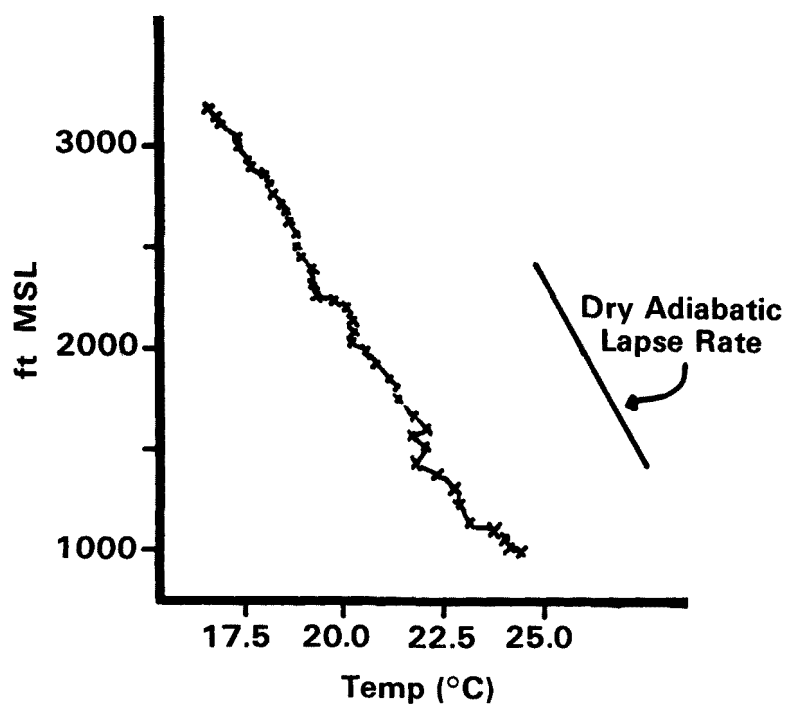
Figure A-35. Temperature soundings, 4 September 75, 1238-1244 EST.

Figure A-36. Temperature soundings, 4 September 75, 1402-1404 EST.
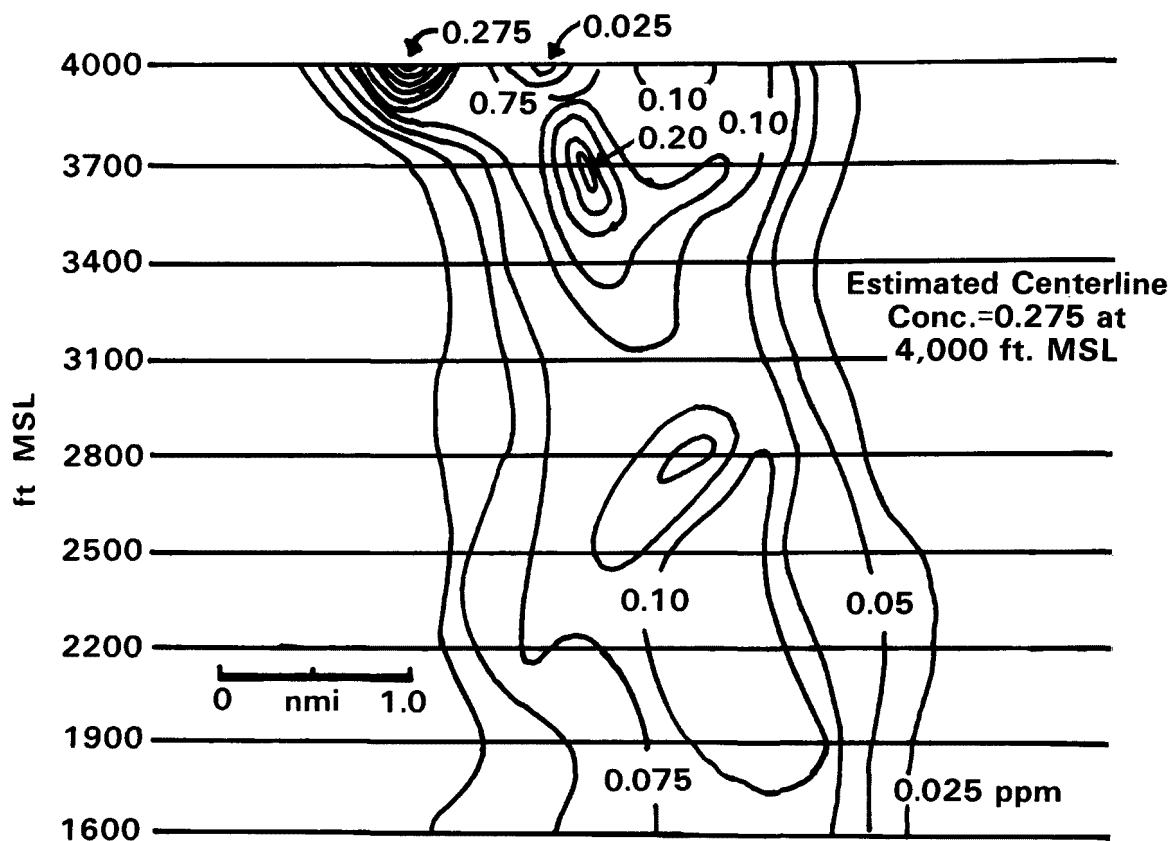
Figure A-37. Sulfur dioxide cross section of Mitchell and Kammer
at 6 nmi southeast of plants, 4 September 75, 1307-1349 EST.
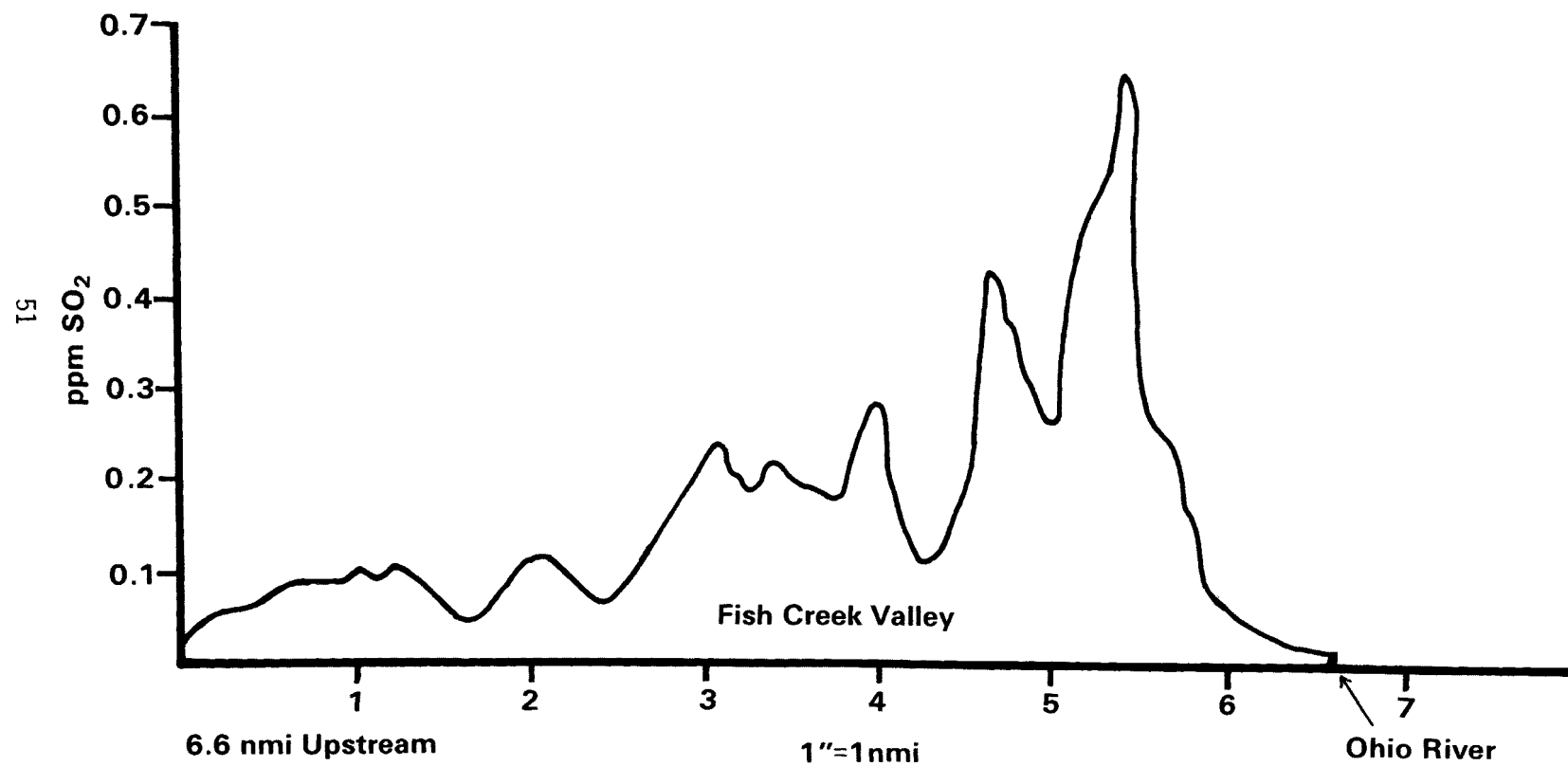
Figure A-38. Low-level flight down Fish Creek Valley, 4 September 75, 1353-1358 EST.

Altitude (ft MSL)	Direction (Degrees mag)	Speed (knots)
2,000	345	9
2,200	328	9

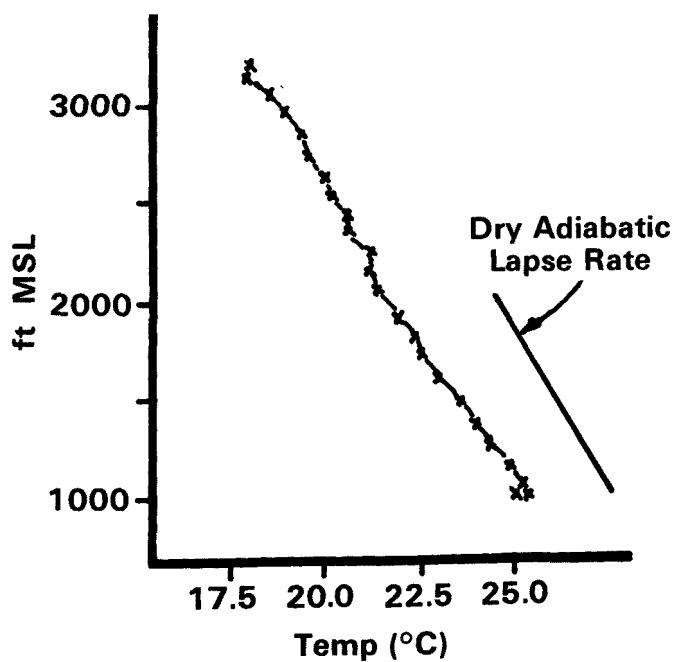TABLE A-20. KAMMER PLANT EMISSIONS AND PLUME DATA, 4 SEPTEMBER 75, 1215-1444 EST

Volumetric Emission Rate (m^3/sec)	SO_2 Emission Rate (g/sec)	Distance (nmi)	Plume Width (ft)	Plume Height (ft MSL)	SO_2 Centerline Concentration (ppm)
640	3,720	6	18,750	2,200	0.19
		6	18,750	3,700	0.21

It is unknown whether the Kammer plume was looping between these two levels or if the plumes from the two stacks maintained their identities.

5 SEPTEMBER 1975, 0903-1245 EST

This flight was a dual helicopter-LIDAR mission. Cross sections were constructed along the 206° and 213° radials of the Bellaire VORTAC. At the start of the mission, there was a temperature inversion based at 2,200 ft MSL. This had burned off by 1230 EST. Figure A-42 is a helicopter cross section of the SO_2 emissions of the Kammer, Mitchell and possibly the Burger power plant plume which is north of the Kammer plant. Approximately 1 hour was taken to collect the information. Figure A-43 is a cross section developed from LIDAR data along the same radial. Approximately 3 minutes was required to collect these data. The units assigned to the LIDAR data are once again relative. The analogs of the LIDAR returns were plotted on rectilinear graph paper with the vertical scale representing height and the horizontal scale representing relative return signal strength at a given level. A series of LIDAR soundings was plotted along the flight of the aircraft and isopleths of equal relative values were drawn. Major features are in close agreement. Both cross sections were drawn to the same scale. There is a possibility that the left hand maximum at 2,900 ft MSL or Figure A-42 was missed due to the 25-second pulse repetition rate of the LIDAR system.

An attempt was made to jointly construct a second cross section along the 213° radial of the Bellaire VORTAC. Formation of clouds below the LIDAR aircraft prevented the accomplishment of its mission. Figure A-45 is the cross section developed by the helicopter.
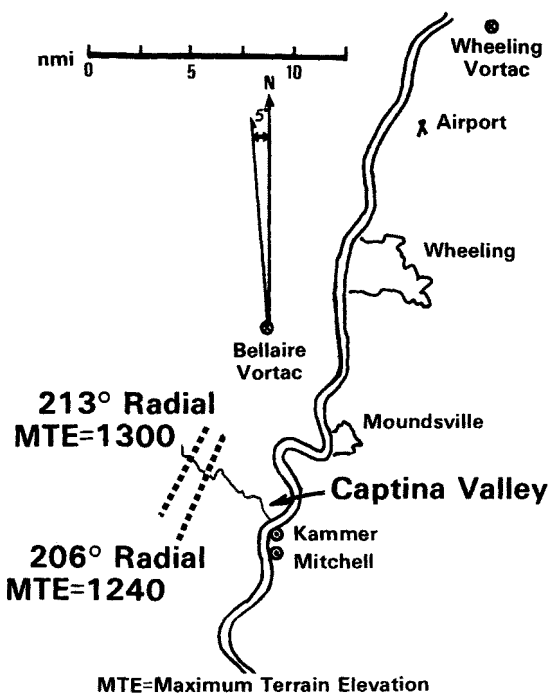
Figure A-39. Helicopter flight,
5 September 75.
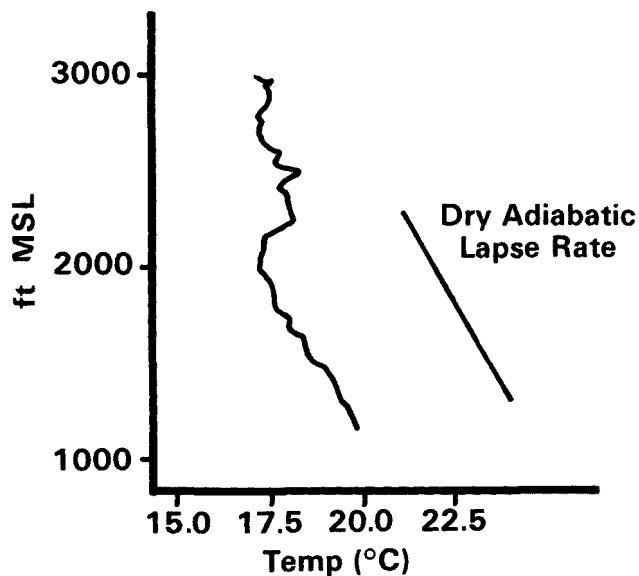
Figure A-40. Temperature sounding,
5 September 75, 0925-0930 EST.
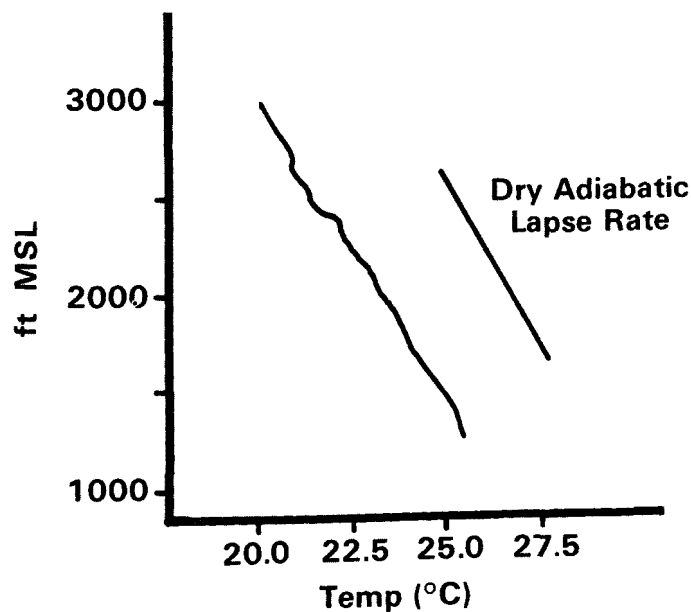
Figure A-41. Temperature sounding, 5 September 75,
1227-1231 EST.
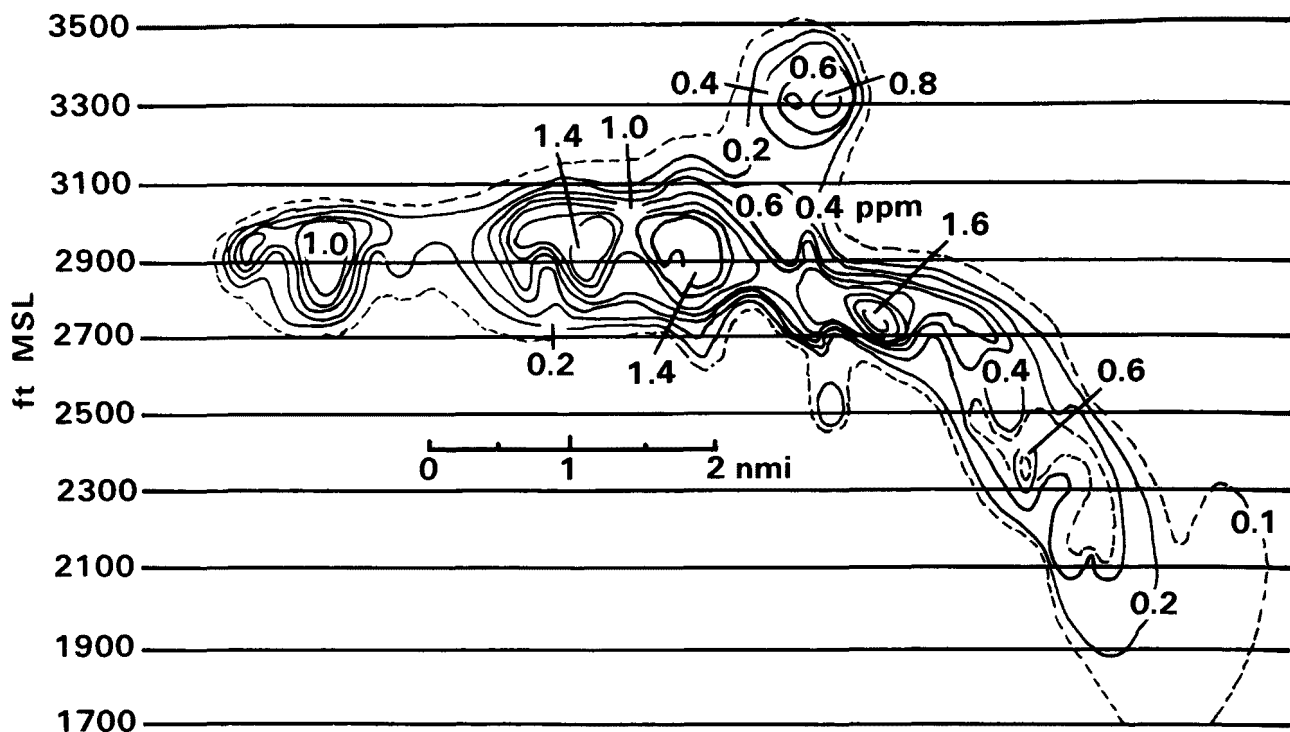
Figure A-42. SO$_2$ cross section of Kammer and Mitchell plumes along the 206° radial of the Bellaire VORTAC, 0936-1040 EST, 5 September 75.
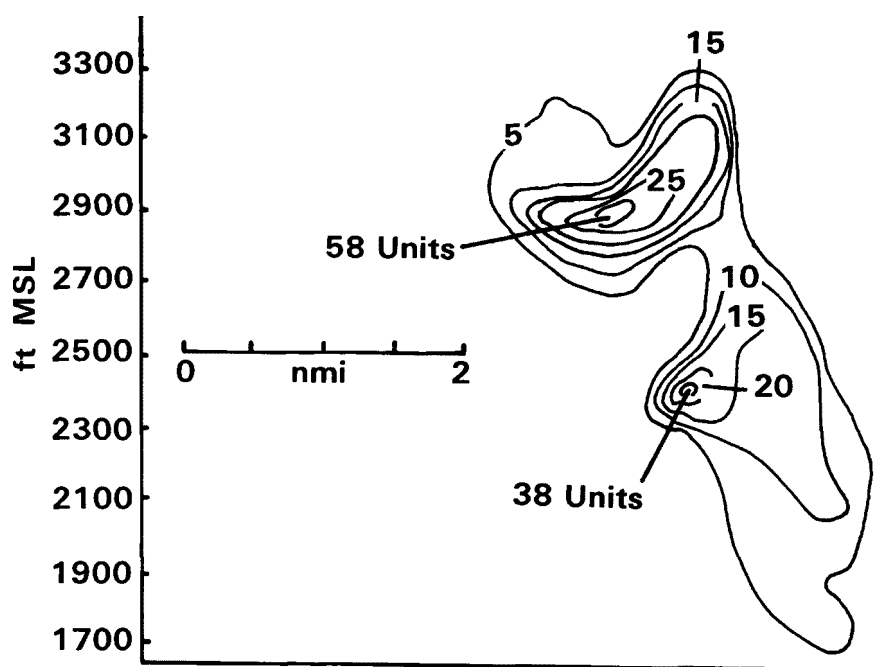
Figure A-43. LIDAR cross section of Kammer and Mitchell plumes on a radial of 213° of the Bellaire VORTAC, approximately 7.5 nmi northwest of the plants, 1030 EST, 5 September 75.
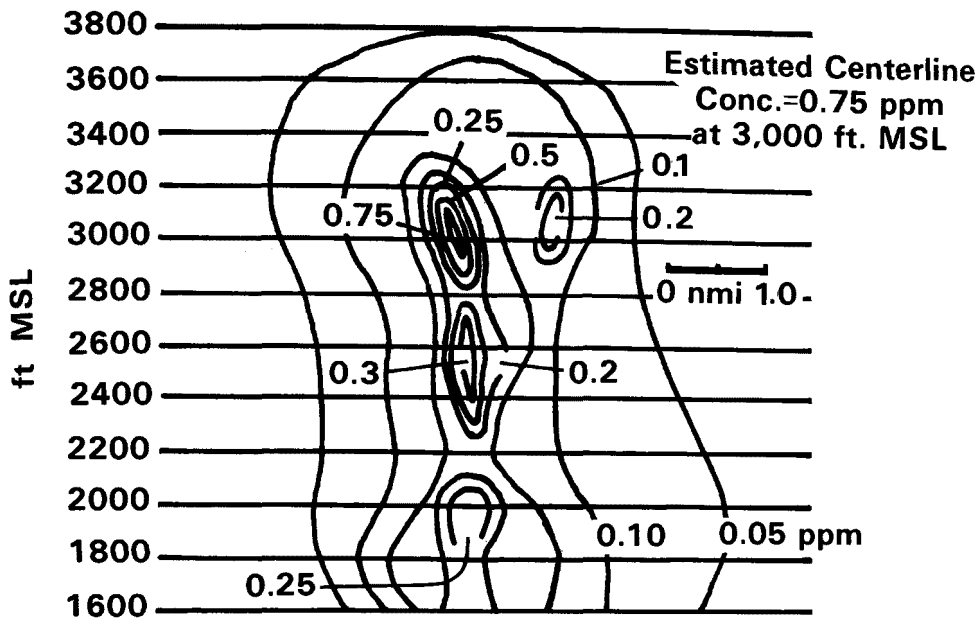
Figure A-44. Sulfur dioxide cross section along 213° radial of Bellaire VORTAC, 5 September 75, 1157-1207 EST.

TABLE A-21. PIBAL WIND INFORMATION, 5 SEPTEMBER 75, 1030-1300 EST

Number of Observations	Height (ft MSL)	Direction (degrees mag)	Measured Speed (m/sec)	Speed (knots)
6	993	162	1.9	4
	1,307	123	2.1	4
	1,621	124	3.2	6
	1,935	149	3.2	6
	2,249	136	5.6	11
	2,563	141	6.7	13
	2,876	149	5.1	10
	3,190	165	5.7	11
	3,504	170	6.3	12
	3,818	156	5.0	10
	4,132	196	4.1	8
	4,446	200	5.5	11
	4,759	205	4.9	10

TABLE A-22. KAMMER PLANT EMISSIONS AND PLUME DATA, 5 SEPTEMBER 75, 903-1245 EST

Volumetric Emission Rate (m³/sec)	SO₂ Emission Rate (g/sec)	Distance (nmi)	Plume Width (ft)	Plume Height (ft MSL)	Centerline Concentration (ppm)
657.5	3,638	4.5	12,660	2,700	1.52
		4.5		2,350 (LIDAR)	
		5.0		2,600	0.33
		Not determined			
		5.0		2,000	
		Not determined			

TABLE A-23. MITCHELL PLANT EMISSIONS AND PLUME DATA, 5 SEPTEMBER 75, 0903-1245 EST

Volumetric Emission Rate (m³/sec)	SO₂ Emission Rate (g/sec)	Distance (nmi)	Plume Width (ft)	Plume Height (ft MSL)	Centerline Concentration (ppm)
280	5,880	4.5	13,980	2,900	1.71
		4.5	10,350	2,800 (LIDAR)	
		5.5	14,690	3,000	

7 SEPTEMBER 1975, 1015-1545 EST

This mission was flown using the LIDAR equipped aircraft. The atmosphere was fairly clean and particulates were uniformly distributed through an approximate 3,000-ft mixing layer. However, one portion of the flight was of special interest. A pass was made over the Kammer and Mitchell plumes at 1015 EST. This portion of the flight was along the 226° radial of the Bellaire VORTAC and intercepted the plume approximately 7.5 nmi northwest of the plants. The returns from these sources strongly suggested that the Kammer plume was at the surface at this time. Visual observations confirmed this fact. Figures A-46 and A-47 are a representation of this portion of the flight. The vertical lines on Figure A-46 are the relative LIDAR returns at and near the surface, associated with both plant plumes and Figure A-47 is a contour plot of the relative signal strengths. No wind data or plant emission data are available for this flight.
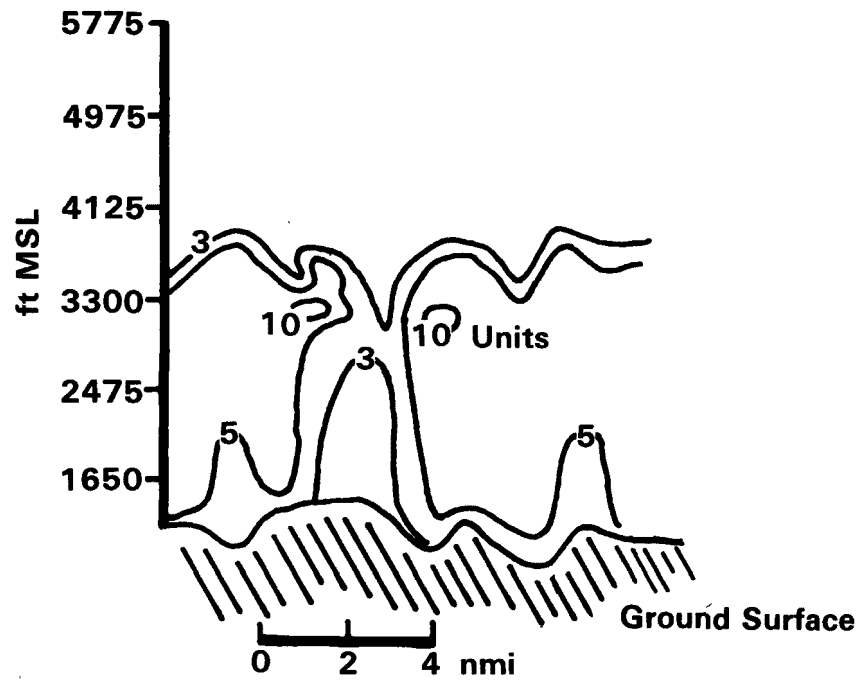
Figure A-45. LIDAR cross section along the 226° radial of the Bellaire VORTAC, 7 September 75, 1038-1044 EST.

Figure A-46. LIDAR returns along the 226° radial of the Bellaire VORTAC, 7 September 75, 1015 EST.

● = Ground Surface at Lidar Data Locations

Figure A-47. LIDAR aerosol light-scattering cross section of the Kammer and Mitchell Plumes 7.5 nmi northwest of plants along the 226° radial of the Bellaire VORTAC, 7 September 75, 1015 EST.

● = Ground Surface at Lidar Data Locations
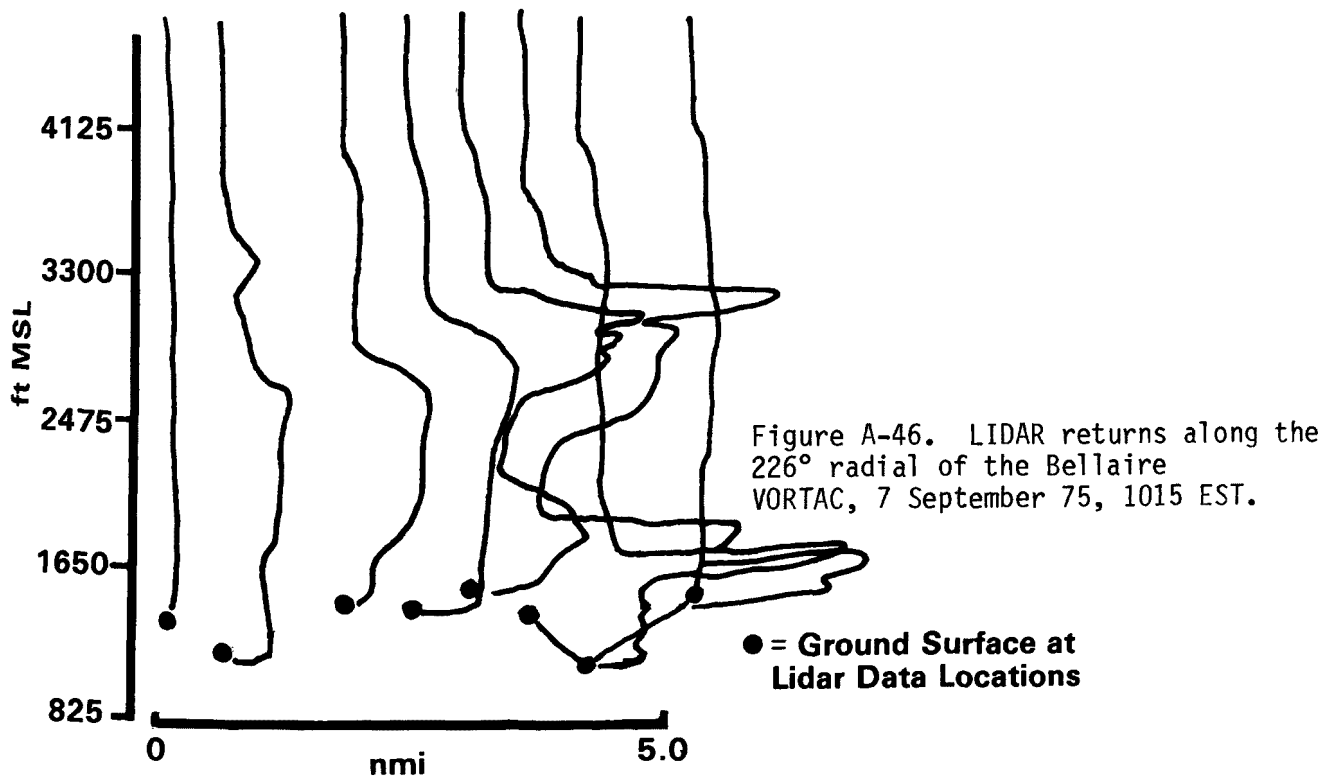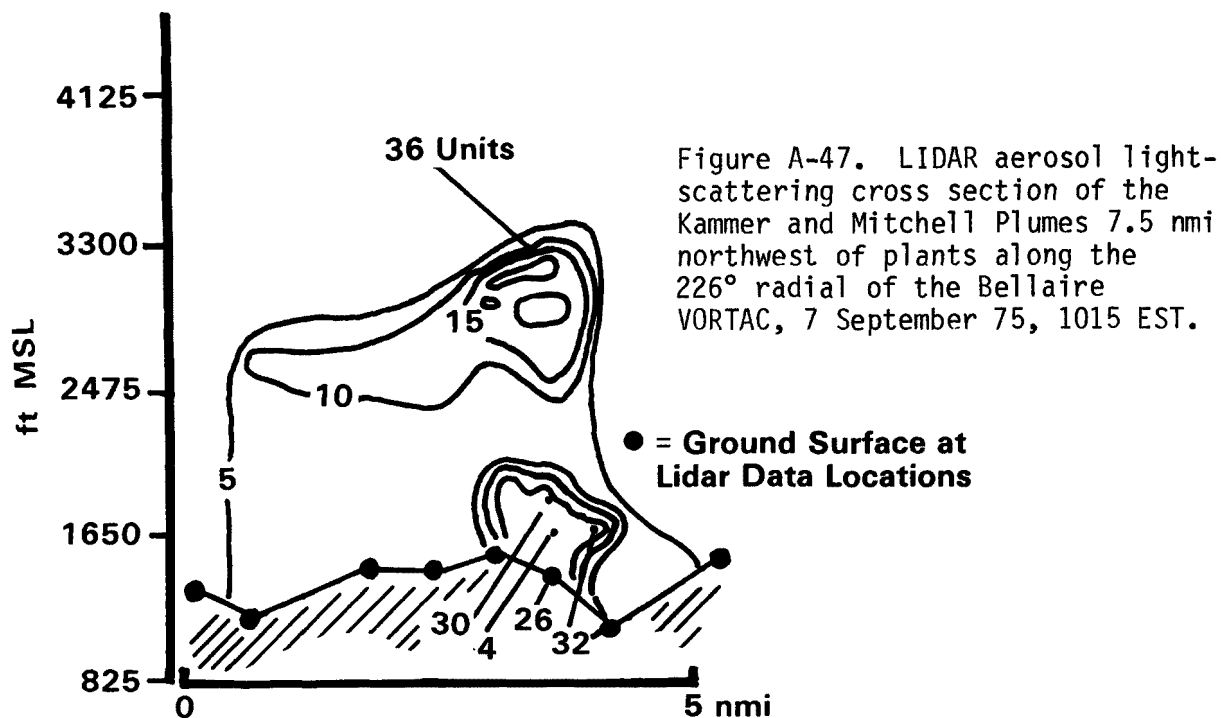
8 SEPTEMBER 1975, 0905-1247 EST

Radials of 157° and 135° were flown from the Bellaire VORTAC by both the helicopter and LIDAR aircraft. At 0938 EST, an inversion between 2,200 and 2,500 ft MSL was observed; nearly neutral conditions were measured above. The Kammer plume was trapped near the surface. By 1236 EST, neutral conditions had developed to 3,700 ft MSL. Visual centerline height of the Mitchell plume was estimated as 2,700 ft MSL.

MTE=Maximum Terrain Elevation
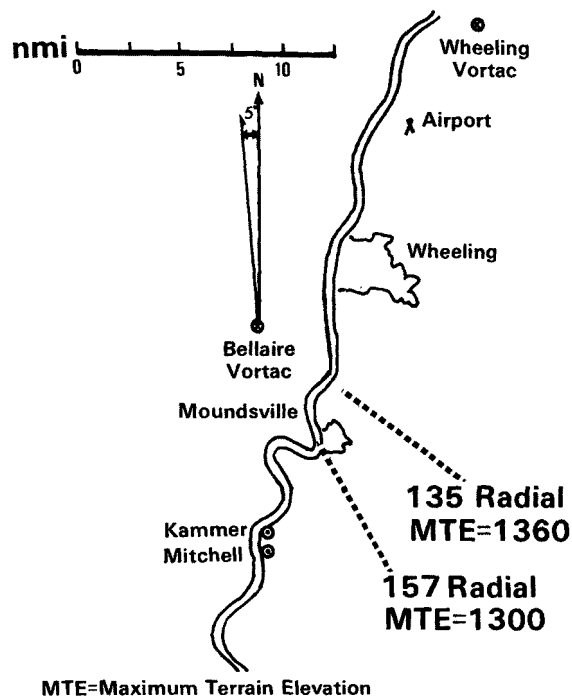
Figure A-48. Helicopter flight, 8 September 75.
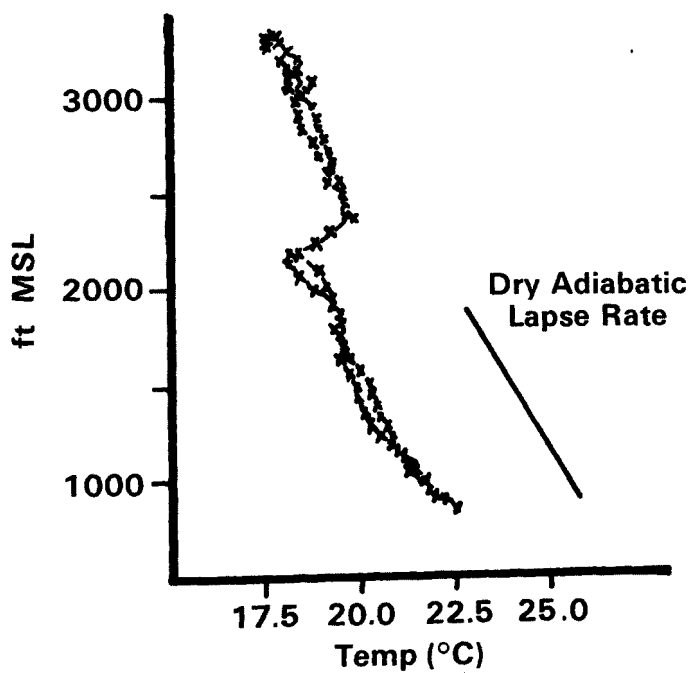
Figure A-49. Temperature sounding, 8 September 75, 0934-0939 EST.
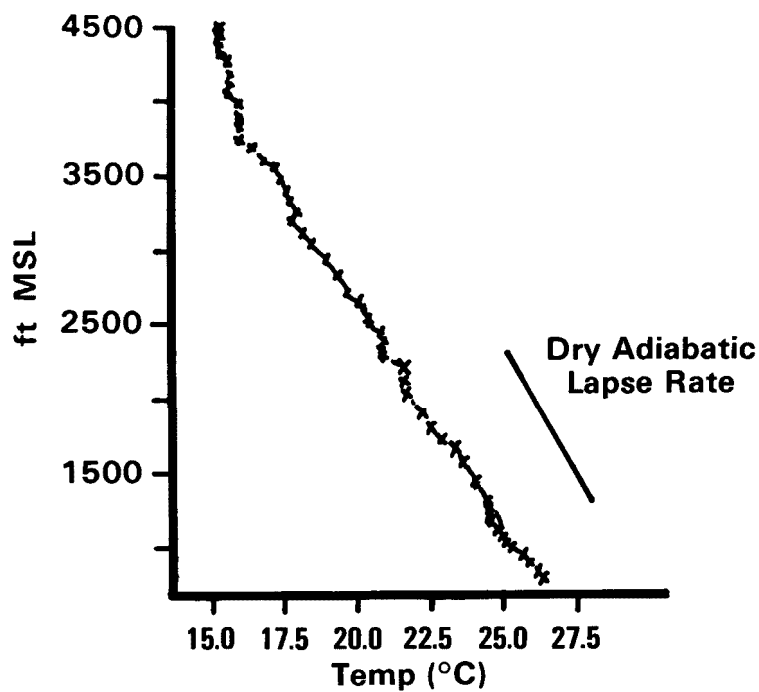
Figure A-50. Temperature sounding, 8 September 75, 1226-1236 EST.
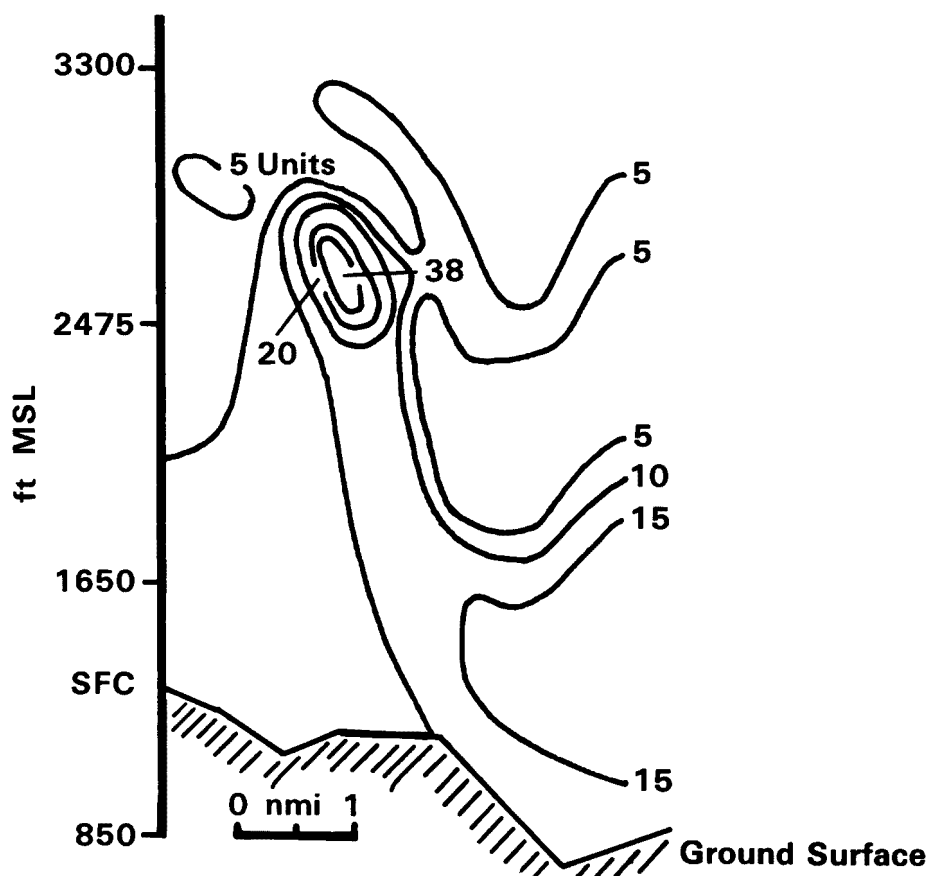
Figure A-51. LIDAR cross section along the 157° radial of the Bellaire VORTAC, 8 September 75, 0950 EST.
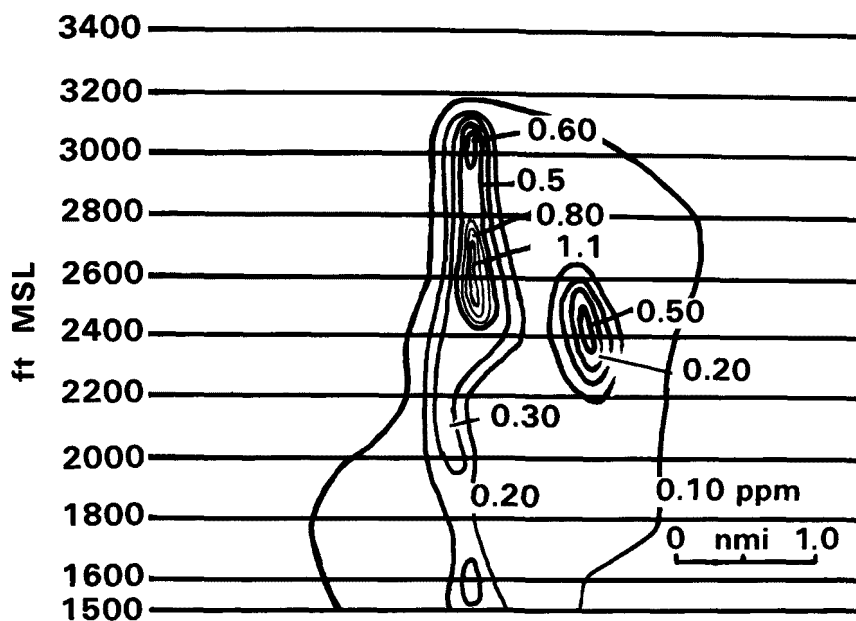
Figure A-52. Sulfur dioxide cross section along the 157°
radial of the Bellaire VORTAC, 8 September 75, 0944-1040 EST.
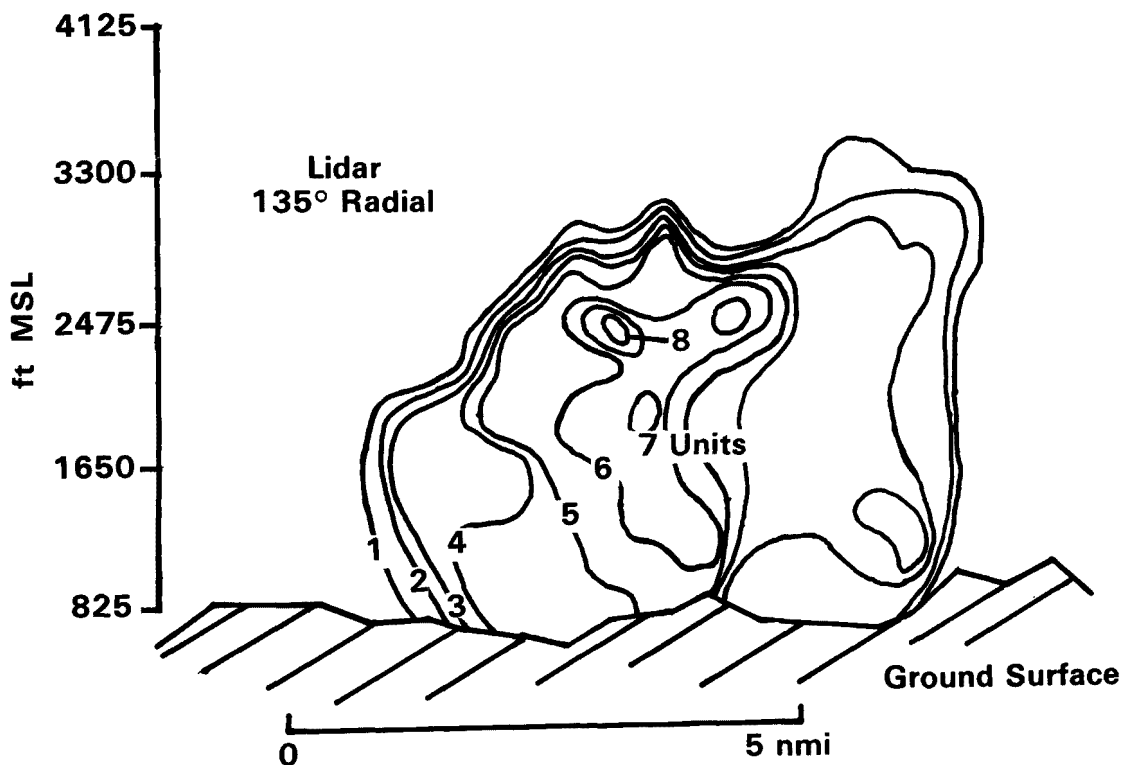
Figure A-53. LIDAR cross section of Kammer and Mitchell along
the 135° radial of the Bellaire VORTAC approximately 8 nmi
northwest of the plants, 8 September 75, 1048-1220 EST.
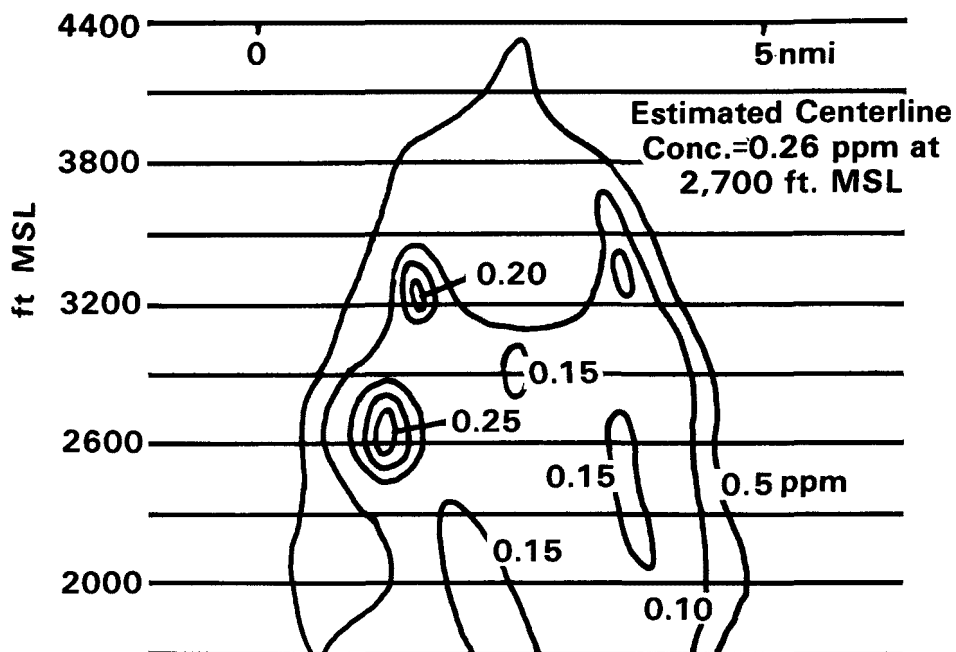
Figure A-54. Sulfur dioxide cross section of Kammer and
Mitchell along the 135° radial of the Bellaire VORTAC
approximately 8 nmi northeast of the plants, 8 September 75,
1048-1220 EST.
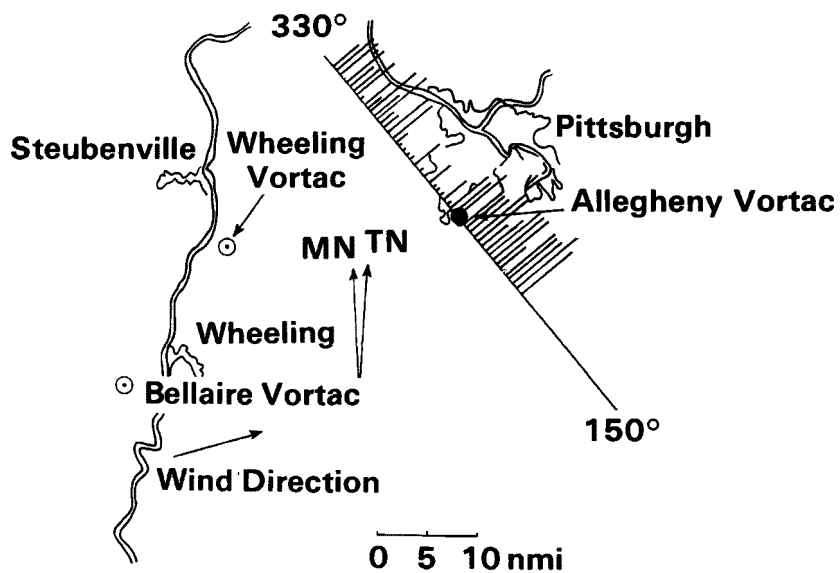
Figure A-555 LIDAR pass along the 150/330° radials of the
Allegheny VORTAC, 8 September 75.

TABLE A-24. PIBAL WIND INFORMATION, 8 SEPTEMBER 75, 1015-1315 EST

Number of Observations	Height (ft MSL)	Direction (degrees mag)	Measured Speed (m/sec)	Speed (knots)
7	993	229	3.3	8
	1,307	223	4.6	9
	1,621	226	5.9	11
	1,935	235	6.4	12
	2,249	233	6.6	13
	2,563	243	7.6	15
	2,876	244	10.2	20
	3,190	247	10.0	19
	3,504	249	11.3	22
	3,818	251	10.7	21
	4,132	254	9.5	19
	4,446	252	10.7	21
	4,759	251	9.8	19
	5,073	263	9.2	18

TABLE A-25. KAMMER PLANT EMISSIONS AND PLUME DATA, 8 SEPTEMBER 75, 0905-1247 EST

Volumetric Emission Rate (m^3/sec)	SO_2 Emission Rate (g/sec)	Distance (nmi)	Plume Width (ft)	Plume Height (ft MSL)	SO_2 Centerline Concentration (ppm)
1,670	2,260	4.5	15,200	2,400 2,475 (LIDAR)	0.50
		8.0	--	2,700 2,475 (LIDAR	--

63

TABLE A-26. MITCHELL PLANT EMISSIONS AND PLUME DATA, 8 SEPTEMBER 75, 0905-1247 EST

Volumetric Emission Rate (m^3/sec)	SO_2 Emission Rate (g/sec)	Distance (nmi)	Plume Width (ft)	Plume Height (ft MSL)	SO_2 Centerline Concentration (ppm)
309	4,486	5	12,540	2,600 2,550 LIDAR	1.17
		9	Not Determined	3,300* 2,500 LIDAR	0.26

*During the time the helicopter was constructing the second cross section, the inversion dissipated and the plumes began to rise rapidly.

9 SEPTEMBER 1975, 0617-0852 EST

This was an early morning flight under stable conditions. An isothermal layer existed between 1,500 and 2,000 ft MSL. Cross sections of the Mitchell plume were constructed at 2 and 5 nmi. The Kammer plume was included in the 5-mile cross section as it was directly under the Mitchell plume. Only one Kammer stack was in operation.
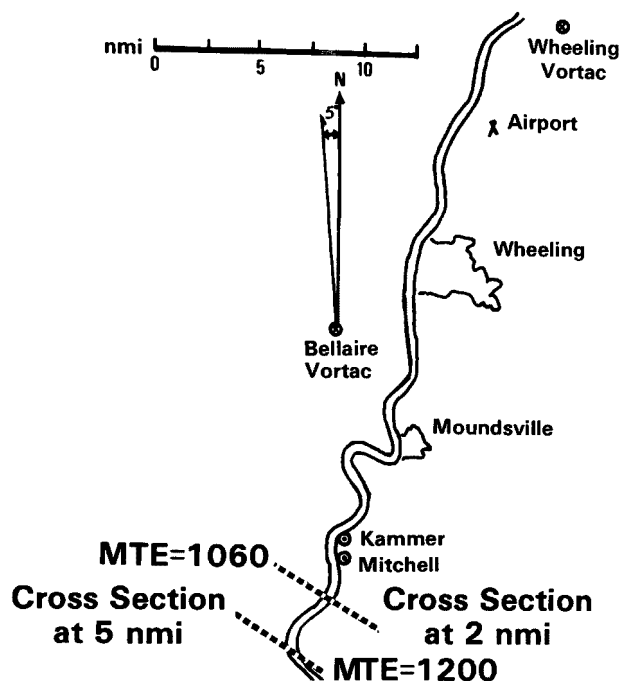
Figure A-56. Helicopter flight,
9 September 75, first flight.
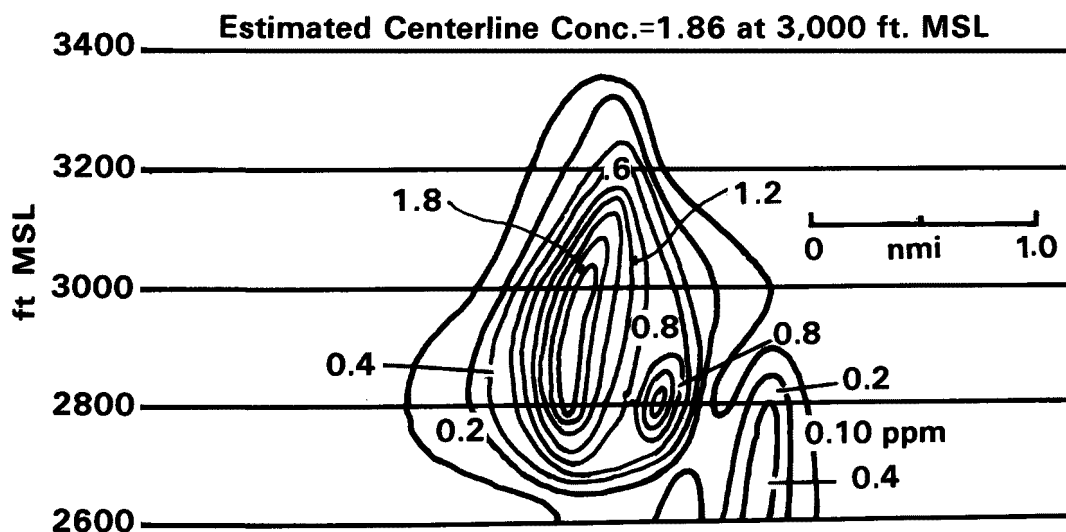
Figure A-57. Sulfur dioxide cross section of Mitchell plant at 2 nmi south of the plant, 9 September 75, 0710-0745 EST.

Figure A-58.   Temperature sounding, 9 September 75, 0656-0700 EST.
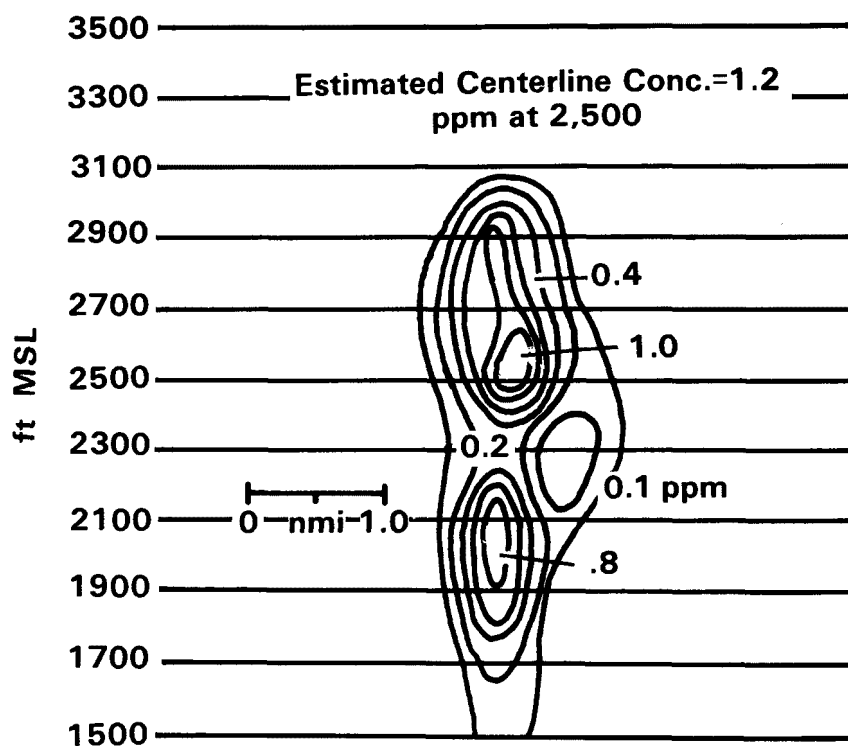
Figure A-59.   Sulfur dioxide cross section of Kammer and Mitchell at 5 nmi southwest of the plants, 5 September 75, 0816-0826 EST.

TABLE A-27. PIBAL WIND INFORMATION, 9 SEPTEMBER 75, 0715-0915 EST

Number of Observations	Height (ft MSL)	Direction (degrees mag)	Measured Speed (m/sec)	Speed (knots)
5	993	31	3.3	6
	1,307	18	3.8	7
	1,621	33	4.6	9
	1,953	36	5.4	11
	2,249	34	6.8	13
	2,563	39	5.5	11
	2,876	33	5.6	11
	3,190	25	4.5	9
	3,504	14	5.2	10
	3,818	342	6.6	13
	4,132	343	6.1	12
	4,446	341	8.7	17

TABLE A-28. KAMMER PLANT EMISSIONS AND PLUME DATA, 9 SEPTEMBER 75, 0617-0952 EST

Volumetric Emission Rate (m³/sec)	SO_2 Emission Rate (g/sec)	Distance (nmi)	Plume Width (ft)	Plume Height (ft MSL)	SO_2 Centerline Concentration (ppm)
628.0	3,854	5.5	6,590	2,200	1.15

A traverse of the Kammer plume at 1500 ft MSL (740 ft AGL) and approximately 4 nmi from the Kammer plant indicated a maximum SO_2 concentration of 0.19 ppm SO_2.

67

TABLE A-29. MITCHELL PLANT CHARACTERISTICS AND PLUME DATA, 9 SEPTEMBER 75,
0617-0952 EST

Volumetric Emission Rate (m³/sec)	SO₂ Emission Rate (g/sec)	Distance (nmi)	Plume Width (ft)	Plume Height (ft MSL)	SO₂ Centerline Concentration (ppm)
1717.2	8,343	2	5,520	3,000	1.86
		5	9,120	2,700	0.87

9 SEPTEMBER 1975, 1027-1331 EST

This flight was flown under slightly unstable conditions. A zigzag pattern (much the same as that of 28 August 75) was flown at 1,300-1,500 ft MSL through the lower portion of the Mitchell plume from approximately 24 nmi back to the plant. There is a possibility that other sources cross-polluted these data.
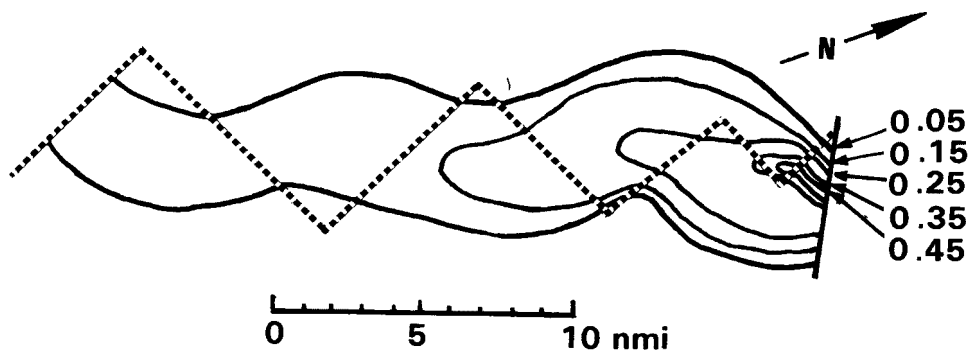
Figure A-60. Helicopter measurement of the horizontal distribution of SO₂ associated with the Mitchell plume, 9 September 75, 1130-1212 EST.
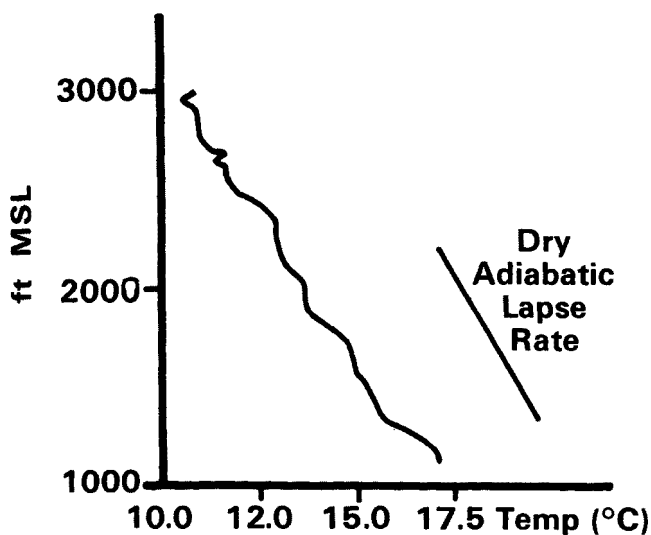
The flight path was at an altitude of approximately 100-300 ft AGL. An absolute maximum of 0.86 ppm was recorded at 1,500 ft MSL, 1 nmi from the plant. A traverse of the plume approximately 3 nmi and 300-900 ft AGL recorded a maximum of 0.62 ppm SO_2. It is noted that the plant had nominal loading at this time. Light winds were observed throughout the mission. A temperature sounding indicated near-neutral conditions.

Figure A-61. Temperature sounding taken at 1055-1059 EST, 9 September 75.

TABLE A-30. PIBAL WIND INFORMATION, 9 SEPTEMBER 75, 1130-1400 EST

Number of Observations	Height (ft MSL)	Direction (degrees mag)	Measured Speed (m/sec)	Speed (knots)
6	993	21	4.5	9
	1,307	18	4.5	9
	1,621	16	3.9	8
	1,935	25	3.8	7
	2,249	18	4.4	9
	2,563	21	4.0	8
	2,876	12	2.6	5
	3,190	19	2.5	5
	3,504	23	2.9	6
	3,818	21	3.6	7
	4,132	16	3.7	7
	4,446	339	5.1	10
	4,759	339	6.3	12

TABLE A-31. PLANT EMISSION DATA, 9 SEPTEMBER 75, 1039-1330 EST

Plant	Volumetric Emission Rate (m^3/sec)	SO_2 Emission Rate (g/sec)
Kammer	661	3,855
Mitchell	1,720	8,345

10 SEPTEMBER 1975, 0924-1255 EST

The purpose of this mission was to construct joint helicopter LIDAR cross sections along selected radials of the Bellaire VORTAC. Unfortunately, the LIDAR data were lost during processing. In addition, the helicopter data system failed from 1000-1134 EST. It was possible to construct one cross section along the 232° radial. This track was approximately 7.5 nmi from Kammer and 8 nmi from Mitchell. Near-neutral conditions were observed. Light winds produced highly concentrated plumes. Four relative maxima were found. The two maxima at 2,800 and 3,200 ft MSL may be the result of the Kammer plume changing altitudes during the helicopter sampling period or the two Kammer plumes may have maintained their identities. At 0955 EST, visual inspection of the plumes indicated that the Kammer plumes had combined and had a plume stabilization height of 2,800 ft MSL at 1104 EST; it was noted that the Mitchell plume was rising and was topped at 4,000 ft MSL. A spiral through both the Mitchell and Kammer plumes at 1237 EST indicated that the Mitchell plume centerline was then at 3,700 ft MSL and the Kammer plume had a single maximum at 3,300 ft MSL. At 1224 EST, a traverse was made under the Kammer plume at altitudes ranging from 140-800 ft AGL. A maximum concentration of 0.20 ppm SO_2 was observed.

70
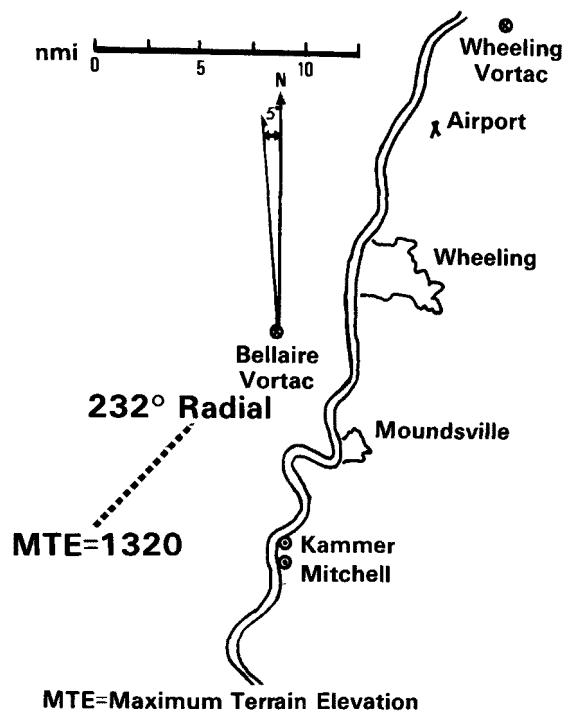
Figure A-62. Helicopter flight, 10 September 75.
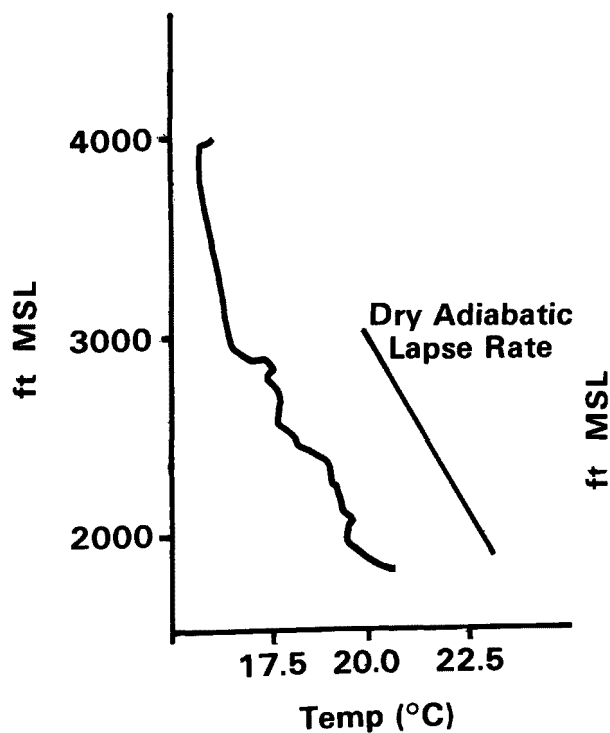
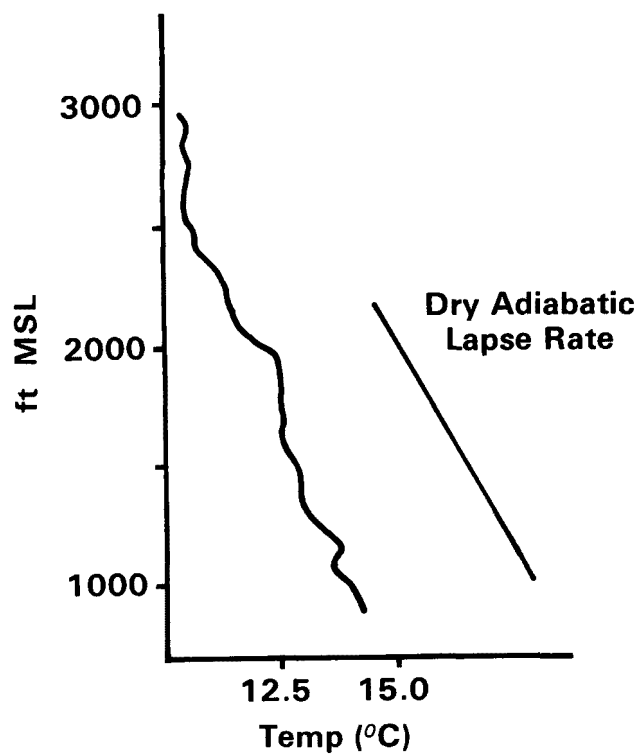Figure A-63. Temperature sounding, 10 September 75,
1238-1247 EST.
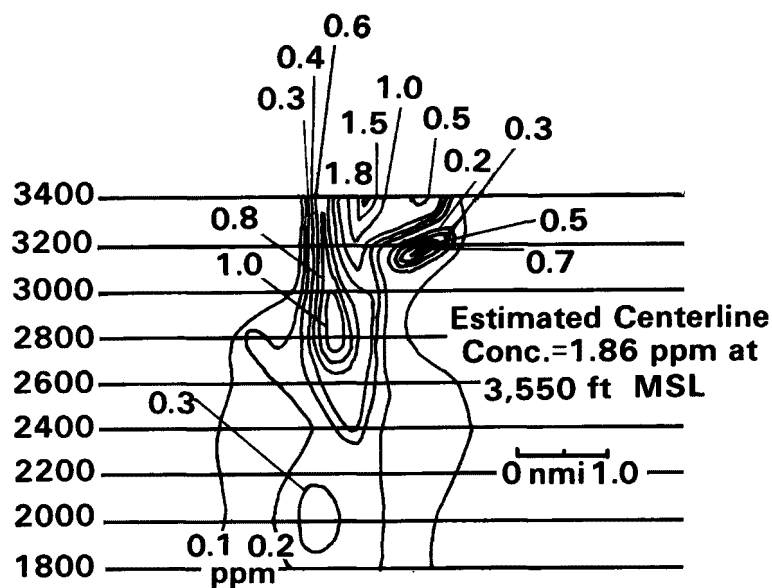
Figure A-64. Sulfur dioxide cross section of Kammer and Mitchell at 8 nmi northwest of the plants, 10 September 75, 1039-1227 EST.

TABLE A-32. PIBAL WIND INFORMATION, 10 SEPTEMBER 75, 1030-1330 EST

Number of Observations	Height (ft MSL)	Direction (degrees mag)	Measured Speed (m/sec)	Speed (knots)
7	993	139	1.6	3
	1,307	107	0.9	2
	1,621	69	1.2	2
	1,935	81	1.6	3
	2,249	120	1.5	3
	2,563	140	2.6	5
	2,876	147	3.1	6
	3,190	143	4.1	8
	3,504	140	3.3	6
	3,818	164	2.2	4
	4,132	192	1.6	3
	4,446	221	2.8	5

TABLE A-33. KAMMER PLANT EMISSIONS AND PLUME DATA, 10 SEPTEMBER 75,
0924-1255 EST

Volumetric Emission Rate (m^3/sec)	SO_2 Emission Rate (g/sec)	Distance (nmi)	Plume Width (ft)	Plume Height (ft MSL)	SO_2 Centerline Concentration (ppm)
910	4,020	7.5	17,226	2,800	0.84
		7.5	Not Determined	3,200	

TABLE A-34. MITCHELL PLANT EMISSIONS AND PLUME DATA, 10 SEPTEMBER 75,
0924-1255 EST

Volumetric Emission Rate (m^3/sec)	SO_2 Emission Rate (g/sec)	Distance (nmi)	Plume Width (ft)	Plume Height (ft MSL)	SO_2 Centerline Concentration (ppm)
1740.4	11,214	8.0	9,120	3,550	1.86

11 SEPTEMBER 1975, 0831-1109 EST

A flight was made by the helicopter to measure the Mitchell and Kammer plumes at 2 and 5 nmi. A cross section was constructed at 10 nmi of the Kammer, Mitchell and Burger plumes. The strong winds, 4-15 m sec, were measured along with surprisingly stable conditions.

nmi 0   5   10
N

Wheeling
Vortac
Airport
Wheeling
Cross Section
at 10 nmi
Bellaire
Vortac
MTE=1160
Moundsville
Kammer
Mitchell

MTE=Maximum Terrain Elevation
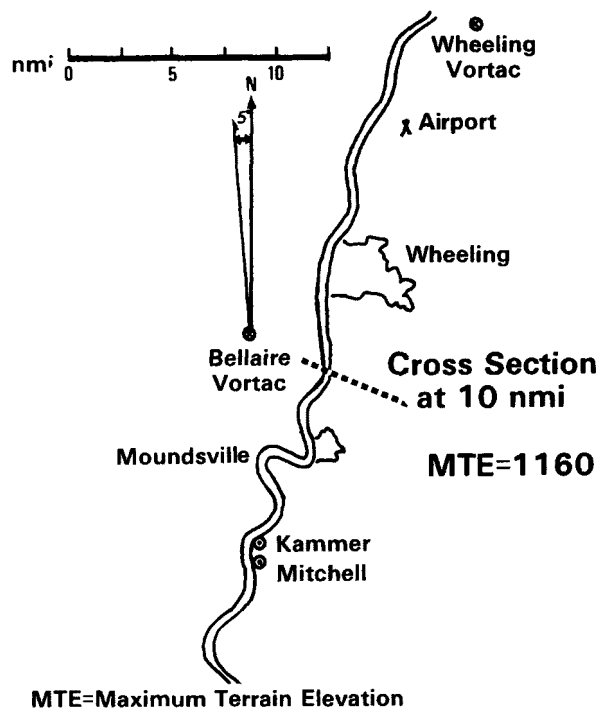
Figure A-65. Helicopter flight,
11 September 75, first flight.

Dry Adiabatic
Lapse Rate

(Composite)

ft MSL

3000

2000

17.5   20   22.5
Temp (°C)
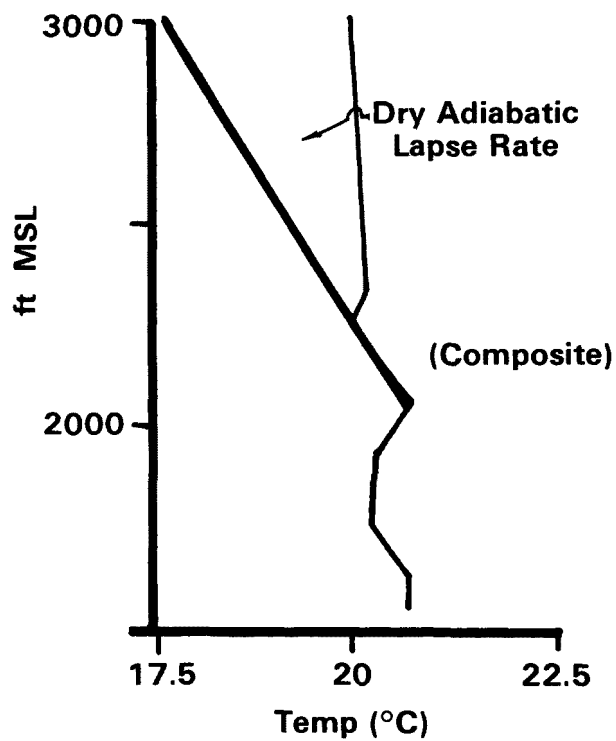
Figure A-66. Temperature sounding,
11 September 75, a.m. composite.

74
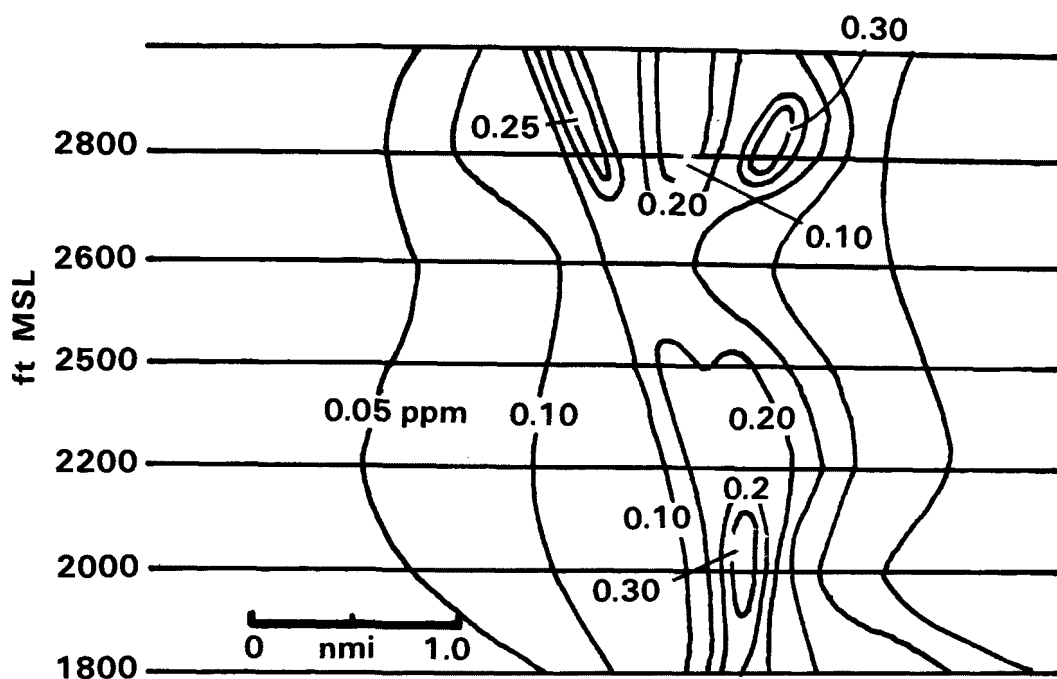
Figure A-67. SO$_2$ cross section of Kammer and Mitchell plumes
10 nmi northeast of plants, 11 September 75, 0958-1047 EST
(Estimated centerline concentration equals 0.3 ppm at 2800 ft MSL).

TABLE A-35. PIBAL WIND INFORMATION, 11 SEPTEMBER 75, 1015-1145 EST

Number of Observations	Height (ft MSL)	Direction (degrees mag)	Measured Speed (m/sec)	Speed (knots)
4	993	200	4.5	9
	1,307	199	6.1	12
	1,621	201	7.3	14
	1,935	204	9.6	18
	2,249	214	11.9	23
	2,563	224	13.6	27
	2,876	225	15.6	30
	3,190	230	15.5	30
	3,504	230	18.4	36
	3,818	233	13.7	27
	4,132	282	15.2	30

TABLE A-36.   KAMMER PLANT EMISSIONS AND PLUME DATA, 11 SEPTEMBER 75,
0831-1109 EST

Volumetric Emission Rate (m^3/sec)	SO_2 Emission Rate (g/sec)	Distance (nmi)	Plume Width (ft)	Plume Height (ft MSL)	SO_2 Centerline Concentration (ppm)
910	4,020	2	8,100	1,950	1.20
		5	Not Determined	1,900	0.54
		10	12,160	2,000	0.35

TABLE A-37.   MITCHELL PLANT EMISSIONS AND PLUME DATA, 11 SEPTEMBER 75,
0831-1109 EST

Volumetric Emission Rate (m^3/sec)	SO_2 Emission Rate (g/sec)	Distance (nmi)	Plume Width (ft)	Plume Height (ft MSL)	SO_2 Centerline Concentration (ppm)
1763.5	10,720	2	3,540	2,350	1.10
		5	12,160	2,050	0.36

11 SEPTEMBER 1975, 1346-1423 EST

Nearly neutral conditions with moderately strong winds, 3.5-10 m/sec, were observed during this flight. Upon arriving at Kammer, it was noted that the plume was hitting the hills to the northwest of the plant at a distance of approximately 1.5 nmi. A series of 22 passes was made along the side of the hill. The mean value of the maxima was 0.15 ppm SO_2 during the 32 minutes required to collect the data. It then began to rain and the helicopter returned to base.

76

TABLE A-38.   PIBAL WIND DATA, 11 SEPTEMBER 75, 1315-1415 EST

Number of Observations	Height (ft MSL)	Direction (degrees mag)	Measured Speed (m sec)	Speed (knots)
2	993	192	5.3	10
	1,301	197	4.4	9
	1,621	196	6.6	13
	1,935	197	6.8	13
	2,249	194	9.0	15
	2,563	197	9.5	19
	2,876	196	10.8	21
	3,190	204	11.8	23
	3,504	207	13.2	27
	3,818	211	15.0	29
	4,132	212	16.9	33

TABLE A-39.   KAMMER PLANT EMISSIONS, 11 SEPTEMBER 75, 1234-1336 EST

Volumetric Emission Rate (m^3/sec)	SO_2 Emission Rate (g/sec)
10,403	3,829

MTE=Maximum Terrain Elevation
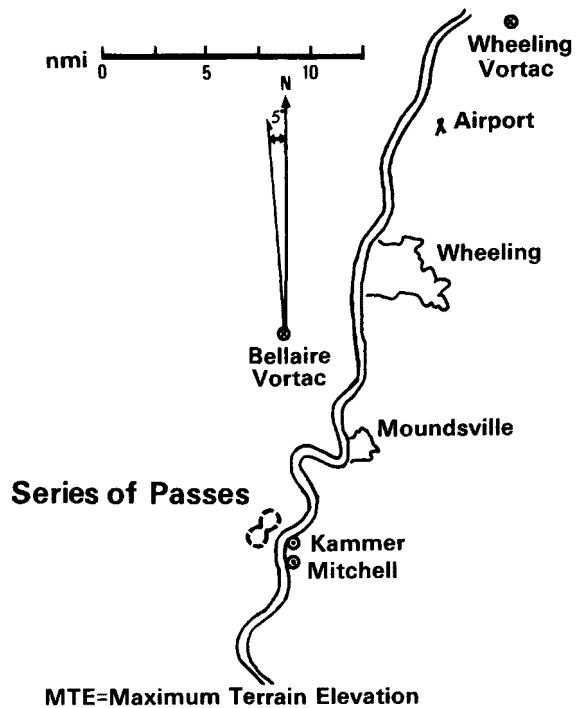
Figure A-68. Helicopter flight, 11 September 75, second flight.
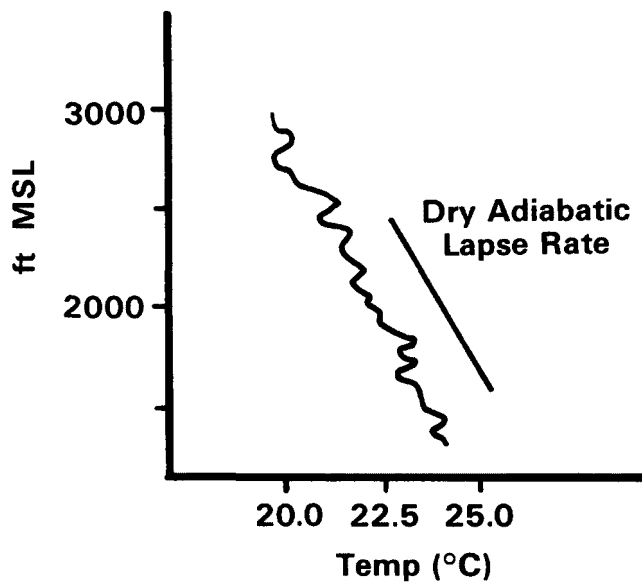
Figure A-69. Temperature sounding, 11 September 75, 1346-1350 EST.

APPENDIX B. WIND DATA

Single theodolite wind measurements were taken in the vicinity of the Kammer and Mitchell plants. An effort was made to take these observations 1 to 2 miles downwind from the smoke stacks. These locations were between 610 and 680 ft MSL, with most of the observations being taken at 680 ft MSL. The mean of all the soundings taken during the period of each flight is included in the discussion of each flight so that the winds may be computed for effective stack heights and so that the mixing layer heights may be estimated.

To supplement these data and to verify their accuracy, helicopter drift measurements were made during sampling missions to determine wind speed and direction. Table B-1 provides a comparison of data for similar altitudes obtained from these two methods.

TABLE B-1. COMPARISON OF HELICOPTER AND PIBAL WINDS

Date (1975)	Helicopter Wind Direction Degrees (mag)	Helicopter Wind Speed (knots)	Pibal Mean Wind Direction Degrees (mag)	Pibal Mean Wind Speed (knots)
2 Sep	321	10	290	9
	303	5	284	7
5 Sep	203	17	149	6
8 Sep	271	23	243	15
	299	20	246	19
9 Sep	034	16	039	11
	021	6	025	9
	029	12	036	11
	070	12	025	7
10 Sep	102	7	143	8
3 Sep*	257	6 (at 2258 ft MSL)		
	279	8 (at 1900 ft MSL)		
4 Sep*	345	9 (at 2000 ft MSL)		
	328	9 (at 2000 ft MSL)		

*No pibal wind measurements were taken on these dates.

The average directional difference between the two measurement methods was +28 degrees while the average difference in speed was 3.8 kn. These are equivalent to a graphically determined average vector difference of 6.2 kn. It must be noted that the pibal and helicopter wind measurements were not taken in juxtaposition. Pibal measurements were taken in the Ohio River Valley, while the helicopter was sampling; the helicopter drift measurements were generally taken coming from or returning to the airport during flights between 2,000 and 3,200 feet MSL over undulating terrain. Taking this into account, it is felt that the helicopter drift measurements offer substantiation of the quality of the pibal wind measurements.

The helicopter drift calculations for wind speed and direction were made using position data obtained from VORTAC stations in Bellaire, Ohio, and Wheeling, West Virginia. Heading and air speed were obtained from helicopter instruments. In Figure B-1, point A is the Wheeling VORTAC and point B is the Bellaire VORTAC. Coordinates for these two points can be determined in relation to some distant coordinate axes positioned so that all points for consideration in any problem would be in the first quadrant of that set of axes. Point (X_1, Y_1) is the beginning point of the measured flight. Values for X_1 and Y_1 can be obtained using distances a_1 and b_1 obtained from the VORTAC stations and c, the distance between A and B, in this manner, using the law of cosines. This law is:

$$\angle F_1 = \cos^{-1} \frac{(b_1{}^2 + c^2 - a_1{}^2)}{2b_1 c}$$

The line through A and B makes an angle of 36 degrees to true north so that $\angle F_1 + 36$ is the angle of b_1 to true north. Then:

$$X_1 = X_4 + b_1 \sin (\angle F_1 + 36)$$

$$Y_1 = Y_4 + b_1 \cos (\angle F_1 + 36)$$

Similarly, to determine values for X and Y the coordinates of the end point of the measured flight, the following equation applies.

$$\angle F_2 = \cos^{-1} \frac{(b_2{}^2 + c^2 - a_2{}^2)}{2b_2 c}$$

Then:

$$X_2 = X_4 + b_2 \sin (\angle F_2 + 36)$$

$$Y_2 = Y_4 + b_2 \cos (\angle F_2 + 36)$$

Using true heading, TH, which in this case is the indicated heading minus 5 degrees for magnetic correction, X_3 and Y_3 can be determined.

$$X_3 = X_1 + SZ(\sin TH)$$

$$X_3 = Y_1 + SZ(\sin TH)$$

where S = airspeed*
Z = length of time of the measured flight

The magnitude of the wind vector can then be found using the distance formula:

$$\text{Wind Speed} = \sqrt{(X_2 - X_3)^2 + (Y_2 - Y_3)^2}$$

The wind direction is found using the following equation.

$$\angle Q = \tan^{-1} \frac{X_2 - X_3}{Y_2 - Y_3}$$

From this,

$$\text{Wind Direction} = F_3 + 180, \text{ if } Y_2 - Y_3 > 0$$

$$= F_3 + 360, \text{ if } X_2 - X_3 > 0, \text{ and } Y_2 - Y_3 < 0$$

$$= F_3, \text{ if } X_2 - X_3 < 0 > Y_2 - Y_3$$
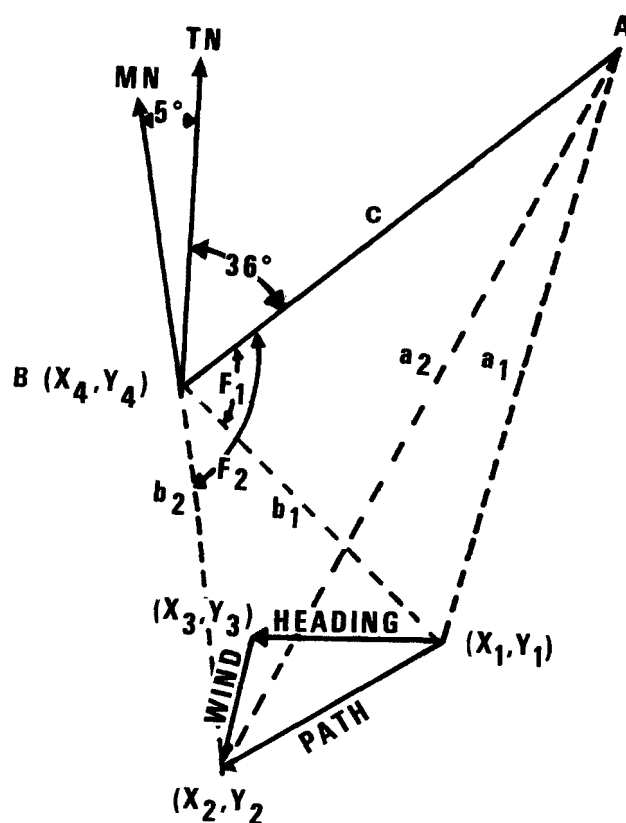
Figure B-1. Representation of wind calculations.

APPENDIX C. DETERMINATION OF HORIZONTAL AND VERTICAL
DISPERSION COEFFICIENTS

The values of the standard deviations, σ_y and σ_z, used in the summary were calculated from actual plume measurements. Values of the horizontal standard deviation, σ_y, were determined from plume width measurements using the well-known relationship, 2.15 σ_y equals the distance to one-tenth the centerline concentration in a horizontal direction, or by our definition of plume width, plume width is equal to 4.3 σ_y. Values of the vertical standard deviation, σ_z, were estimated assuming the relationship:

$$\frac{\sigma_y \text{ (Measured)}}{\sigma_y \text{ (Flat Terrain)}} = \frac{\sigma_z \text{ (Computed)}}{\sigma_z \text{ (Flat Terrain)}}$$

This estimation was necessary because of the frequency of less than Visual Flight Rules (VFR) conditions near the upper extent of the plumes and because the helicopter was not always able to fly low enough to ascertain the lower limits of the plume. In addition, the Kammer and Mitchell plumes were frequently stacked in the vertical, making it impossible to determine in the vertical where one plume ended and the other began.

In a very limited number of cases it was possible to measure σ_z in the downward direction. The downward direction was chosen so the effects of possible stable layers above the plumes would not be measured. Table C-1 presents a comparison of the mean vertical standard deviation, $\overline{\sigma}_z$, for flat terrain for computed and measured cases.

TABLE C-1. DOWNWARD STANDARD DEVIATIONS FOR FLAT TERRAIN, COMPUTED AND
MEASURED

Plant	$\overline{\sigma}_z$ Flat Terrain	$\overline{\sigma}_z$ Computed	$\overline{\sigma}_z$ Measured Downward
Kammer (3 cases)	76 m	125 m	92 m
Mitchell (4 cases)	74 m	156 m	138 m

Although no firm conclusions can be drawn from these limited data, it would appear that the actual values of σ_z are closer to the computed values than they are to the values for flat terrain. Typically, the vertical distribution of the effluent is with the maximum portion in the upper half of the plume (Schiermeier 1971). This would mean that the upward σ_z values should be smaller than the downward values of σ_z.

It is of interest to note that the values of σ_y associated with the Mitchell plume are on the average 1.1 times greater than the values for flat terrain (Turner 1969), while a comparison of the measured values of σ_y associated with the combined Kammer plume with the values associated with flat terrain shows that the Kammer σ_y values are on the average 2.0 times greater.

Figures C-1 and C-2 give a comparison of the measured values with the flat terrain values. The difference between the behavior of the two plumes can be explained by the fact that the Mitchell station has a 336-meter stack, while the two stacks of the Kammer station are 183 meters in height. The very high release altitude of the Mitchell station resulted in a plume stabilization height which was frequently above the effects of surface roughness and topography.
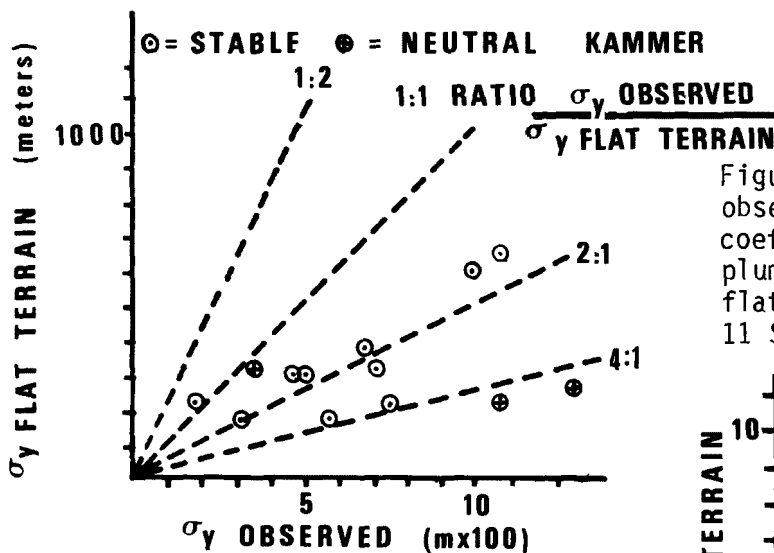
Figure C-1. Comparison of observed horizontal dispersion coefficients for the Kammer plume with those developed for flat terrain, 25 August - 11 September 75.

Figure C-2. Comparison of computed vertical dispersion coefficients for the Kammer plume with those developed for flat terrain, 25 August - 11 September 75.
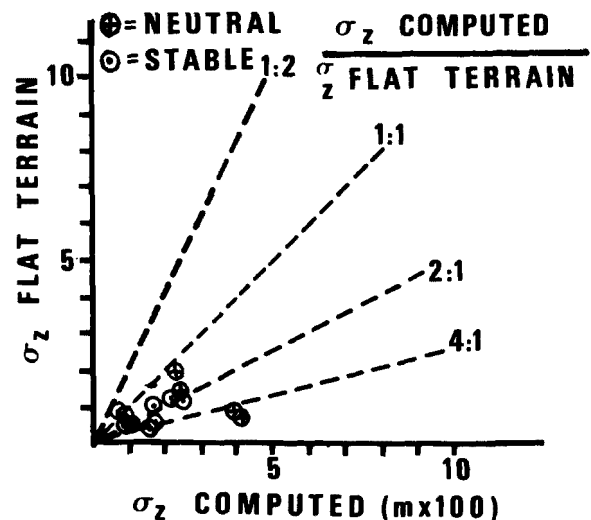
Figures C-3 through C-6 offer a comparison of the ratios of the measured σ_y values to the flat terrain σ_y values and downwind distance. The ratio for the Mitchell plant is fairly constant with distance, reinforcing the idea that the Mitchell plume is frequently high enough to be unaffected by the effects of topography.

The mean value of the ratio is higher at 3.7 kilometers (2 nmi) than at greater downwind distances (see Figures C-5 and C-6). It is hypothesized that the terrain-induced scale of turbulence in the horizontal is near the effective eddy size at this distance (Sutton 1932). This same enhancement of dispersion close to the source has been observed by McElroy and Pooler (1968), who investigated dispersion over metropolitan St. Louis, Missouri. They concluded that when the plume becomes much larger than the eddies associated with mechanical turbulence, the extent of the dispersion approaches that of open country.
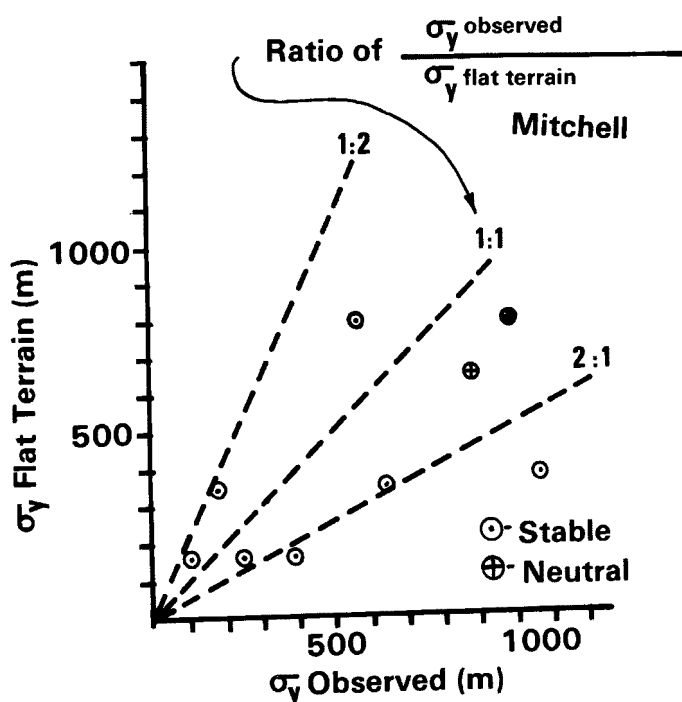
Figure C-3. Comparison of observed horizontal dispersion coefficients for the Mitchell plume with those developed for flat terrain, 25 August - 11 September 75.
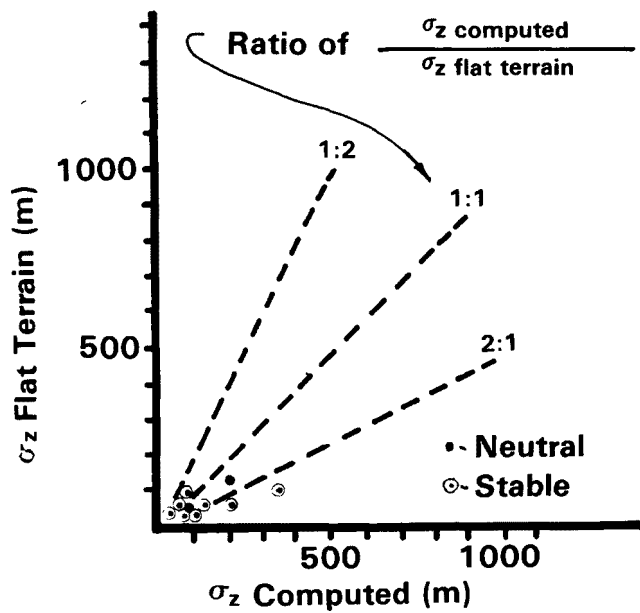
Figure C-4. Comparison of calculated vertical dispersion coefficients with those developed for flat terrain, 25 August - 11 September 75.
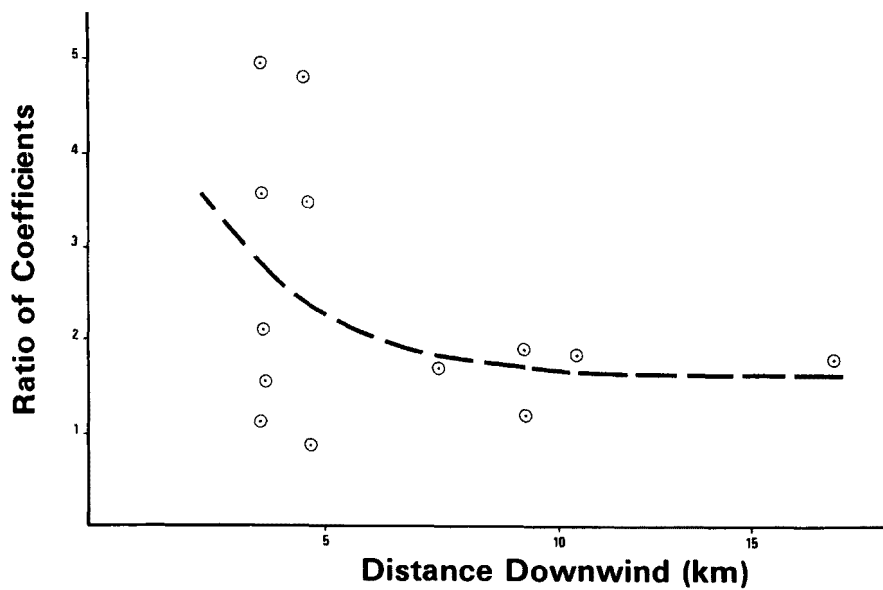
Figure C-5. Ratios of measured horizontal dispersion coefficients to coefficients for flat terrain, Kammer plume, 25 August - 11 September 75.
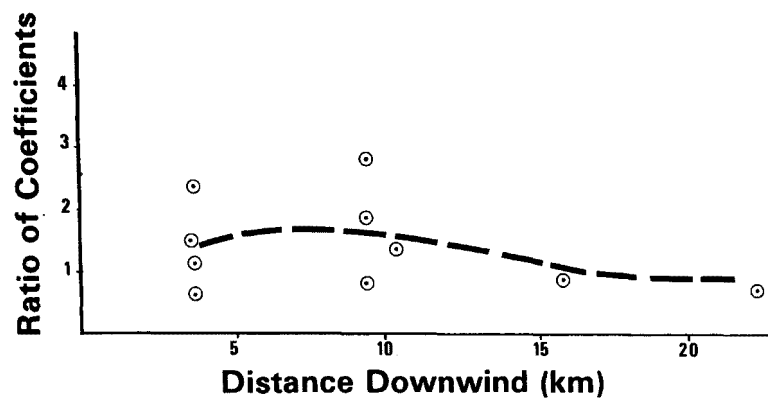
Figure C-6. Ratios of measured horizontal dispersion coefficients to coefficients for flat terrain, Mitchell plume, 25 August - 11 September 75.

APPENDIX D. FLUX CALCULATIONS FROM PLUME CROSS SECTIONS

The three cross sections that were constructed on the morning of 29 August 1975 were chosen as the basis for calculations of the flux of SO_2 from the Kammer power plant. The cross sections were chosen for the following reasons: a) stable atmospheric conditions, b) moderately strong wind speeds, c) three cross sections were available in a 2-hour period, and d) no other plumes were in the area.

Flux is defined as follows.

$$\text{Flux} = \text{Concentration} \times \text{Area} \times \text{Wind Speed}$$

$$= \frac{\mu g}{m^3} \times m^2 \times \frac{m}{sec}$$

$$= \frac{\mu g}{sec}$$

The actual hourly flux from the plant was computed from the daily coal consumption, the sulfur content, and the hourly power generation data. These data were provided to EPA Region III by the Ohio Power Company on 5 October 1975. The hourly flux of SO_2 was computed as follows:

Hourly SO_2 Generation =

$$\text{Daily Coal} \times \text{Percent Sulfur} \times \frac{\text{Hourly Production}}{\text{Daily Consumption}} \times 2$$

The factor of 2 was included because the molecular weight of SO_2 is twice that of sulfur.

Flux was estimated from the cross sections as follows:

a. A plot of isopleths of concentration was made on rectilinear coordinate paper representing vertical and horizontal distribution of SO_2.

b. A planimeter was used to measure areas of equal concentrations.

c. Concentrations were converted from parts per million to micrograms per cubic meter by the relationship:

$$\frac{\mu g}{m^3} = \text{ppm} \times \frac{\text{molecular weight}}{0.024}$$

d. The areas of equal concentration were multiplied by the wind speed and concentration to give flux.

e. These results were summed to give total flux.

The results of these calculations are given in Table D-1.

TABLE D-1. FLUX CALCULATIONS

Time (EST)	Distance (nmi)	Actual Flux (kg/hr)	Calculated Flux (kg/hr)	% of Actual
0831-0918	2	13,744	13,244	96
0923-0943	4	13,774	12,483	91
1021-1041	2	13,744	13,949	101

APPENDIX E. HELICOPTER SYSTEM DESCRIPTION

By: J. Jeffrey van Ee, EMSL-LV

Three probes located on the right forward side of the helicopter supply air to the instruments (Table E-1) located in the helicopter cabin. One probe is used for the gas-phase instruments; the other two probes are used for particulates. One of these probes is used exclusively for the nephelometer; the other probe is used to collect particulate samples for microscopic and chemical analyses. All three 1-1/2-inch diameter aluminum probes are coated with Kynar to minimize interactions with the walls. Air is forced through two of the probes by ram-air pressure with the air exhausting to the rear of the helicopter. One of these probes supplies air to the nephelometer. A heater is used to minimize the effect of moisture on visibility measurement. All of the gas phase instruments sample air from the other probe through Teflon tubing and 5-micrometer Teflon filters. Air for the third probe is sampled isokinetically using a special probe tip and an air pump.

Output voltages from the instruments are converted to Binary Coded Decimal (BCD) characters using a Monitor Labs (ML 7200) data acquisition system. These data are recorded on 7-track magnetic tape using a Cipher 70 tape deck. Instruments are scanned by the ML 7200 at a selected scan rate of 2 to 5 seconds. The magnetic tape is processed by a digital computer and a printout of calibrated engineering units is obtained.

Particulates are collected for laboratory analysis by either impaction or filtration. For microscopic analysis, particulates are collected on Nucleopore elements using a commercial six-stage Anderson impactor. A membrane filter is used as the final filter. The required 1 cubic foot per minute (cfm) flow rate is achieved using a limited orifice. For chemical analyses of particulates, x-ray fluorescence is frequently used. Millipore 1-micrometer Fluoropore filters are used together with a high-capacity pump to obtain high volumes of air samples in relatively short times. (The exact sample time required to identify a certain pollutant depends on the sensitivity of the analysis and the expected ambient air concentration.)

TABLE E-1. HELICOPTER INSTRUMENTATION

PARAMETER	INSTRUMENT*	MEASUREMENT METHOD	CALIBRATION STANDARD	METHOD OF CALIBRATION
CO	Beckman 7000	Dual Isotope Fluorescence	NBS traceable CO/N_2 gas	Dilution of gas with Bendix Dynamic Calibration System
SO_2	Meloy SA160 with H_2S scrubber	flame phometric	NBS certified permeation	Method described in _Federal Register_
Temperature/ Dewpoint	Cambridge CS-137	thermistors	fixed resistors	Procedure recommended by manufacturer
NO/NO_x	Monitor Labs 8440	NO: Chemiluminescent reaction with O_3 NO_2: Conversion of NO_2 to NO in Moly converter; subsequent reaction with O_3	NO-NBS traceable NO/N_2 gas NO_2- GPT of NO with O_3 to generate NO_2/NO mixture	Dilution of gas using Bendix Dynamic Calibration System
O_3	REM612B	Chemiluminescence	O_3 source calibrated with _Federal Register_ KI method	A Dasibi O_3 monitor is calibrated against a standard ozone source. The Dasibi is used to check the calibration of the field-based O_3 source
Visibility	MRI 1550B nephelometer	90° light scattering	Freon 12	Procedure recommended by manufacturer
Altitude	Computer Instrument Corp., Model 8000	Pressure		The airport altitude is compared to the ground-based altimeter reading
Particulates	Anderson 6 stage impactor	Electron & Optical Microscopy X-ray fluorescence		The 1 cfm flow rate is achieved using a limiting orifice
	37 mm, millipore 1 micron fluoro-pore filters	X-ray fluorescence		Sample flow is obtained by measuring the pressure drop across the filter
Position	Collins DME 40 and Bendix RVA-33-A VOR	Triangulation accurate to within 0.1 NM		

91

APPENDIX F.   CALIBRATION STANDARDS AND PROCEDURES

By: J. Jeffrey van Ee, EMSL-LV

Nearly all of the gas-phase instruments used by the Monitoring Operations Division of EMSL-Las Vegas are calibrated with National Bureau of Standards (NBS) traceable gases. Secondary CO and NO standards are diluted to ambient levels using a Bendix Dynamic Calibration System (DCS) Model 8851. Zero air is provided by an AADCO 737 zero air generator. This instrument used a molecular sieve process to generate dry, pure air. Dilution flows are measured with a Hastings Mini-flow Calibrator (Model HBM-1). These soap bubble flowmeters are traceable to NBS volumetric standards.

Sulfur dioxide is generated from an NBS permeation tube, maintained at constant temperature, in the Bendix DCS. To ensure the existence of a stable SO_2 source, dry air continuously flows over the tube during the whole time of the project. When ambient source concentrations of SO_2 are expected to exceed one part per million (ppm), an SO_2-in-aluminum-cylinder standard and the Bendix DCS are used to calibrate the 1-10 ppm range of the Meloy SA-160.

Calibration of the SO_2 monitor is complicated by the fact that SO_2 is a reactive pollutant, yet it is not all that difficult because an adequate standard source (the NBS certified permeation tube) exists for this pollutant. Calibration of an ozone monitor is made more difficult because it is a highly reactive pollutant and no adequate standard source for O_3 exists at this time. A temperature and current controlled UV-lamp source is used to generate ozone. Dry air is used in this process. Following the Neutral Buffered Potassium Iodide (NBKI) method described in the Federal Register, a Dasibi-AH ozone monitor (using an uncalibrated ozone generator in the process) is calibrated. The Dasibi instrument uses an ultraviolet (UV) absorption process that has proven to be quite stable over long periods of time (3-4 weeks). With this instrument, the stability of an ozone source in the field can be monitored and this source can be calibrated to a NBKI EPA reference method performed in the laboratory. Using this calibration method, the chemiluminescent ozone monitor can be effectively calibrated with the accuracy inherent in the NBKI method itself. Unfortunately, many problems exist with the NBKI method. For this reason, the calibration of the Dasibi must be checked with an ozone source that has been calibrated using the gas-phase titration of ozone with a National Bureau of Standards NO Standard Reference Material (SRM).

PROCEDURES

Lab-oriented air pollution instruments, operating in an aircraft environment, experience wide variations of temperature, pressure, humidity,

and vibration during a helicopter flight. To ensure the collection of the best possible data all instruments are zeroed and spanned daily. In addition, the gas-phase instruments are given zero gas during a flight with the instrument reading recorded on tape.

On the ground, after a flight, the instruments are first zeroed. This is a hands-off zero with no adjustments being made to the instrument. The instrument reading is simply recorded. This operation is referred to as the "post-flight zero." Next, the instruments are adjusted to give a zero output value with a zero input. This is the "pre-flight zero." Next, a "post-flight span" is performed. No instruments are adjusted at this time; the span value is simply recorded. Finally all the instruments are adjusted to read the span input value in the "pre-flight span." The instruments are now calibrated for the next flight after checking the zero and span drift that occurred during the preceding flight.

DATA REDUCTION AND INTERPRETATION

Several corrections are made to the data collected from the aircraft. First, linear corrections are made to account for the zero and span drift that occurs over a 1-day period. In many of the new electronic air pollution instruments being marketed today, daily instrument drift is minimal. Operation of these instruments in a helicopter environment tends to increase this drift. To reduce the error associated with this drift, the inflight zero, ground-level zero and span data (obtained from the calibration procedures described above) are used. Electronic instrument drift is presently accounted for using the inflight zero data. Instrument drift caused by changes in flow rates and contamination of the sensor package is taken into account with the daily zero and span calibrations. While this method of correcting data is not perfect, it is the best practical method available to account for the temperature, flow rate changes, etc., experienced by an instrument during a flight.

All span calibrations of the helicopter instrumentation are referred to standard temperature and pressure (STP) conditions (25°C, 760 mmHg). These corrections are identical to the corrections normally made in the calibration of a ground-based air pollution instrument. When the helicopter instrumentation measures pollution at different temperatures and altitudes, the required STP corrections become more complicated. Confusion often arises when one speaks of correcting data reported in terms of parts per million (ppm, a volume/volume rate) for changes in atmospheric temperature and pressure. In reality, an instrument that is calibrated with a gas (the concentration being reported in terms of ppm) actually measures the pollutant on a mass per second basis. Thus, corrections for changes in temperature and pressure must be made to the data. Unfortunately, these corrections are not straightforward. Instrument manufacturers employ a variety of techniques to stabilize their instruments. The use of thermoelectric coolers, temperature compensated electronics, ovens, regulators, and critical orifices prevents one from using the ideal gas law to correct airborne-based data to STP conditions. At the present time, an environmental chamber is being used to obtain the true variation in span response caused by variations in temperature and pressure.

With this information, it will be possible to reduce the errors inherent with the placement of lab-oriented instrumentation in an aircraft environment. With the exception of the carbon monoxide instrument, all of the environmental chamber work, up to this point, has shown the corrections for temperature and pressure to be small when the helicopter samples air within a few thousand feet of the ground. For example, the SO_2 instrument span value would decrease by approximately 0.03 ppm if the helicopter sampled air 4,000 feet above the ground. Thus, the complex span (gain) corrections for temperature and pressure are not being made at this time.

Table F-1 lists the lag and response times measured on the instrumentation. Currently, a computer-based convolution integral technique to correct the helicopter data for instrument response is being developed. In the absence of such a technique no corrections are being made to the data listed on the computer printout. Fortunately, response-time corrections can be neglected (and little error results) when an aircraft flies through slowly varying, widely dispersed pollution. In plume sampling these corrections become more significant. With some of the graphic plume presentations, graphical techniques have been subjectively used to obtain a truer picture of the plume. Given the amount of uncertainty inherent with current modeling methodology, it is not unreasonable to use the best available airborne plume measurement data even though a sizeable, undefinable amount of uncertainty exists with the data.

TABLE F-1. AVERAGE RESPONSE TIMES AND MINIMUM DETECTABLE CONCENTRATIONS

Parameter	Average Response Times[1] Lag	0-90%	Minimum Detectable[2] Concentration
CO	5 sec	11 sec	0.1 ppm
SO_2		variable	0.005 ppm
Temperature/Dew point			$\dfrac{-60° \text{ F}}{10\% \text{ Rel. Hum.}}$
NO/NO_x	9.5	4	approx. 2 ppb
O_3	7.5	5	0.01 ppm
Visibility		<1	b_{scat} - 0.1

1. These figures are typical for the instrumentation maintained by EMSL-Las Vegas.

2. These figures were obtained from the manufacturers' literature.

APPENDIX G. PLUME RISE CALCULATIONS

An examination of the Mitchell data was begun in an attempt to normalize the plume rise data. First, a comparison of the observed plume rises with those derived by Briggs (1968) through dimensional analysis was made.

Table G-1 (equations 1 through 3) considers the case of a windy day and buoyancy-dominated plume.

TABLE G-1. DIMENSIONAL ANALYSIS PLUME RISE RELATIONS

Type of Rise	Plume Rise Formula	
Transitional	$\Delta h = 2.0\ F^{1/3}u^{-1}x^{2/3}$	(1)
Stable	$\Delta h = 2.6\ (F/u)^{1/3}\ s^{-1/3}$	(2)
Neutral	$\Delta h = 10^3\ Fu^{-3}$	(3)

where Δh = plume rise (m)
         F = buoyancy flux ($m^4 sec^{-3}$)
         u = wind speed (m sec^{-1})
         x = downwind distance (m)
         s = stability parameter (sec^{-2})

The buoyancy flux for the equations in Table G-1 was obtained in the following manner:

For a hot source---

$$F = \frac{gQ_h}{\pi C_p\ T}$$ (4)

where g = gravitational constant
         Q_h = heat emission rate
         C_p = specific heat, constant pressure
             = density
         T = temperature

96

or,

$$F = 3.7 \times 10^{-5} \left| \frac{m^4 \ sec^3}{cal \ sec} \right| x \ Q_h \left| J/sec \right| \tag{5}$$

and

$$Q_h = Q_m C_p \Delta T \tag{6}$$

where C_p = 1.42×10^3 (m^2-sec^2-deg^{-1})
Q_m = mass emission rate (kg-sec^{-1})
ΔT = temperature difference (°K)

and,

$$Q_v = 22.4 \times 10^{-3} \frac{Q_m}{M_w} \frac{T}{273} \tag{7}$$

where Q_v = volumetric flow rate (m3-sec-1)
T = exit temperature (°K)
M_w = gram molecular weight of 1 mole of gas, or 0.029 kg

or,

$$Q_m = \frac{Q_v M_w}{22.4 \times 10^{-3}} \frac{273}{441} \tag{8}$$

Therefore,

$$Q_h = 166,156 \ Q_v \tag{9}$$

The stability parameter, s, was calculated in the following manner (Briggs, 1969):

$$s = \frac{g}{T} \frac{\partial \Theta}{\partial Z} \tag{10}$$

where $\frac{\partial \Theta}{\partial Z} = \frac{\partial T}{\partial Z} + 9.8°C/km$, and $\frac{\partial T}{\partial Z}$ = lapse rate

Θ = potential temperature
T = mean ambient temperature through which plume rises
g = gravitational constant

The results obtained with either the second or third Briggs equation (equation 2 or 3, as applicable) are shown in Table G-2.

TABLE G-2. PLUME RISE CALCULATED FROM THE BRIGGS EQUATIONS BASED ON DIMENSIONAL ANALYSIS

Date	Stability	Stability Parameter(s)	Buoyancy Flux F	Wind Speed (m sec^{-1})	Calculated Δh (m)	Observed Δh (m)
27 Aug	N	-0.111	1,258	10.0	1,258	386
27 Aug	N	-0.111	1,258	10.0	1,258	347
3 Sep	N	0.000	1,591	5.0	12,728	378
3 Sep	N	0.000	1,591	5.0	12,728	408
3 Sep	N	0.000	1,591	5.0	12,728	500
5 Sep	N	0.000	1,702	5.0	13,616	317
5 Sep	N	0.000	1,702	5.1	13,616	341
8 Sep	S	1.000	1,887	7.6	16	226
8 Sep	N	-0.057	1,887	10.8	1,497	438
9 Sep	S	0.130	10,545	5.0	88	347
9 Sep	S	0.130	10,545	5.5	111	356
10 Sep	N	0.100	10,693	2.6	608,366	569
11 Sep	S	0.328	10,841	12.5	36	149
11 Sep	S	0.328	10,841	9.0	46	58

These are, of course, not satisfactory calculations of plume rise.

The next calculations involve use of the formula for neutral conditions as suggested by Briggs et al. (1968). Recognizing that there was only nominal loading on the plant, unsatisfactory results were obtained for the neutral cases using:

$$\Delta h = 400\frac{F}{u^3} + 3r\frac{w}{u}$$

where r = stack radius
      w = exit velocity

The average of the calculated values for the period 27 August through 8 September (a period of nominal plant loading) agrees within 1% of the observed plume rise values. However, the values obtained for the period 9 through 11 September are too high due to the extremely high buoyancy fluxes generated when the Mitchell plant is in full operation.

TABLE G-3. A COMPARISON OF COMPUTED TO OBSERVED PLUME RISE FOR NEUTRAL CASES

Date	Calculated Plume Rise (m)	Observed Plume Rise (m)
27 Aug	549	386
	549	347
3 Sep	5,182	376
	5,182	408
	5,182	500
5 Sep	5,538	317
	5,537	347
8 Sep	1,780	438
	2.4×10^5	569
9 Sep	796	356
10 Sep	1,692	569
11 Sep	884	149
	867	58

TABLE G-4. VOLUMETRIC EMISSION RATES (Cramer 1976)* AND ASSOCIATED BUOYANCY FLUXES FOR THE MITCHELL PLANT

Date	Time (EST)	Volumetric Emission Rate (m^3/sec)	Buoyancy Flux (m^4-sec^{-3})
9 Sep	0617-0856	1717	10,545
	1027-1331	1720	10,555
10 Sep	0924-1255	1740	10,693
11 Sep	0831-1109	1764	10,841

*Cramer, H.E., personal communication, 1976

These values are on the order of twice the volumetric emissions of the Kammer plant. This fact, coupled with the high release altitude (366 m AGL), the large stack diameter (10.06 m) and the high exit velocity (30.3 m/sec), makes it not surprising that the formulae developed for smaller plants are not applicable. An inspection of the formula given by equation 1 suggests that the u^{-1} term might be varied to give better results as the F and x terms are nearly constant in this treatment. Therefore, various exponential values were assigned to the value u with the results shown in Table G-5.

TABLE G-5. PLUME RISE CALCULATED USING VARIOUS EXPONENTS OF u COMPARED TO OBSERVED PLUME RISE

Date	Calculated Plume Rise u^{-1} (m)	Calculated Plume Rise $u^{-1.1}$ (m)	Calculated Plume Rise $u^{-1.5}$ (m)	Calculated Plume Rise $u^{-1.6}$ (m)	Observed Plume Rise (m)
9 Sep	876	745	391	333	347
	796	671	339	286	356
10 Sep	1,692	1,537	1,049	953	569
11 Sep	884	686	250	194	149
	861	695	289	231	58

This approach gives fair results for the observations taken on 9 September when there were moderate wind speeds. However, the results for 10 September (u = 2.6 m-sec^{-1}) and 11 September (u = 12.6 and 9 m-sec^{-1}) are less than satisfactory. It was decided to develop a relationship between wind speed and plume rise through a curve-fitting process. The assumption is that the data may be fitted using an exponentially decreasing function. The possibilities considered were:

$$f_1(x) = Ae^{-ku} \qquad (12)$$

and

$$f_2(x) = Ae^{-ku^2} \qquad (13)$$

where u = wind speed (m/sec)

Parameters A and k were found using the values associated with the lower wind speed (2.6 m/sec, 569 m) and a second value obtained by drawing a smooth curve through a plot of wind speed versus plume rise. The second value (10.75 m/sec, 103.5 m) was halfway between the values associated with the higher wind speeds (9 m/sec, 58 m and 12.5 m/sec, 149 m). The equations are:

$$f_1(u) = 980.0e^{-0.209u} \qquad (14)$$

and

$$f_2(u) = 632.6e^{-0.1566u^2} \qquad (15)$$

A comparison of the fit of these two curves is shown in Table G-6.

TABLE G-6. COMPARISON OF THE FIT OF TWO POSSIBLE CURVES TO DESCRIBE PLUME RISE AS A FUNCTION OF WIND SPEED FOR HIGH FLUX CASES OF THE MITCHELL PLUME

(m/sec)	Observed Plume Rise (m)	Plume Rise from $f_1(u)$ (m)	Plume Rise from $f_2(u)$ (m)
2.6	569	569	569
5.0	347	345	428
5.5	356	311	394
9.0	58	149	178
12.5	149	72	55

The standard deviation associated with $f_2(u)$ is 49 m and the standard deviation for $f_1(u)$ is 80 m. Therefore, $f_2(u)$ was selected. Figure G-1 presents a comparison of the observed and calculated plume rises using equation 1 for low flux cases and equation 14 for the high flux cases.

The Kammer plume rise was handled in a similar manner. The Briggs formulae shown in equations 1, 2, and 3 were considered.
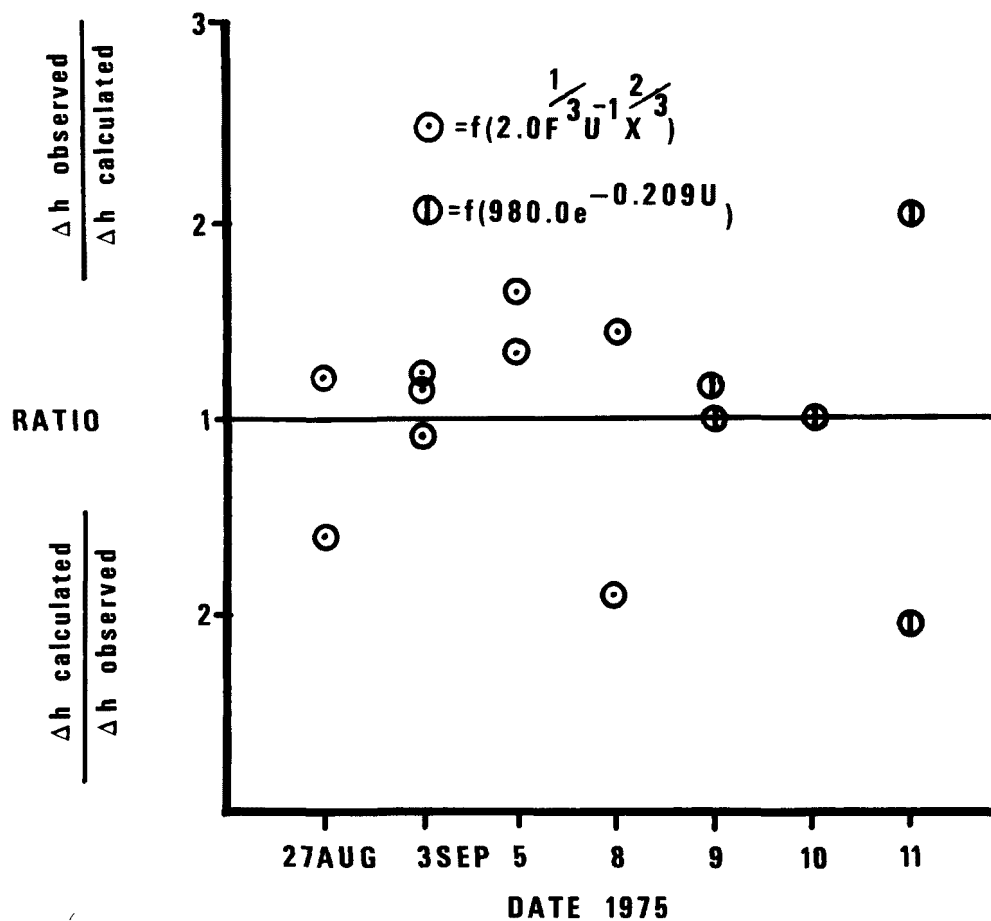
Figure G-1. Comparison of observed and calculated plume rises for the Mitchell plant, 27 August - 11 September 75.

Table G-7 presents the parameters used in these calculations. Once again, x = 1 km was chosen as the downwind distance where stabilization takes place. The plume rise measurements for 8 September were not included since a strong inversion capped the Kammer plume.

TABLE G-7. PARAMETERS USED IN PLUME RISE CALCULATIONS FOR THE KAMMER PLANT

Date	Stability	Stability Parameter (sec^{-2})	Wind Speed (m/sec)	Buoyancy Flux (m^4/sec^3)
27 Aug	Neutral	-0.11	2.7	6.07×10^3
28 Aug	Neutral	0.08	5.3	6.14×10^3
	Neutral	0.08	5.3	6.14×10^3
29 Aug	Stable	0.32	8.8	5.99×10^3
	Stable	0.32	8.8	5.99×10^3
	Stable	0.32	8.8	5.99×10^3
2 Sep	Neutral	0.00	4.6	6.07×10^3
3 Sep	Neutral	0.00	3.5	6.36×10^3
4 Sep	Neutral	0.00	4.5	3.92×10^3
5 Sep	Neutral	0.00	5.5	4.03×10^3
	Neutral	0.00	6.0	4.03×10^3
8 Sep	Stable	Inversion	6.6	4.11×10^3
	Stable	Inversion	6.6	4.11×10^3
9 Sep	Stable	0.13	4.4	4.07×10^3
10 Sep	Neutral	0.10	3.1	5.59×10^3
11 Sep	Stable	0.33	9.2	5.88×10^3
	Stable	0.33	9.2	5.88×10^3

Table G-8 presents the results obtained by an application of the three equations (equations 1, 2, and 3) to calculations of plume rise for the Kammer plant.

TABLE G-8. COMPARISON OF CALCULATED TO OBSERVED PLUME RISE FOR THE KAMMER PLANT

Date	Observed Plume Rise (m)	Plume Rise Calculated from Eq. 1 (m)	Plume Rise Calculated from Eq. 2 (m)	Plume Rise Calculated from Eq. 3 (m)
27 Aug	232	1,348		3.08×10^6
28 Aug	841	690	63	4.12×10^5
	1,116	690	63	4.12×10^5
29 Aug	293	414	33	8.79×10^4
	262	414	33	8.79×10^4
	308	414	33	8.79×10^4
2 Sep	354	791		6.24×10^5
3 Sep	811	1,057		1.48×10^6
4 Sep	567	702		4.30×10^5
5 Sep	506	578		2.42×10^5
	384	530		1.87×10^5
8 Sep	354	Inversion		1.43×10^5
	293	Inversion		1.43×10^5
9 Sep	262	727	50	4.78×10^5
10 Sep	475	1,142	68	1.88×10^6
11 Sep	216	391	32	7.55×10^4
	201	391	32	7.55×10^4

Equations 2 and 3 yield unsatisfactory results. Once again, equation 1 gives the best results. However, the average calculated value was 50 percent too high. We therefore have introduced a factor of 0.66 to the equation.

$$\Delta h = 0.66(2.0 \ F^{1/3}u^{-1}x^{2/3})$$

An application of this factor gives the results shown in Table G-9. Figure G-2 is a graphical representation of these results.

104

TABLE G-9. ADJUSTED CALCULATED VS. OBSERVED PLUME RISE FOR THE KAMMER PLANT

Date	Calculated Plume Rise (m)	Observed Plume Rise (m)
27 Aug	895	232
28 Aug	458	841
	458	1,116
29 Aug	275	293
	275	262
	275	308
2 Sep	525	354
3 Sep	702	811
4 Sep	466	567
5 Sep	336	506
	336	384
9 Sep	174	262
10 Sep	758	475
11 Sep	260	216
	260	201
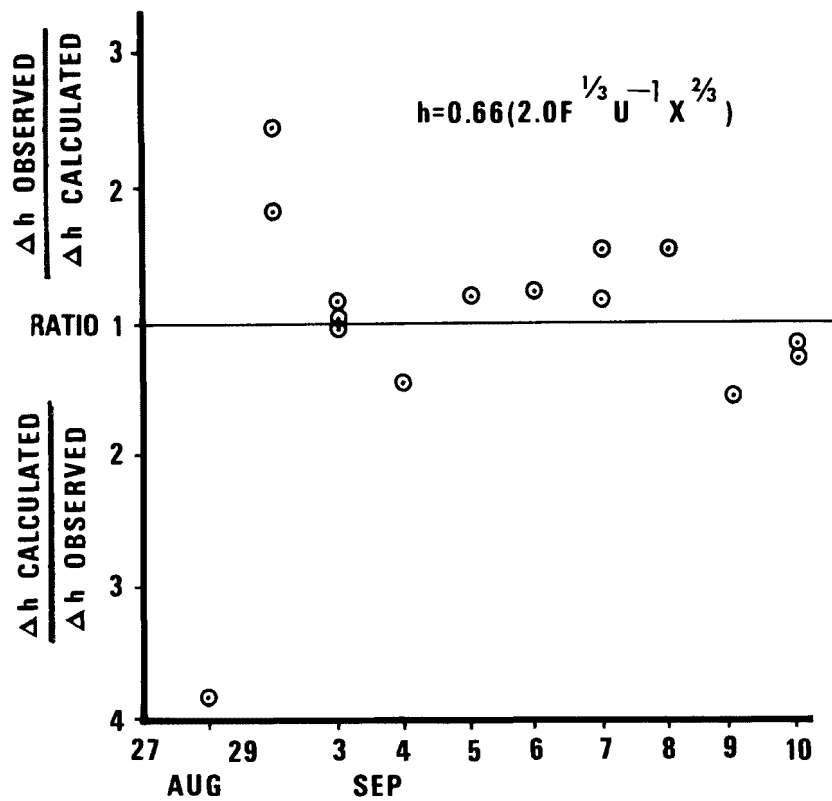
Figure G-2. Comparison of observed and calculated plume rises for the Kammer plant, 27 August - 11 September 75.

16. ABSTRACT

A field study was conducted during August and September 1975 to measure parameters of effluent plumes from two coal-fired electric generating stations near Wheeling, West Virginia. This data report presents plume heights, plume horizontal and vertical dispersion, and plume centerline and maximum low altitude sulfur dioxide concentrations. Plume parameters were observed with a helicopter-borne air quality monitoring system and an airborne Light Detection and Ranging (LIDAR) system which measured aerosol light scattering. Plume cross sections in terms of sulfur dioxide concentrations and aerosol light scattering were simultaneously obtained with the helicpoter and LIDAR systems and are presented for comparison. Estimates of sulfur dioxide fluxed in the effluent plumes were prepared from the helicopter sulfur dioxide plume cross sections and the transport winds. Sulfur dioxide flux estimates derived from helicopter data agree within 10 percent with flux estimates derived from coal consumption and sulfur content data for three cases in stable atmospheres with moderate wind speeds. Plume rise formulas have been developed for the two plants.

17.	KEY WORDS AND DOCUMENT ANALYSIS	
a. DESCRIPTORS	b. IDENTIFIERS/OPEN ENDED TERMS	c. COSATI Field/Group
Electric power generation Air pollution Environmental surveys Helicopters Wind meteorology Sulfur dioxide	Kammer and Mitchell electric power stations, West Virginia Helicopter air quality measurements	04B 07B 17H 20F
18. DISTRIBUTION STATEMENT RELEASE TO THE PUBLIC	19. SECURITY CLASS *(This Report)* UNCLASSIFIED	21. NO. OF PAGES 116
	20. SECURITY CLASS *(This page)* UNCLASSIFIED	22. PRICE A06